NASA CR-168323

NASA

National Aeronautics and
Space Administration

CLEAN CATALYTIC COMBUSTOR PROGRAM

FINAL REPORT

By

E.E. Ekstedt, T.F. Lyon,
P.E. Sabla, and W.J. Dodds

General Electric Company
Aircraft Engine Business Group
Cincinnati, Ohio 45215

Prepared for

National Aeronautics and Space Administration

NASA Lewis Research Center
Contract NAS3-22003

1. Report No.	2. Government Accession No.	3. Recipient's Catalog No.
NASA CR-168323		

4. Title and Subtitle	5. Report Date
Clean Catalytic Combustor Program	November 1983
	6. Performing Organization Code
7. Author(s)	8. Performing Organization Report No.
E.E. Ekstedt, T.F. Lyon, P.E. Sabla, and W.J. Dodds	
	10. Work Unit No.
9. Performing Organization Name and Address	
General Electric Company Aircraft Engine Business Group Cincinnati, Ohio 45215	11. Contract or Grant No. NAS3-22003
	13. Type of Report and Period Covered Contractor Report Oct 1979 - July 1982
12. Sponsoring Agency Name and Address	
National Aeronautics and Space Administration Washington, D.C. 20546	14. Sponsoring Agency Code

15. Supplementary Notes

Project Manager, A.J. Szaniszlo
NASA-Lewis Research Center,
Cleveland, Ohio 44135

16. Abstract

A combustor program was conducted to evolve and to identify the technology needed for, and to establish the credibility of, using combustors with catalytic reactors in modern high-pressure-ratio aircraft turbine engines.

Two selected catalytic combustor concepts were designed, fabricated, and evaluated. The combustors were sized for use in the NASA/General Electric Energy Efficient Engine (E^3). One of the combustor designs was a basic parallel-staged double-annular combustor. The second design was also a parallel-staged combustor but employed reverse flow cannular catalytic reactors.

Subcomponent tests of fuel injection systems and of catalytic reactors for use in the combustion system were also conducted.

Very low-level pollutant emissions and excellent combustor performance were achieved. However, it was obvious from these tests that extensive development of fuel/air preparation systems and considerable advancement in the steady-state operating temperature capability of catalytic reactor materials will be required prior to the consideration of catalytic combustion systems for use in high-pressure-ratio aircraft turbine engines.

17. Key Words (Suggested by Author(s))	18. Distribution Statement
Catalytic Combustor Low Emission Combustor Fuel Injection Pollutant Emissions Aircraft Turbine Combustor	Unclassified - Unlimited

19. Security Classif. (of this report)	20. Security Classif. (of this page)	21. No. of Pages	22. Price*
Unclassified	Unclassified	144	

* For sale by the National Technical Information Service, Springfield, Virginia 22161

FOREWORD

The work described herein was conducted by the General Electric Aircraft Engine Business Group under Contract NAS3-22003. The program was jointly funded by NASA and the Air Force. The NASA Project Manager was Andrew J. Szaniszlo.

Catalytic reactors were designed and fabricated by Engelhard Industries Division of the Engelhard Corporation.

TABLE OF CONTENTS

TABLE OF CONTENTS (Concluded)

LIST OF ILLUSTRATIONS

LIST OF ILLUSTRATIONS (Continued)

LIST OF ILLUSTRATIONS (Continued)

LIST OF ILLUSTRATIONS (Concluded)

LIST OF TABLES

1.0 SUMMARY

The objective of this program was to develop the technology needed for the design of combustion systems utilizing catalytic reactors and to determine the feasibility of the use of these combustion systems in modern high-pressure ratio, high-temperature, aircraft gas-turbine engines.

The program was conducted in two phases. During Phase I, a total of six combustion systems were designed and analyzed for performance, life, cost, weight, and reliability. The two most promising of these combustors were a basic parallel-staged system and a parallel-staged combustor with reverse flow cannular catalytic reactors. The basic parallel-staged combustor utilized an annular pilot stage with 30 fuel nozzles. The pilot is utilized for all operation up to 60% engine thrust. The main stage has an annular catalytic reactor mounted inboard of the pilot and is used along with the pilot for all engine operation above 60% thrust. The reverse flow combustor also has an annular pilot with 30 fuel nozzles but uses 30 cylindrical catalytic reactors for the main stage. In the reverse flow system, the catalytic reactors are mounted outboard of the pilot stage.

During Phase II, which is the subject of this report, 60° sector combustors of the two designs selected from Phase I were designed, fabricated, and evaluated in a series of four-atmosphere pressure tests. The combustors were designed for the NASA/General Electric Energy Efficient Engine (E^3).

In addition to the sector combustor performance tests, subcomponent tests were conducted on several catalytic reactor designs and on fuel and air premixing systems. These subcomponent tests were conducted at pressures up to 11 atmospheres. The catalytic reactor subcomponent tests were to select a configuration and generate pressure corrections for the lower pressure sector-combustor tests.

During the sector combustor tests, excellent performance capability was demonstrated for a combustion system utilizing a catalytic reactor. Gaseous emissions (oxides of nitrogen, unburned hydrocarbons, and carbon monoxide) were more than 25% below the Environmental Protection Agency (EPA) standards as they were proposed for the landing - takeoff cycle for class T-2, newly

certified engines in the March 24, 1978 Federal Register. Oxides of nitrogen levels of 3.0 grams per kilogram of fuel were also demonstrated for normal cruise operating conditions. Other performance chracteristics such as pressure drop, pattern factor, liner temperature, combustion efficiency, and combustor light off appear to present no significant problems for the combustion system with a catalytic-reactor main stage. Pilot-stage smoke at the 60% power condition before the main stage is fueled, which cannot be fully evaluated in a four-atmosphere test, represents a concern item and should be evaluated at higher (actual engine) pressure. However, the smoke measurements made during the sector combustor tests indicated very low smoke levels.

In order to achieve high combustion efficiency in the catalytic reactor main stage at the 60% engine power condition, it was necessary to reduce the reference velocity in the catalytic reactor from the original design value of 30 m/s by 50%. Considerable improvement in combustion efficiency with operating pressure level was demonstrated in the subcomponent catalytic reactor tests, however. Therefore, a reference velocity design value of 24 to 27 m/s should be adequate for high performance levels at actual engine pressure conditions based on the results of this program.

The major limitation for the use of combustion systems with catalytic reactors appears to be the continuous operating temperature capability of the catalytic reactors. It was necessary to operate the catalytic reactors at the continuous operating temperature limit of 1700 K at cruise conditions in order to meet the NO_x emissions goal (3 g/kg) of the program. Considerable advancement in the operating temperature capability of catalytic reactor materials will be required for successful application of catalytic combustors to very high pressure ratio, high temperature engines of the type considered in this study.

Baseline testing was conducted with both of the combustors. The reverse flow combustor was selected for the final tests. The reverse flow configuration was selected over the basic parallel-staged combustor because of length, maintenance, and performance considerations.

During this program, considerable effort was necessary to develop fuel and air premixing systems with adequate fuel air uniformity for use with a catalytic combustor.

2.0 INTRODUCTION

The ability of catalytic combustors to promote stable combustion of lean fuel/air mixtures with flame temperatures less than 1800 K, provides the potential for obtaining ultra-low nitrogen oxides emissions levels in combustion systems utilizing catalytic reactors. Improved combustion system life is another potential benefit obtained from the use of catalytic reactors due to the reduced gas temperatures in the combustion zone. In standard combustion systems with droplet burning, primary zone gas temperatures can reach stoichiometric flame temperature levels locally and radiation levels from the primary zone are relatively high. However, in a catalytic combustor, the gas temperature is at the much lower flame temperature value associated with the average premixed fuel/air ratio. Therefore, the flame radiation levels are significantly lower due to the reduced flame temperature and because of reduced quantity of soot particles associated with lean premixed flames. Other potential benefits of catalytic combustors include improved turbine life because of reduced pattern factors, improved temperature profiles, and improved combustion stability at low fuel/air ratios.

The effort covered by this report is Phase II of a two-phase program initiated by NASA and conducted by the General Electric Company. The program involves investigating the potential for applying catalytic combustion to modern high-pressure-ratio gas turbine engine combustion systems.

Phase I (Reference 1) had the objective to design and analyze six different conceptual designs employing catalytic combustion. Based on the analysis performed during Phase I, two parallel-staged, fixed geometry designs were identified as the most promising concepts. Results of the design studies indicated that cruise oxides of nitrogen (NO_x) emissions could be reduced by an order of magnitude relative to current technology levels by the use of catalytic combustion. During the Phase II program, the two most promising concepts identified during Phase I were designed, fabricated, and evaluated in an extensive series of tests. Initially, subcomponent tests of the fuel preparation systems for the catalytic reactor were conducted. Next, several cannular catalytic reactors were tested at pressures up to 11 atmospheres to

select the catalytic reactor to be used in the sector combustor tests and to generate correlations to use for later pressure corrections to the catalytic reactor performance in the lower pressure sector combustor tests. Finally, 60° sector combustor tests were conducted at pressures up to four-atmospheres to determine the combustion system performance. The combustion system performance was determined at light off, idle, approach power, 60% engine power, cruise, climb, and takeoff conditions. Actual engine operating conditions were used at light off and idle. Above these power levels, the tests were conducted at four-atmospheres inlet pressure. However, corrections to the measured data were estimated from previously determined correlations (Reference 2) and also from the correlations determined in the single-can catalytic reactor subcomponent tests.

Performance measurements included gaseous emissions, smoke, combustion efficiencies, combustor metal temperatures, pressure drop, and combustor exit temperature profiles.

3.0 PROGRAM GUIDELINES

3.1 COMBUSTOR PERFORMANCE

The overall program goal was to evolve the technology needed for the design of combustion systems utilizing catalytic reactors and to determine the feasibility of using these combustion systems in modern high-pressure-ratio, high-temperature aircraft gas turbine engines. Of particular importance was the achievement of ultra-low NO_x emissions while at the same time meeting all of the normal performance requirements of modern high performance combustion systems. Specific program pollutant emission and combustor performance goals for this program are as follows:

- Oxides of nitrogen (NO_x) levels of 3.0 grams per kilogram of fuel or less at normal cruise operating conditions.
- Gaseous pollutant emissions levels 25% below the U.S. Environmental Protection Agency (EPA) emissions standards for the landing-takeoff cycle for class T-2, newly certified engines. For purposes of this discussion, these are taken to be the proposed standards published in the March 24, 1978 Federal Register (Reference 3), and are as follows (with the 25% reductions):

  Hydrocarbons - 2.5 grams per kilonewton thrust

  Carbon Monoxide - 18.8 grams per kilonewton thrust

  Oxides of Nitrogen - 24.8 grams per kilonewton thrust

- Smoke Number - 15
- Combustion efficiency of 99.5% at idle, 99.9% at takeoff, and 99% at other operating conditions.
- Combustion system pressure loss of less than or equal to 5.5% of compressor discharge pressure.
- Exit temperature pattern factor and profile factors of less than or equal to 0.25 and 0.15, respectively.
- Combustor liner metal temperatures of no more than 1144 K.

3.2 REFERENCE ENGINE

The engine selected as the reference engine for the Phase I program and for this Phase II program is the NASA/General Electric advanced Energy Efficient Engine, which is typical of the high pressure ratio, high bypass ratio engines that will be developed for commercial aviation service within the next 10 to 20 years. This reference engine is a direct drive fan, mixed exhaust flow version of a series of turbofan engines evaluated as a part of the recently completed NASA-sponsored Energy Efficient Engine Preliminary Design and Integration Study Program (Reference 4). An engine layout drawing is shown in Figure 1.

A major objective of the E^3 program is to obtain a 12% reduction in specific fuel consumption (SFC) at cruise conditions relative to the CF6 family of engines.

Low SFC values at cruise conditions are achieved with the E^3 by efficiency improvements in its various components and by an increase in cycle pressure ratio at cruise conditions. At sea level static conditions, the overall pressure ratio of the E^3 is the same as that of the CF6-50 engine (30:1), but at maximum cruise conditions, the E^3 cycle pressure ratio is 35.8 to 1, resulting in considerably higher combustion system inlet pressures and temperatures.

The E^3 cycle is especially appropriate as a reference engine cycle for the proposed program because the combustor high inlet-air pressures and temperatures of this cycle at cruise conditions are indicative of the trend of future commercial engine development. As a consequence of the high pressures and temperatures, the achievement of low NO_x at cruise conditions will become more difficult to accomplish and also, as explained in the following discussion, the design of practical catalytic combustion systems will become a much greater challenge.

Cycle parameters for the reference E^3 at important operating conditions are presented in Table 1 (SI units) and Table 2 (Customary units). These reference engine cycle operating parameters are the same as were used in the Phase I program. Included in these tabulations are (1) the four EPA-specified

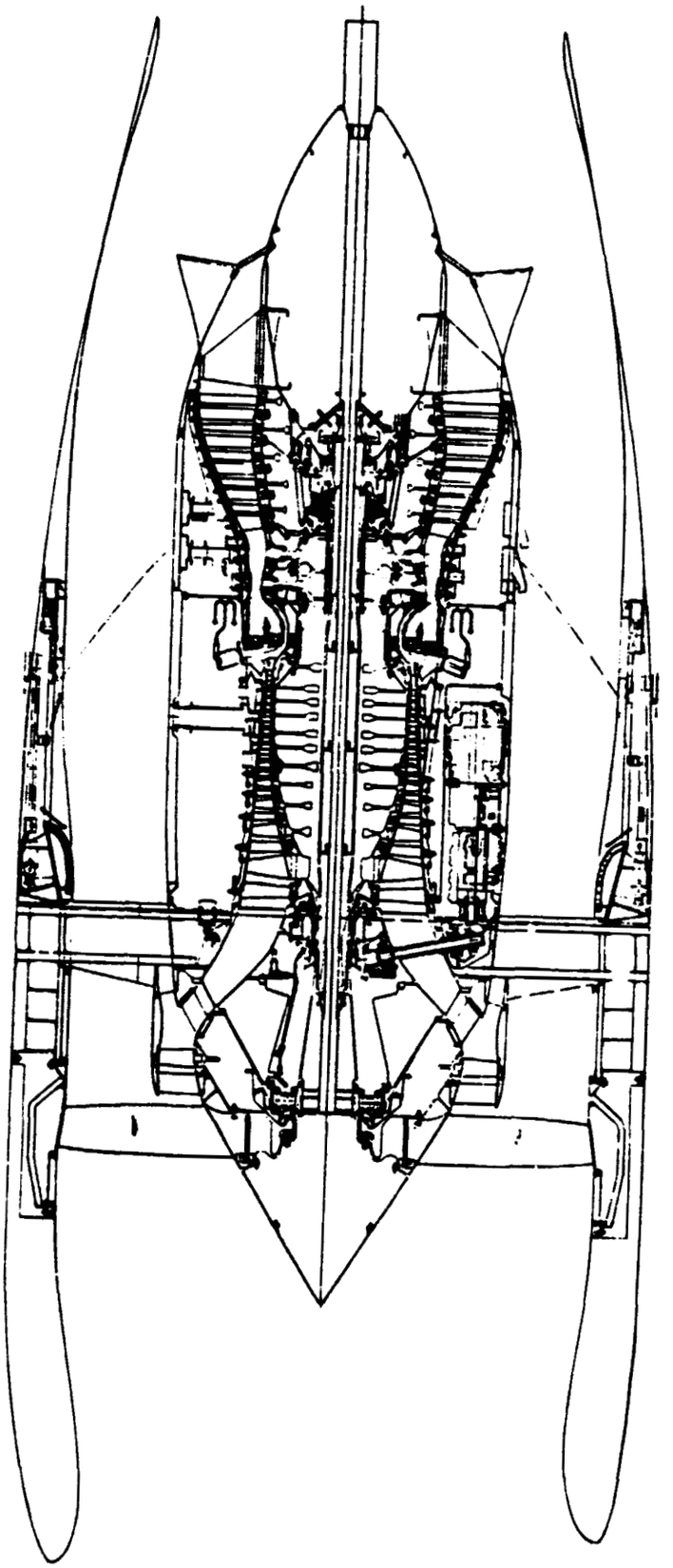

Figure 1. E^3 Reference Engine.

Table 1. Reference Engine Cycle Parameters (SI Units).

Cycle Point Ambient Conditions	Idle Std Day	30% Approach Std Day	60% Std Day	85% Climb Std Day	100% Takeoff Std Day	Hot Day Takeoff +15 K	Very Hot Day Takeoff +35 K	Max. Cruise +10 K	Normal Cruise +10 K	Min. Cruise +10 K
h_o, Flight Altitude, km	0	0	0	0	0	0	0	10.7	10.7	10.7
M_o, Flight Mach No.	0	0	0	0	0	0	0	0.80	0.80	0.80
F_N, Installed Net Thrust, kN	9.74	48.70	97.42	138.04	162.36	162.39	137.29	37.47	29.98	14.99
W_3, Compressor Exit Airflow, kg/s	10.70	28.76	43.84	55.20	61.69	60.06	51.71	26.99	23.95	17.74
W_{36}, Combustor Airflow, kg/s	9.53	25.58	39.04	49.12	54.93	53.48	46.04	24.04	21.32	15.79
P_{T3}, Compressor Exit Total Pressure, MPa	0.401	1.183	1.965	2.626	3.020	3.007	2.589	1.306	1.121	0.774
T_{T3}, Compressor Exit Total Temperature, K	485.0	632.6	717	781.6	813.8	851.3	864.3	782.1	745.1	676.9
T_{T4}, Combustor Exit Total Temperature, K	940.3	1135.3	1378	1528.7	1617.7	1693.1	1691.8	1595.1	1488.4	1289.4
W_f, Fuel Flow, kg/s	0.1136	0.3546	0.7496	1.0948	1.3399	1.3867	1.1752	0.5887	0.4680	0.2743
f_{36}, Combustor Fuel/Air Ratio, g/kg	11.9	13.9	19.2	22.3	24.3	25.9	25.5	24.5	22.0	17.4
M_3, Compressor Exit Mach No.(1)	0.281	0.296	0.29	0.286	0.283	0.282	0.285	0.281	0.282	0.289

(1)Assumes A_{e3} = 314.4 cm^2

Table 2. Reference Engine Cycle Parameters (Customary Units).

Cycle Point Ambient Conditions	Idle Std Day	30% Approach Std Day	60% Std Day	85% Climb Std Day	100% Takeoff Std Day	Hot Day Takeoff +27° F	Very Hot Day Takeoff +63° F	Max. Cruise +18° F	Normal Cruise +18° F	Min. Cruise +18° F
h_o, Flight Altitude, k ft	0	0	0	0	0	0	0	35.0	35.0	35.0
M_o, Flight Mach No.	0	0	0	0	0	0	0	0.80	0.80	0.80
F_N, Installed Net Thrust, lb	2190	10,948	21,900	31,032	36,501	36,506	30,864	8423	6740	3369
W_3, Compressor Exit Airflow, pps	23.6	63.4	96.66	121.7	136.0	132.4	114.0	59.5	52.8	39.1
W_{36}, Combustor Airflow, pps	21.0	56.4	86.07	108.3	121.1	117.9	101.5	53.0	47.0	34.8
P_{T3}, Compressor Exit Total Pressure, psia	58.2	171.5	285	380.9	438.0	436.1	375.5	189.4	162.6	112.2
T_{T3}, Compressor Exit Total Temperature, ° F	413	679	830	947	1005	1072	1096	948	881	759
T_{T4}, Combustor Exit Total Temperature, ° F	1233	1584	2020	2292	2452	2588	2585	2411	2219	1861
W_f, Fuel Flow, pph	902	2814	5949	8689	10,634	11,006	9327	4672	3714	2177
f_{36}, Combustor Fuel/Air Ratio	0.0119	0.0139	0.0192	0.0223	0.0243	0.0259	0.0255	0.0245	0.0220	0.0174
M_3, Compressor Exit Mach No.(1)	0.281	0.296	0.29	0.286	0.283	0.282	0.285	0.281	0.282	0.289

(1) Assumes $A_{e3} = 48.7$ in^2

operating conditions for calculating landing-takeoff cycle emissions levels, (2) 60% power conditions where the catalytic reactor is first fueled, and (3) cruise operating conditions where ultra-low NO_x emission levels are being sought. Mission studies indicate that the largest proportion of commercial flight will occur at the normal cruise point, a power setting that is 75% of the maximum cruise thrust.

The reference engine combustor and the interface dimensions which were used as guidelines in this program are shown in Figure 2. As in the Phase I program, combustion system length and outer casing diameter were allowed to deviate from the baseline design values in order to accommodate the catalytic combustor designs. The standard E^3 combustor, which is an ultra-short, double-annular design was based on the NASA/General Electric Experimental Clean Combustor Program (ECCP) results (References 5 and 6). The combustion system is 29.6 cm long from the compressor discharge to the turbine inlet. The combustion system has 30 fuel nozzles in both the pilot dome and the main-stage dome. The pilot is located outboard of the main stage. Double-wall, impingement-cooled liner construction is used to provide long life. The pilot-stage is designed for low dome velocities and provides excellent light off and low power operation including low idle emissions. The main-stage has relatively high velocities (21 m/s) and is designed for lean combustion at high power for low levels of oxides of nitrogen and low smoke.

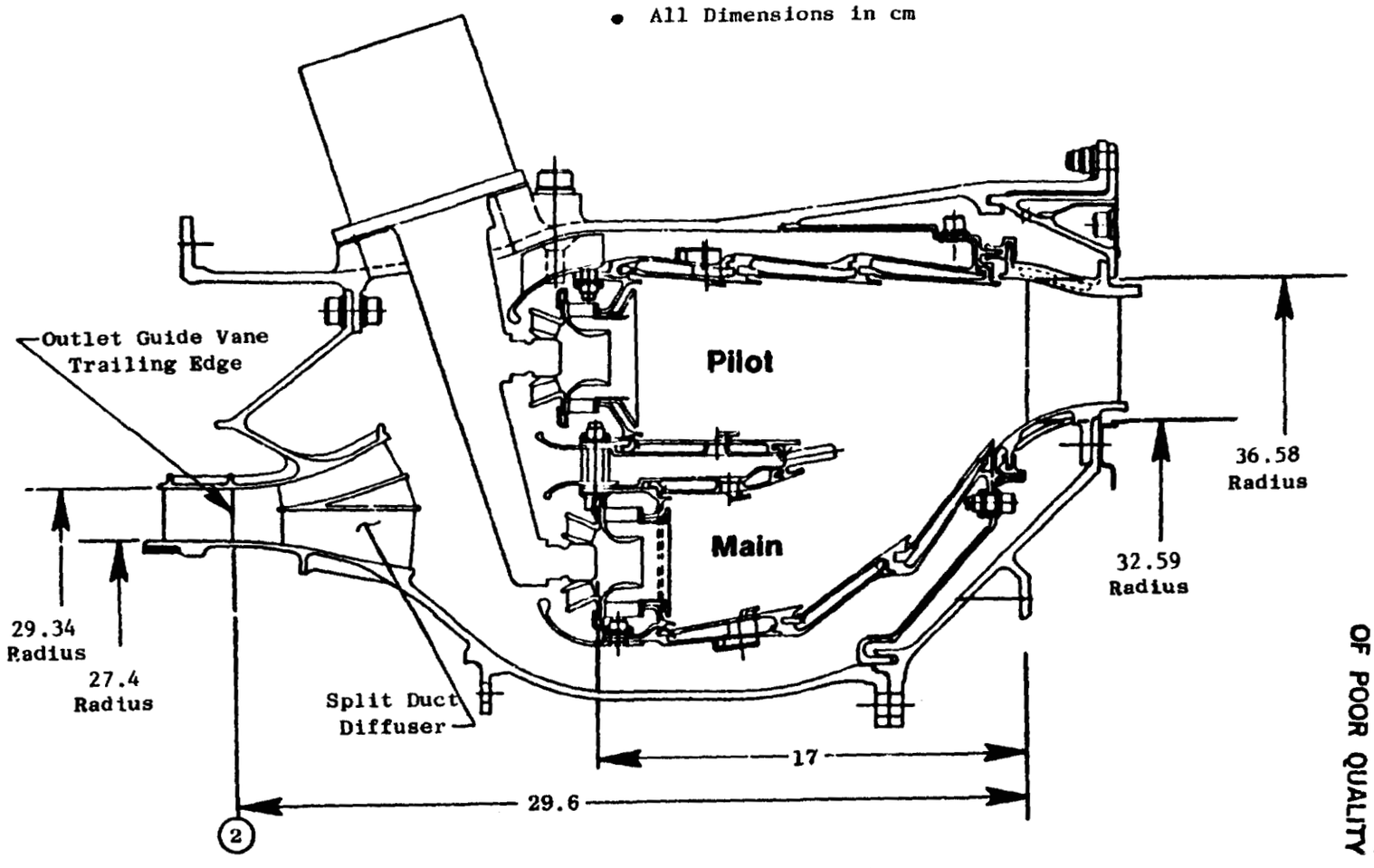

Figure 2. Reference Engine Combustion System.

4.0 CATALYTIC COMBUSTOR DESIGNS

The two promising combustors selected from the Phase I program for experimental verification and evaluation are illustrated in Figure 3. One is referred to as a basic parallel-staged combustor and the other as a reverse-flow, parallel-staged combustor. In order to accommodate the catalytic reactors and the premixing fuel system, some increase in overall combustion system length and revision of the combustor casing were required relative to the ultra-short and compact E^3 combustion system. The basic parallel-staged combustor length was 38.9 cm from the compressor discharge to the turbine inlet versus 29.6 for the standard E^3 system. The length for the reverse-flow combustor was 29.6 cm which is the same as the E^3 combustor; however, the catalytic reactors and premixing fuel/air system overlap the compressor aft end diameter.

4.1 BASIC PARALLEL-STAGED COMBUSTOR

The basic parallel-staged combustor, Figure 3(a), has a pilot stage with 30 fuel nozzles and counterrotating primary and secondary swirl cups. The pilot stage is used for combustor light off and for providing engine power up to the 60% point. Therefore, it was sized to provide rich mixtures and low velocities for good low-power performance. For power levels greater than 60%, fuel is simultaneously supplied to the pilot and main stage (catalytic reactor). The primary zone of the pilot dome has thermal barrier coating to minimize cooling airflow for improved low-power operation and for reduced pollutant emissions (Reference 7).

The main stage of this combustor is located radially inboard of the pilot stage and has a streamlined inlet section for fuel/air premixing and an annular catalytic reactor. The premixing duct was designed for a fuel residence time of 2 ms in order to provide an autoignition safety margin of approximately 100% for the most severe operating condition which is engine sea level takeoff (Reference 8). The duct length from the point of fuel injection to the catalytic reactor inlet was approximately 13 cm. The duct exit contours were designed to match the predicted free streamline boundaries for airflow

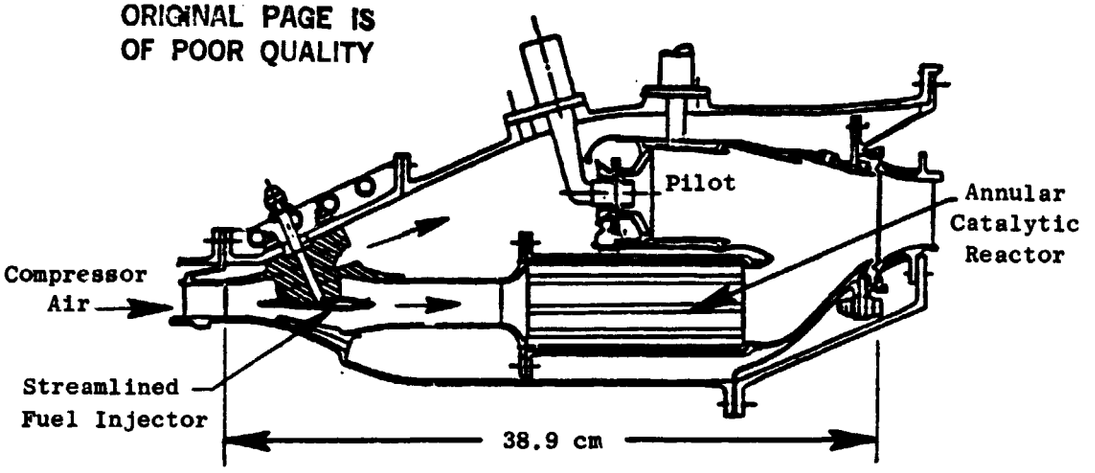

(a) Basic Parallel-Staged Combustor

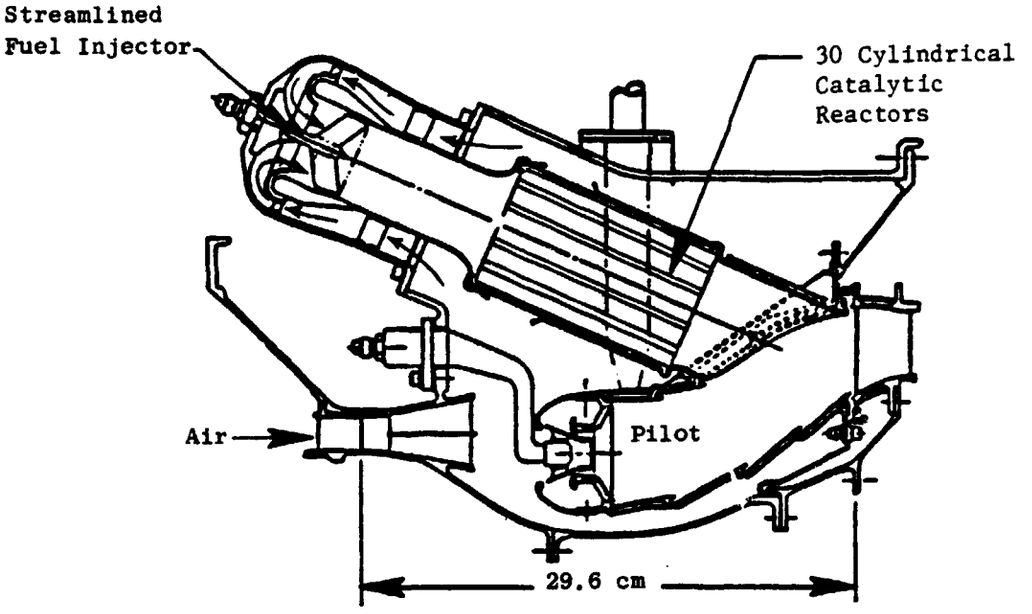

(b) Reverse-Flow Parallel-Staged Combustor

Figure 3. Two Promising Baseline Combustor Designs.

entering the reactor with approximately 50% area blockage at the reactor inlet. This was to avoid any flow separation and the resulting high residence-time zones which would promote autoignition. The fuel injector is a streamlined annular ring in the premixing duct inlet. Fuel orifices are located to provide cross-stream injection. The catalytic reactor is 12.7 cm long and has a radial height of 5.4 cm. The catalytic reactor has an Engelhard proprietary catalyst on a ceramic monolith with multiple axial channels for gas flow. The assembled reactor is supported by a compliant layer of ceramic fibers approximately 0.2 to 0.3 mm thick.

The design reference velocity for the catalytic reactor is 30 m/s. Approximately 53% of the combustor air flows through the catalytic reactor. Approximately 20% of the air is introduced into the combustor through the pilot swirl cups. The remainder of the air is used for cooling and dilution. The combustor design equivalence ratios are shown for several operating conditions in Table 3.

Table 3. Combustor Equivalence Ratios.

Operating Condition	Pilot Primary Zone	Catalytic Reactor
Idle	0.7	0
60% Power Before Transition	1.1	0
60% Power After Transition	0.25	0.35
Takeoff	0.43	0.40

Several simplifications were introduced for the 60° sector combustor test hardware. Figure 4 shows the sector combustor design. Figures 5, 6, and 7 are photographs of the test hardware parts. The aft inner and outer liners used conventional film cooling geometry instead of the impingement and convective cooled liner geometry proposed for an engine combustor. Also, a simplified fuel injector consisting of a flattened tube was used instead of the

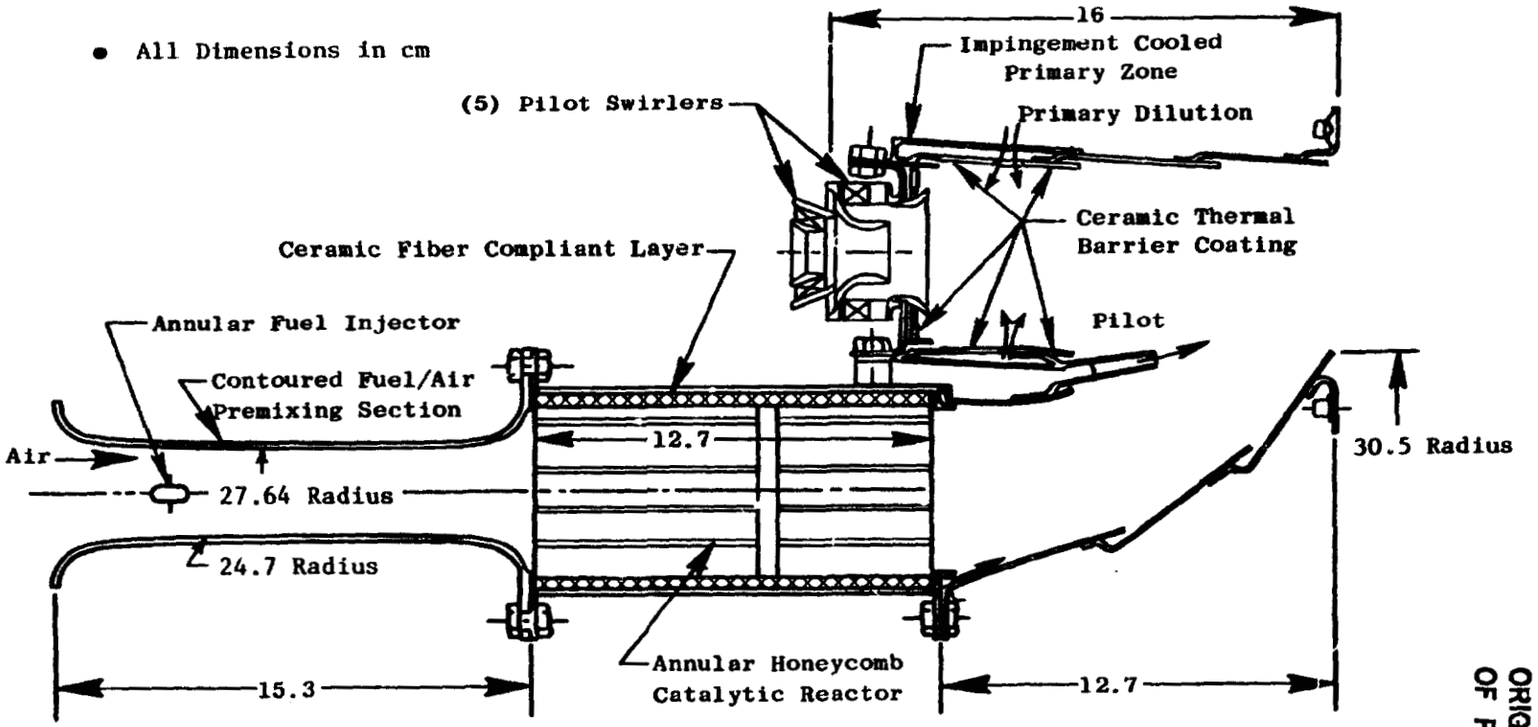

Figure 4. Parallel-Staged 60° Sector Combustor.

Figure 5. Parallel-Staged Sector Combustor Downstream View of Pilot and Main Stages.

Figure 6. Parallel-Staged Sector Combustor Partial Assembly Showing Swirler Inlets.

Figure 7. Parallel-Staged Sector Combustor Liners (Pilot-Stage Thermal Barrier Coating).

streamlined injector illustrated in Figure 3(a). The fuel holes were 0.34 mm diameter and were spaced 0.9 cm apart. The simplifications introduced for the test hardware should have no significant effect on the sector combustor performance.

4.2 REVERSE-FLOW PARALLEL-STAGED COMBUSTOR

The reverse flow combustor, Figure 3(b), has the annular pilot stage on the inboard side of the catalytic reactors. The main stage uses 30 cylindrical catalytic reactors which are 6.1 cm in diameter by 12.7 cm long. Thirty swirl cups are used in the pilot stages. Cylindrical premixing ducts with exit wall contours to match the predicted airflow streamline contours and with a fuel residence time of 2 ms are used with this combustor. The catalytic reactors of this concept discharge into the gas stream from the pilot stage through short ducts. The transition ducts are convectively cooled. Impingement cooling is used for the outer liner in the region where it intersects the transition ducts.

The design reference velocity, flow splits, and equivalence ratios for this combustor are nominally the same as those of the basic parallel-staged combustor (Table 3). A significant and attractive feature of the reverse-flow combustor design is that individual catalytic reactors could be replaced in service without removing the combustion system from the engine. Also, the overall length from the compressor discharge to the turbine nozzle diaphragm is the same as for the basic E^3 combustion system.

Figure 8 shows a cross section of the 60° sector combustor as designed for the component test program. Figures 9 and 10 are photographs of the disassembled sector combustor hardware. For the component test program, the aft inner liner was film-cooled as were the ducts just aft of the catalytic reactor. Considerable effort, described later, was devoted to development of the fuel injection system for the main stage catalytic combustor. The design used in the 60° sector combustor tests (Figure 8) is different than the streamlined version shown in Figure 3(b).

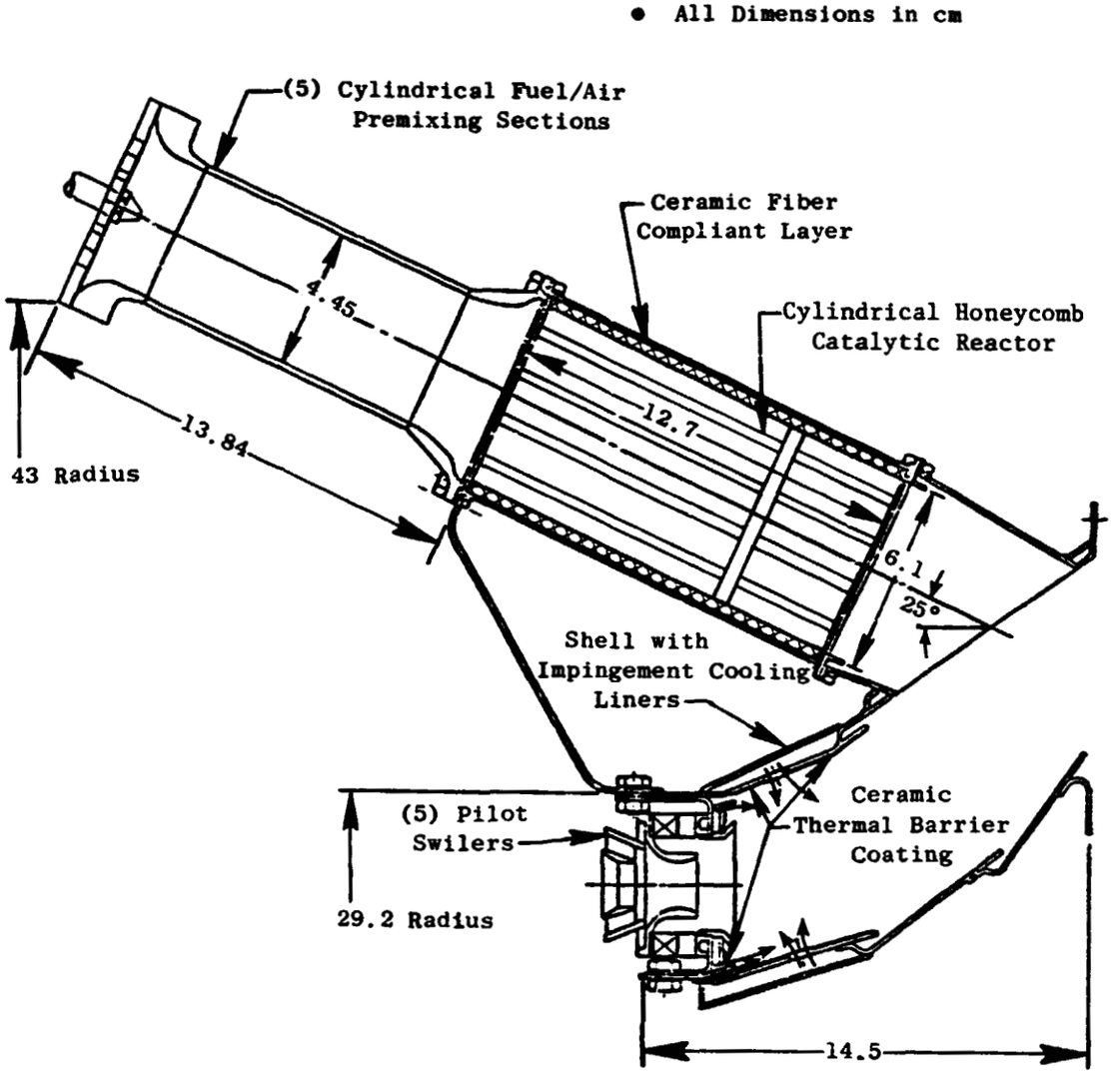

Figure 8. Reverse-Flow 60° Sector Combustor.

Figure 9. Reverse-Flow Sector-Combustor Assembly Showing Juncture of Main Stage Exit with the Pilot Stage.

Figure 10. Reverse-Flow Sector-Combustor Inlet Premixing Duct and Catalytic Reactor As Supplied with Housing.

5.0 TEST FACILITIES AND PROCEDURES

5.1 SECTOR COMBUSTOR FACILITY AND RIG

All of the combustion tests were conducted in the Advanced Combustion Laboratory at Evendale, Ohio. This laboratory very adequately supplied all of the services for the combustion testing required by this program. Air at pressures up to 2.1 MPa was supplied from a central air system at flow rates up to 4.5 kg/s. Jet-A fuel was used for this program and was supplied by a pipeline from large storage tanks located elsewhere in the plant. Test rig inlet conditions were controlled and monitored from a console located in the control room adjacent to the test cell.

The combustion system performance and emissions tests for both the basic parallel-staged and the reverse-flow combustor were conducted in a full-scale, 60°, five-cup sector-combustor test rig. Since the full-annular combustor has 30 nozzles, the pilot dome of the 60° sector combustor had five fuel nozzles and swirl cups. For the reverse-flow sector combustor, a total of four cylindrical catalytic reactors were positioned midway between the five pilot stage swirlers. For the parallel-staged combustor, a full 60° sector catalytic reactor was used.

A schematic of the sector-combustor test rig with the basic parallel-staged combustor installed is presented in Figure 11. However, the reverse-flow sector combustor was also tested in this same test rig. The sector-combustors were mounted in a test plenum chamber that was equipped with air-flow straightening screens downstream of the nonvitiated air supply inlet port. Simulated engine combustion casings were not used in these sector-combustor tests. Any differences in test results from testing without the combustion casings are believed to be negligible since the two combustor configurations have been designed to have relatively low velocities in the inner and outer flow passages around the combustors in the engine configuration.

A photograph of the inlet of the installed reverse-flow combustor is shown in Figure 12. Separate fuel lines were provided to the pilot swirl cups and to the catalytic reactor fuel premixing ducts.

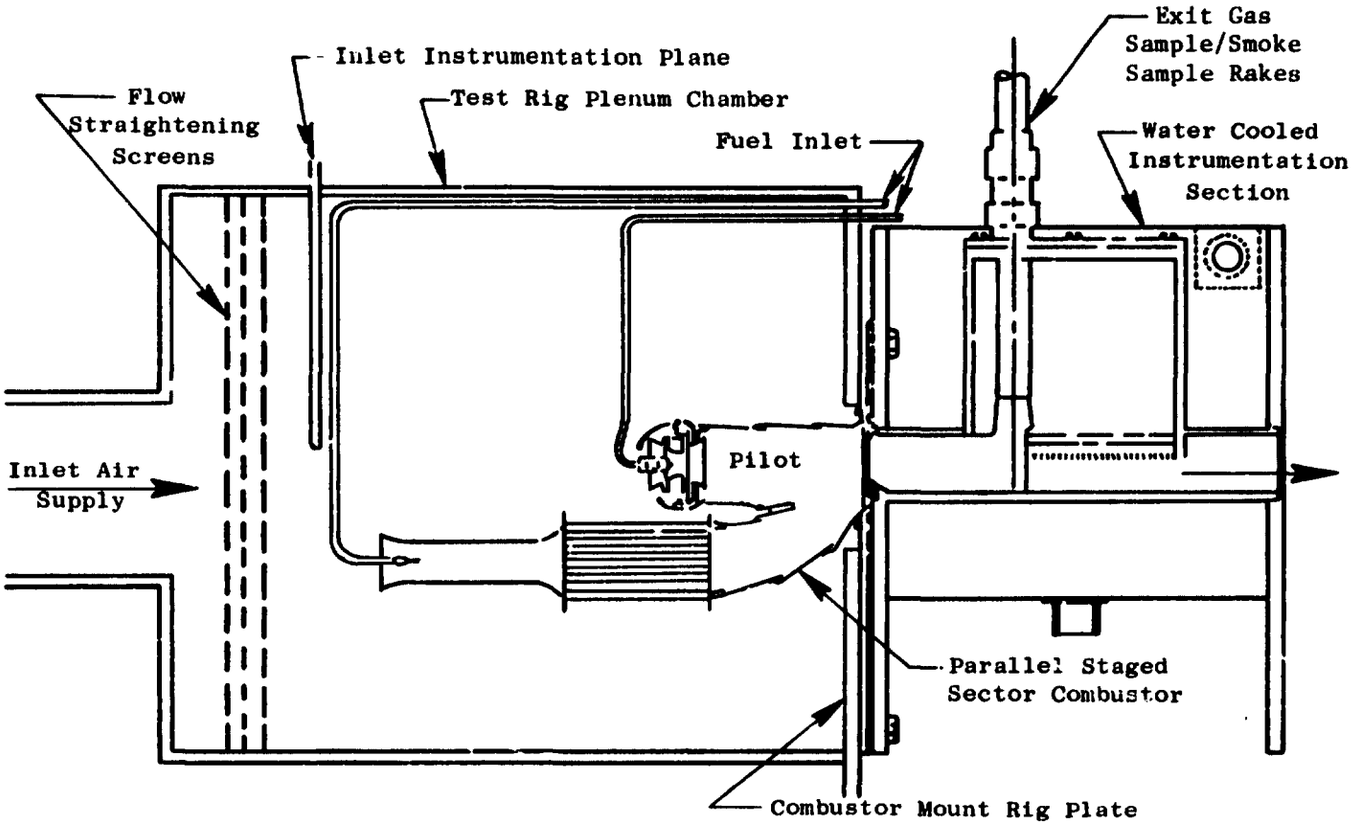

Figure 11. Schematic of the Test Section Used for Performance Evaluation of the 60° Sector Combustor.

Figure 12. Inlet View of the Installed Reverse-Flow Sector Combustor.

5.1.1 Sector-Combustor Instrumentation

Some of the most important measurements made to evaluate the sector-combustor performance during this program were gas samples taken at the combustor exit. These gas samples were used to determine gaseous emissions (NO_x, CO, and HC), smoke, combustor discharge profiles, and combustion efficiency. A photograph of the water-cooled instrumentation section with one gas sampling rake installed is shown in Figure 13. A photograph of a gas sampling rake is shown in Figure 14 and a schematic of a typical sampling element is shown in Figure 15. Each of the sampling elements was designed with a quick-quenching copper probe tip. Quick-quenching was used to suppress any further chemical reaction of the sample within the sampling lines. Both water cooling of the rake body and steam heating of the gas sample lines within the rake were incorporated into the design. Water cooling of the rake body was required to protect the rake from damage due to the high temperature environment at the combustor exit. Steam heating of the gas sampling lines was employed to prevent the condensation of hydrocarbon compounds and water vapor within the sampling lines.

Samples were routed from the test section to the sample-analysis system through stainless steel sample lines. These lines were steam-heated to maintain the sample temperature close to 423 K.

The Contaminants Analyzed and Recorded On-Line (CAROL) system was used to measure gaseous emissions. This system conforms to SAE ARP 1256A (Reference 9) and consists of four basic instruments: a flame-ionization detector (FID) for measuring total HC concentrations, two nondispersive infrared analyzers for measuring CO and CO_2, and a heated, chemiluminescent analyzer for measuring NO and NO_2.

Outputs from the CO, CO_2, HC, and NO_x analyzers of the CAROL system were continuously recorded on strip-chart recorders and manually recorded for later input to an emissions-data-reduction computer program that calculates exhaust-emission concentration indices, combustion efficiency, and sample fuel/air ratio.

Smoke samples were also routed to the control room through the steam heated lines and the smoke levels measured with a test procedure which conforms to SAE ARP 1179A (Reference 10). The smoke measurement console houses

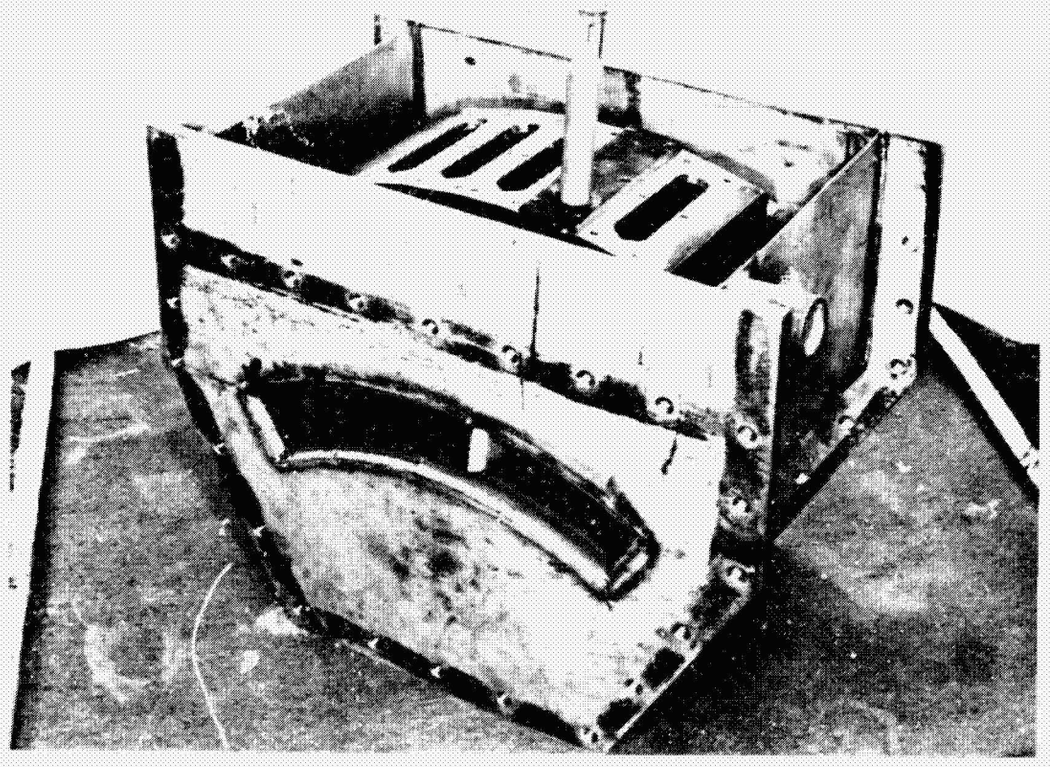

Figure 13. Water-Cooled Exit Instrumentation Section for the Sector Combustors.

Figure 14. Steam-Heated, Water-Cooled Gas Sampling Rake.

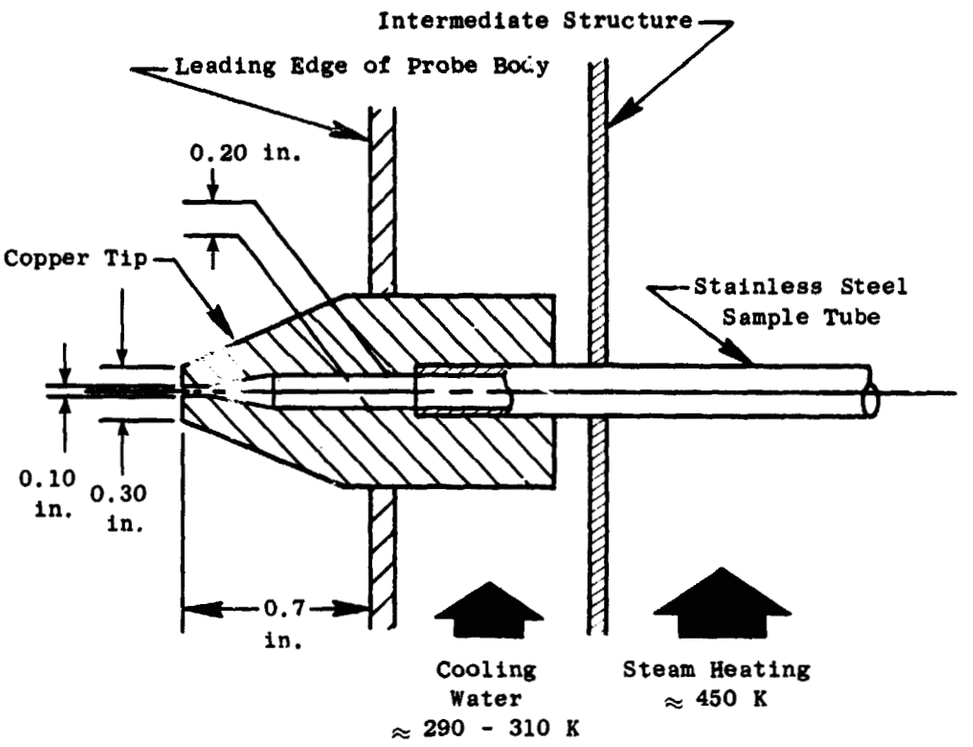

Figure 15. Gas Sample Rake Quick-Quenching Probe Tip Design.

a filtering instrument, water trap, vacuum pump, and flow meter. The filtering unit contains Whatman No. 4 filter paper. It has a fixed filtering area of 3.87 cm^2 and provides a leakproof seal. A water trap is located downstream of the smoke filtering instrument to remove condensed water vapor and condition the gas for flow measurement. A vacuum pump is used to maintain a constant flow rate at low sample pressures. A rotometer is used to monitor the gas sample volume flow rate. An electromechanical timer is used to measure the time required to obtain different sample volumes. The sample volume and time can be used to check gas sample flow rates. The optical density of the smoke spots is read with a Macbeth Model RD 512 densitometer. The smoke number is then calculated according to the procedure listed in ARP 1179A.

Figure 16 shows the location of the gas sample rakes relative to the reverse flow combustor. Two of the rakes were directly in line with pilot swirl cups and two were in line with the catalytic reactors. When the basic parallel stage combustor was tested, the rakes were located in the same positions so that two were in line and two between pilot cups. However, all four of the rake inner elements sampled gases from the catalytic reactors (Reference Figure 5). The five sampling ports on each rake could be read individually or ganged together. For most of the tests, one rake in line with a pilot swirl cup and one rake in line with a catalytic reactor were read individually to determine profile characteristics. The other two rakes were ganged for single samples from each rake. The ganged rake samples generally agreed very well with the average of the individual samples from the rake in an equivalent position relative to the swirl cups or catalytic reactors. No gas samples were taken in line with the end swirl cups to minimize any possible test rig end wall effects.

Both the combustor liner temperatures and the catalytic reactor bed temperatures were also measured. Figure 17 illustrates a typical arrangement for measuring the catalytic reactor exit temperatures for the reverse flow combustor. One sheathed platinum Type B thermocouple (T/C) was mounted at the center of each reactor. For the two end catalysts, six T/C's in addition to the central T/C were used to determine the profile across the reactors. Sheathed

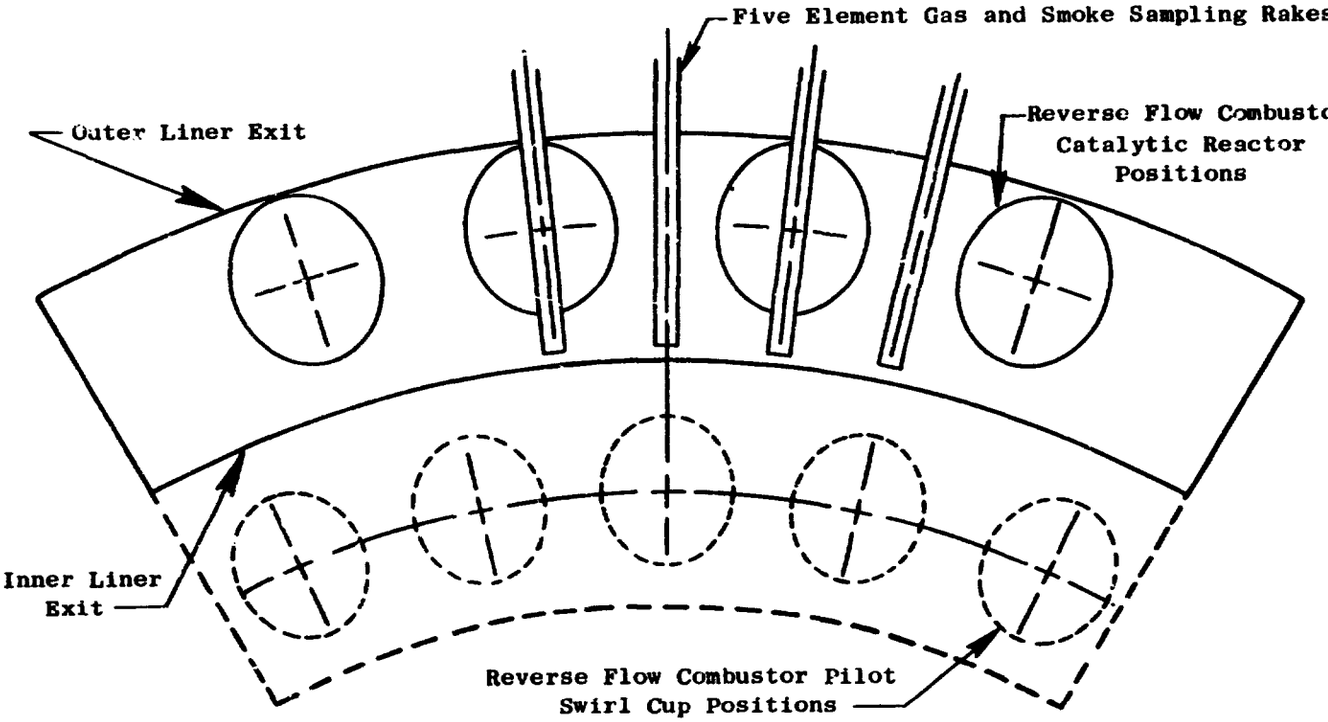

Figure 16. Sector Combustion System Exit Instrumentation Arrangement.

Figure 17. Reverse Flow Combustor Catalytic Reactor Exit Thermocouples.

chromel-alumel T/C's (Type K) were used for the profile measurements. Both types of T/C's were led in from the aft end of the reactors and were held in place with ceramic cement.

Figure 18 shows typical combustor liner metal temperature and combustor wall static pressure drop instrumentation.

5.1.2 Sector Combustor Test Procedures

The sector combustor tests were limited to 0.4 MPa due to test rig structural limitations. This pressure level constraint resulted in true operating conditions for light off and up through engine idle conditions. At high-power conditions, the true engine velocities, temperatures, and fuel/air ratios were used. However, the air flow and fuel flow rates were reduced to scale with the test pressure level. This testing procedure has been successfully utilized in the development of many aircraft gas turbine engine combustion systems. Typical engine conditions used to evaluate the combustor performance were light off, idle, approach, 60% engine power (the condition selected for initial fueling of the catalytic reactor), cruise, climb, and takeoff operation.

Measurements of particular interest at the idle and approach engine power conditions were the combustion efficiency and the CO, HC, and NO_x emissions levels. At the 60% power condition, smoke levels and the combustor discharge radial profile shape while operating on pilot only and combustion efficiency of both stages after switchover to combined operation were the major areas of interest. At cruise, the NO_x emissions level and the radial profile were major parameters to be investigated. At takeoff conditions, NO_x and liner temperatures were the major items of interest. The catalytic reactor operating temperatures and autoignition in the premixing ducts were critical items at all times when the combustor main stages were fueled.

Typical test conditions for the operating points listed above are presented in Table 4. At many of these test conditions, parametric tests were also conducted to determine the effects of reference velocity changes, fuel splits between the pilot and the main stage, fuel/air ratio changes, etc.

Figure 18. Parallel-Staged Combustor Metal Temperature and Wall Static-Pressure Instrumentation.

Table 4. Sector Combustor Test Conditions.

Test Condition	Percent Rated Thrust	Inlet Pressure KPa	Inlet Temperature K	Fuel/Air Ratio	Engine Cycle Pressure MPa
Idle	6	401	485	0.0123	Same
Approach	30	414	636	0.0139	1.21
Reactor Ignition	60	414	717	0.0192	1.97
Cruise	---	414	745	0.0220	1.12
Climb	85	414	781	0.0222	2.63
Takeoff	100	414	814	0.0243	3.02
Ground Start	---	107	300	---	Same

The CAROL gas analysis system was calibrated before each run using the gases indicated in Table 5.

Table 5. Emission Instrument Calibration Gases.

Gas Constituent	Span Gases			
	1	2	3	4
CO_2, %	2.48	3.96	5.85	7.95
CO, ppm	233	447	945	2380
HC*, ppm	268 268	--- 699	--- 1440	--- ---
NO_x**, ppm	29.8 29.8	68 68	--- 287	--- ---

*Calibrated in ppm CH_4 using C_3H_8 span gas.

**Calibrated with NO_x span gas.

Because much of the testing involved operation at or near the catalytic reactor temperature limits, any problems in setting test conditions could lead to hardware damage. Whenever a reactor was overtemperatured, the entire set was replaced in order to assure consistency between the reactors. For the last portion of the testing program, individual fuel control valves were used in the lines to the four catalytic reactors. Using this control system while monitoring the catalytic bed thermocouple readings allowed test points to be set very close to the limiting temperature.

5.2 SUBCOMPONENT TEST RIGS

Extensive subcomponent testing was conducted prior to the full scale sector-combustor tests. The purposes of these subcomponent tests were to:

- Verify that the airflow patterns in the premixing ducts were uniform. Any flow separation could lead to long fuel residence times and auto-ignition during the high temperature combustion tests.

- Conduct screening tests of possible fuel injectors for the premixing sections of the catalytic reactors.
- Conduct fuel mixing and spreading tests of the premixing ducts at pressure levels to be used during the combustion tests.
- Conduct performance tests on catalytic reactors to select a configuration for use during the full-scale sector combustor tests and to generate pressure corrections for catalytic reactor performance to be applied to the 0.41 MPa sector-combustor test data.

Two types of test rigs were used for these tests: ambient pressure and temperature rigs and high pressure rigs.

5.2.1 Ambient Pressure Rigs

The low pressure airflow patterns and fuel injector screening tests were conducted in plastic models of the premixing ducts. Perforated plates were used at the exit of the premixing duct models to simulate the pressure drop of the catalytic reactors and, therefore, give the same airflow patterns as in an actual combustor. In the case of the parallel staged combustor, a flat sector model (two dimensional) was used. Figures 19 and 20 show photographs of this model. Figure 21 shows the premixing duct wall contours.

For the reverse flow combustor with cylindrical catalytic reactors, a full-scale cylindrical model was used for the ambient pressure tests. This model was also constructed of plastic and used a perforated plate to simulate the catalytic reactor flow restriction. A photograph of this model is shown in Figure 22.

Various fuel injectors were evaluated in the two premixing duct types during the ambient pressure screening tests. Typical fuel injector designs for the parallel staged annular ducts are shown in Figure 23 and concentrated on spray rings and spray bars of various types. Fuel injectors considered for the reverse flow coannular ducts are shown in Figure 24. Both spray bars or tubes and pressure atomizing nozzles were evaluated. Fuel nozzles are considered appropriate for use in the cylindrical ducts because the spray patterns (conical) are symmetrical with the ducts.

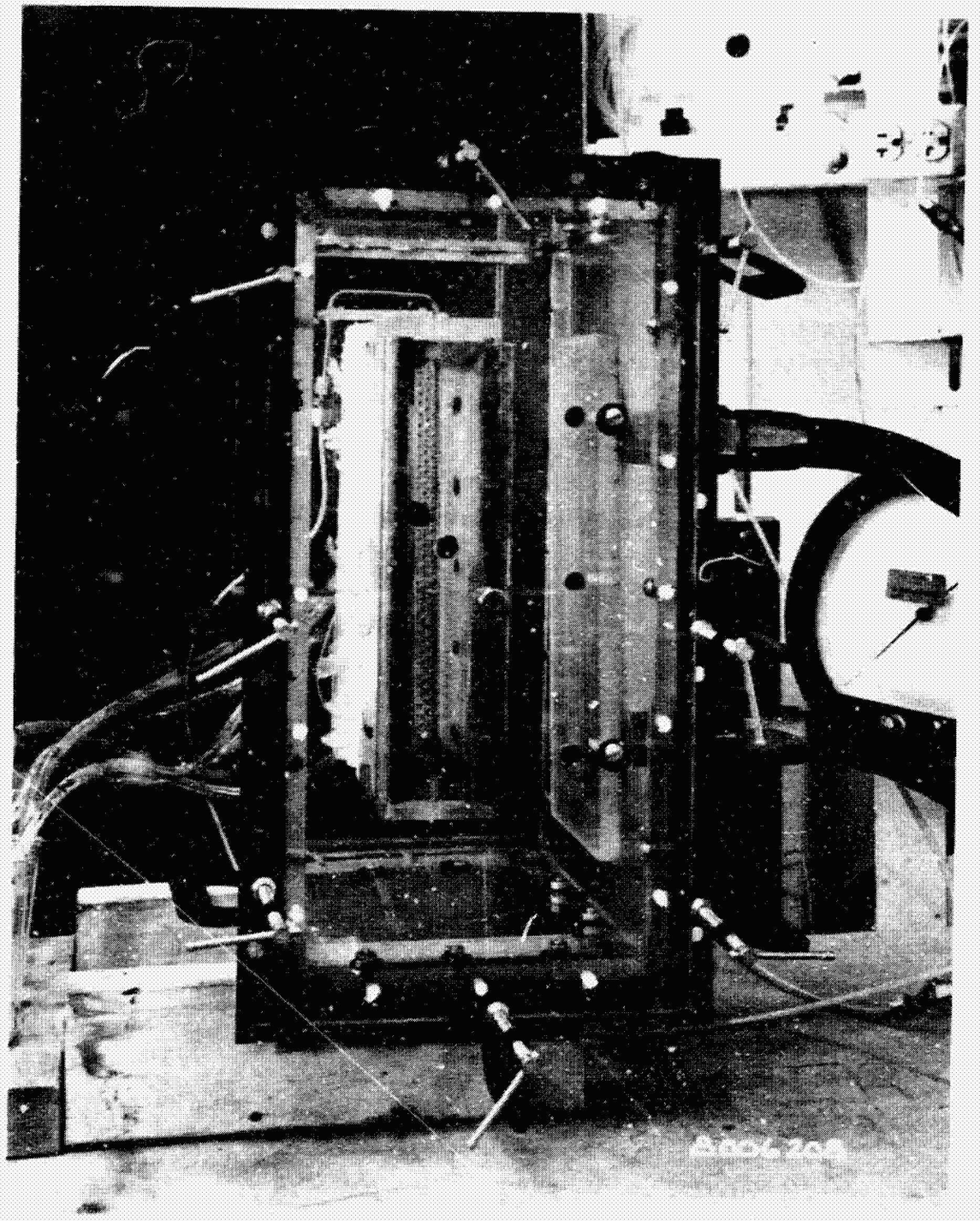

Figure 19. Ambient Pressure Premixing Duct Test Rig for Parallel Staged Combustor (Inlet End).

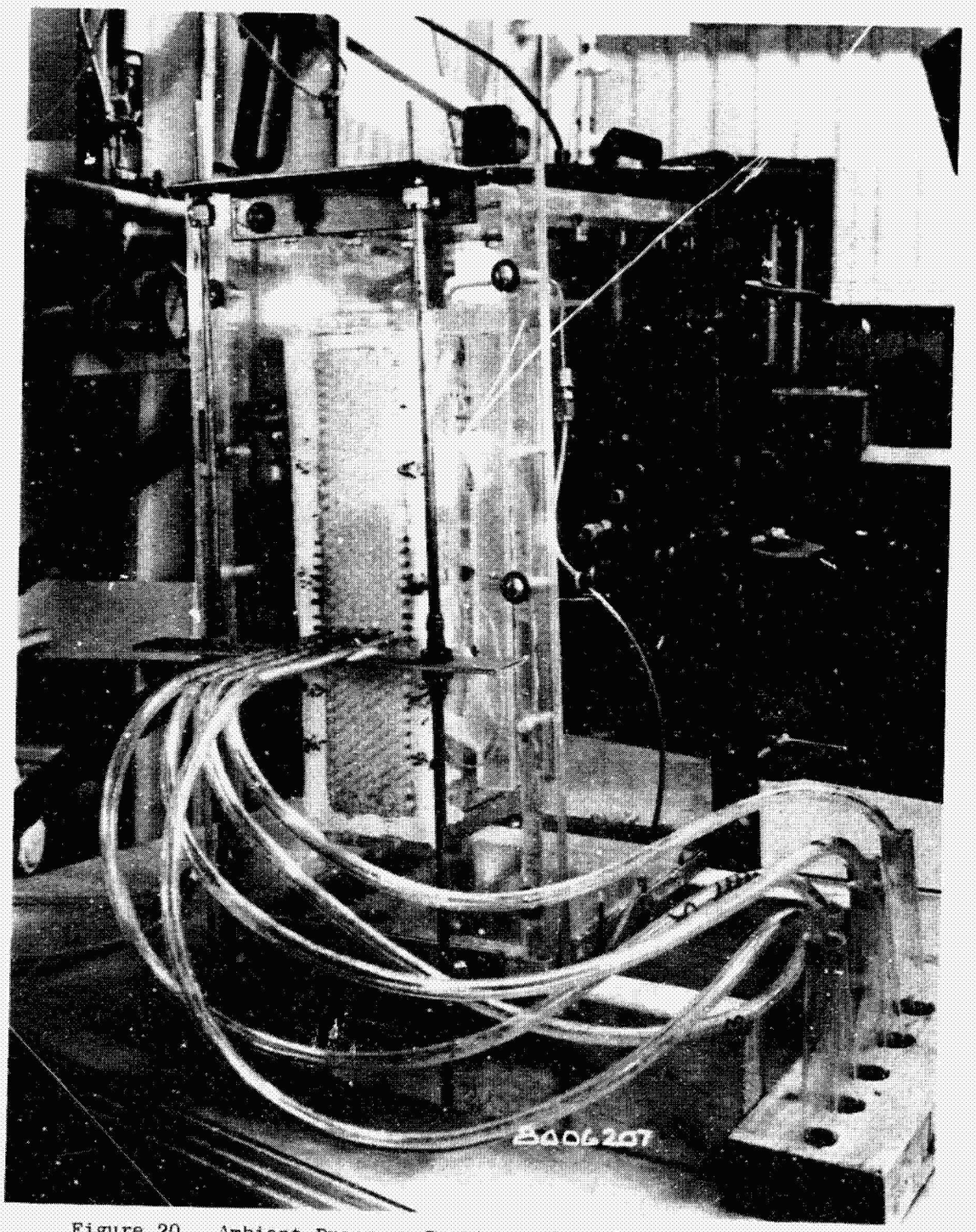

Figure 20. Ambient Pressure Premixing Duct Test Rig for Parallel Staged Combustor (Exit End).

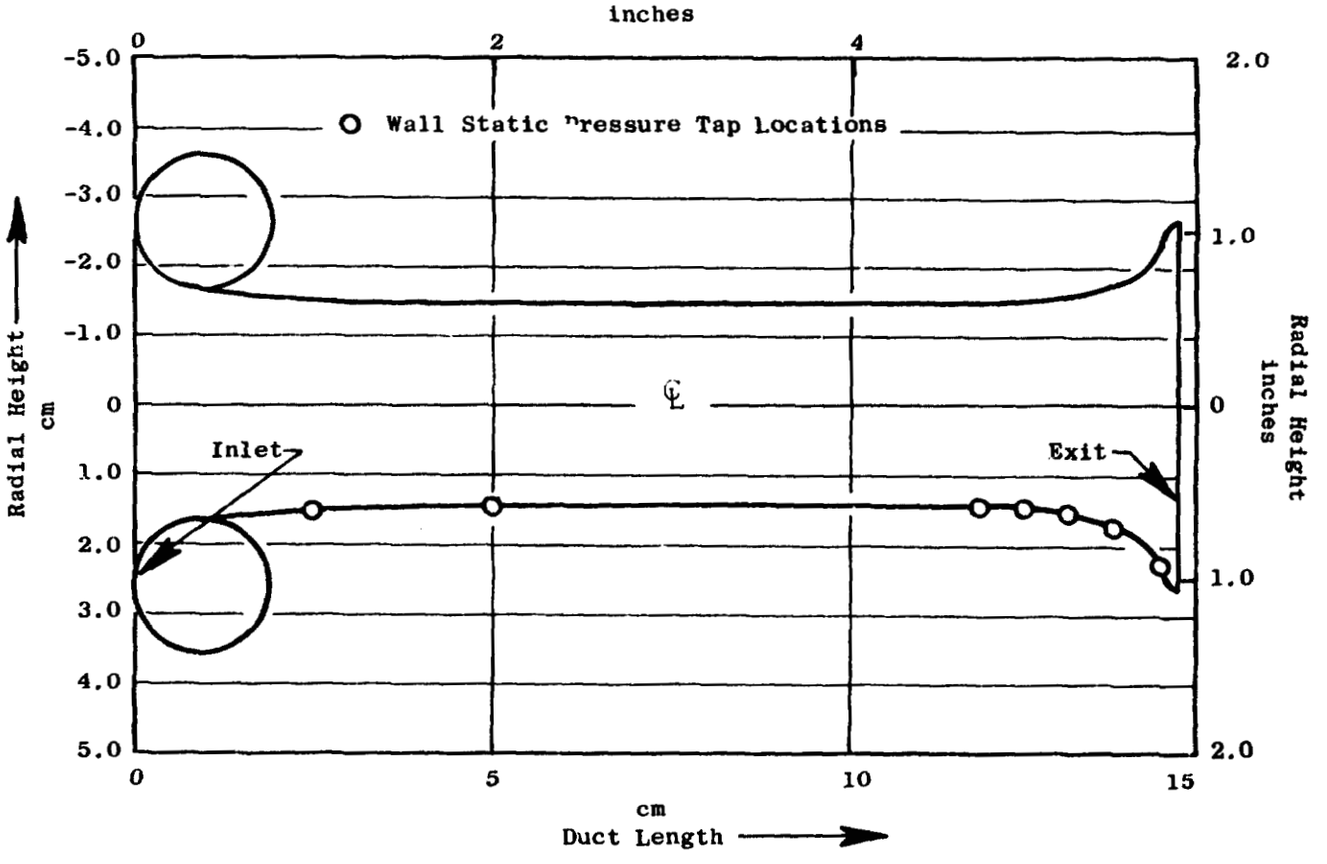

Figure 21. Parallel-Staged Combustor Premixing Duct Wall Contours and Instrumentation

Figure 22. Reverse-Flow Combustor Premixing Duct Ambient Pressure Test Rig.

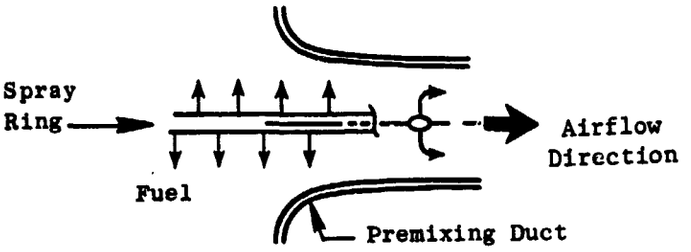

(a) Annular Spray Ring

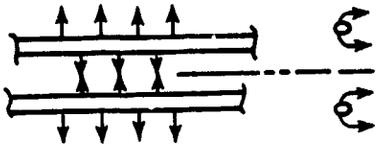

(b) Dual Spray Rings

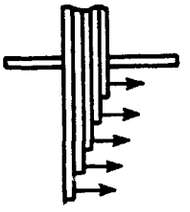

(c) Spray Bars

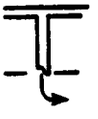

(d) Carburetor Tube

Figure 23. Parallel-Staged Combustor (Annular) Fuel Injector.

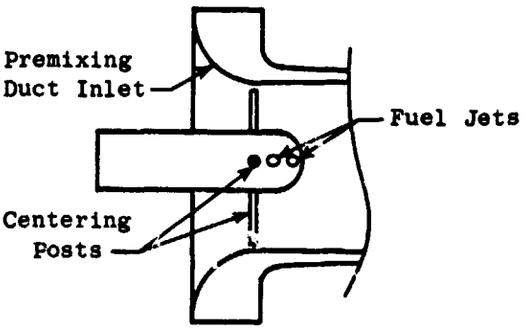

(a) Plain Jet Fuel Tube
(Holes at 45° or 90°)

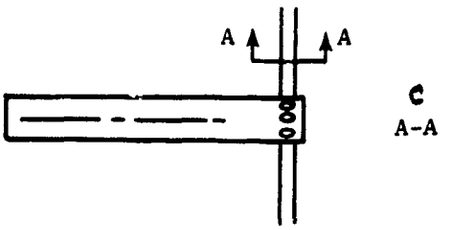

(b) Plain Jet Fuel Tube
With Air Baffles

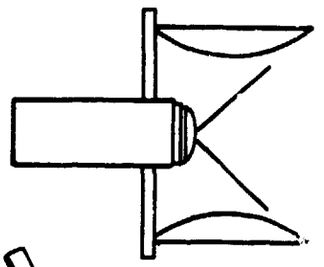

(c) Pressure Atomizing Fuel Nozzle
With Venturi

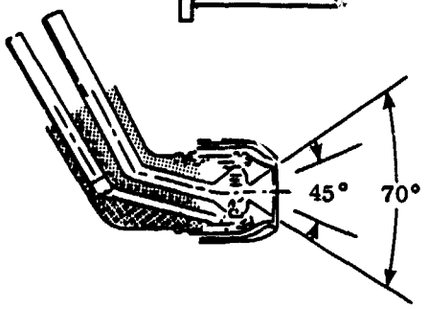

(d) Pressure Atomizing Nozzle
With Dual Spray Angle

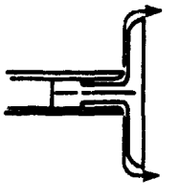

(e) Fuel Tube with Deflector Plate

Figure 24. Reverse Flow Combustor (Cannular) Fuel Injector Designs.

Ambient Pressure Rig Instrumentation

The instrumentation for the ambient pressure duct tests consisted of wall static pressure taps, traversing single-element pressure probes to determine airflow patterns and sampling probes to collect fluid at the discharge of the perforated plates. The wall static pressure tap locations are shown in Figure 21. Total pressure traverse probe positions were at 2.54 cm from the duct inlet, at 2.54 cm from the duct exit and at the exits of the perforated plates. Traversing probes to collect fluid used to simulate fuel were mounted at the duct exit. The fluid collection probes are shown in Figure 20. Graduated cylinders were used to determine the volume of fluid collected from each probe. A similar probe arrangement was used to collect the fluid during tests of the reverse flow combustor premixing duct.

Ambient Pressure Rig Test Procedures

Flow patterns and wall static pressure measurements were conducted with ambient pressure and temperature air. The airflow rates were set to obtain approximately the same pressure loss across the perforated plate as would occur on the catalytic reactors in a combustor (3% to 4%).

During the fuel injector screening tests, water was used to simulate fuel. The objective of these tests was to screen potential fuel injector candidates to achieve uniform fuel (water) distribution at the premixing duct exit. In order to minimize gravitational effects on the water droplets, the test rigs were used in a vertical attitude with the airflow direction from the top to the bottom of the rig.

Test conditions for the ambient tests of the parallel and reverse flow designs are shown in Table 6.

The most important criteria for judging fuel distribution uniformity from the ambient tests with water was the standard deviation, σ, of all of the samples taken. In addition to the overall standard deviation, other statistical data was calculated to further characterize the flow distributions. For the annular duct (parallel-staged combustor) radial and circumferential standard deviations and the kurtosis were also calculated. The radial standard deviation and the kurtosis are based on the averages of the values in each of the

Table 6. Subcomponent Ambient Pressure Test Points.

Cycle Condition	Rated Thrust, %	Combustor Inlet Pressure, kPa	Combustor Inlet Temp, K	Test Rig Airflow, kg/s	Test Rig Liquid/Air Ratio
		Parallel-Staged Concept			
Approach	30	107	289	0.53	0.0070
Approach	30	107	289	0.53	0.0104
Takeoff	100	107	289	0.50	0.0182
Takeoff	100	107	289	0.50	0.022
Cruise	---	107	289	0.50	0.017
Cruise	---	107	289	0.50	0.020
		Reverse-Flow Cannular Concept			
Approach	30	107	289	0.12	0.0070
Approach	30	107	289	0.12	0.0104
Takeoff	100	107	289	0.11	0.0182
Takeoff	100	107	289	0.11	0.022
Cruise	---	107	289	0.11	0.017
Cruise	---	107	289	0.11	0.020

ten circumferential sampling rows used. The kurtosis is a measure of the flatness of peakedness of a distribution curve. A flat distribution has a kurtosis of 1.7, concave curves have a kurtosis less than 1.7, convex curves have a kurtosis greater than 1.7, with the kurtosis of a normal distribution being around 3. The kurtosis of distribution is given by the fourth moment divided by the square of the second moment, or,

$$\text{kurtosis} = \frac{\frac{1}{n}\sum_{i=1}^{n}(Xi - \bar{X})^4}{\left[\frac{1}{n}\sum_{i=1}^{n}(Xi - \bar{X})^2\right]^2}$$

where:

Xi is an individual sample volume

$\bar{X}$ is the average of the grouping in question

and

n is the sample size.

The circumferential distribution data, and the kurtosis, are based on the averages of the values at each of the 18 radial stations.

5.2.2 High Pressure Test Rigs

To verify the performance of the fuel distribution system and duct mixing developed in the ambient tests, tests at sector combustion inlet test conditions were conducted in the sector combustor test rig (Figure 11) for the parallel-staged design. However, for these fuel distribution tests, only the premixing duct and the catalytic reactor were used. The assembly of the duct and the reactor were mounted directly in line with the gas sample rakes of the test rig as shown in Figure 25. In the case of the reverse flow design, a separate test rig was utilized. The cannular catalyst configuration was tested in a high pressure test rig capable of 1.6 MPa and 815 K. The test rig and instrumentation are shown in Figure 26. This test rig consisted of sections of 15 cm diameter, schedule 40 stainless steel pipe with appropriate flanges, instrumentation ports, and a fuel injector mounting boss. The

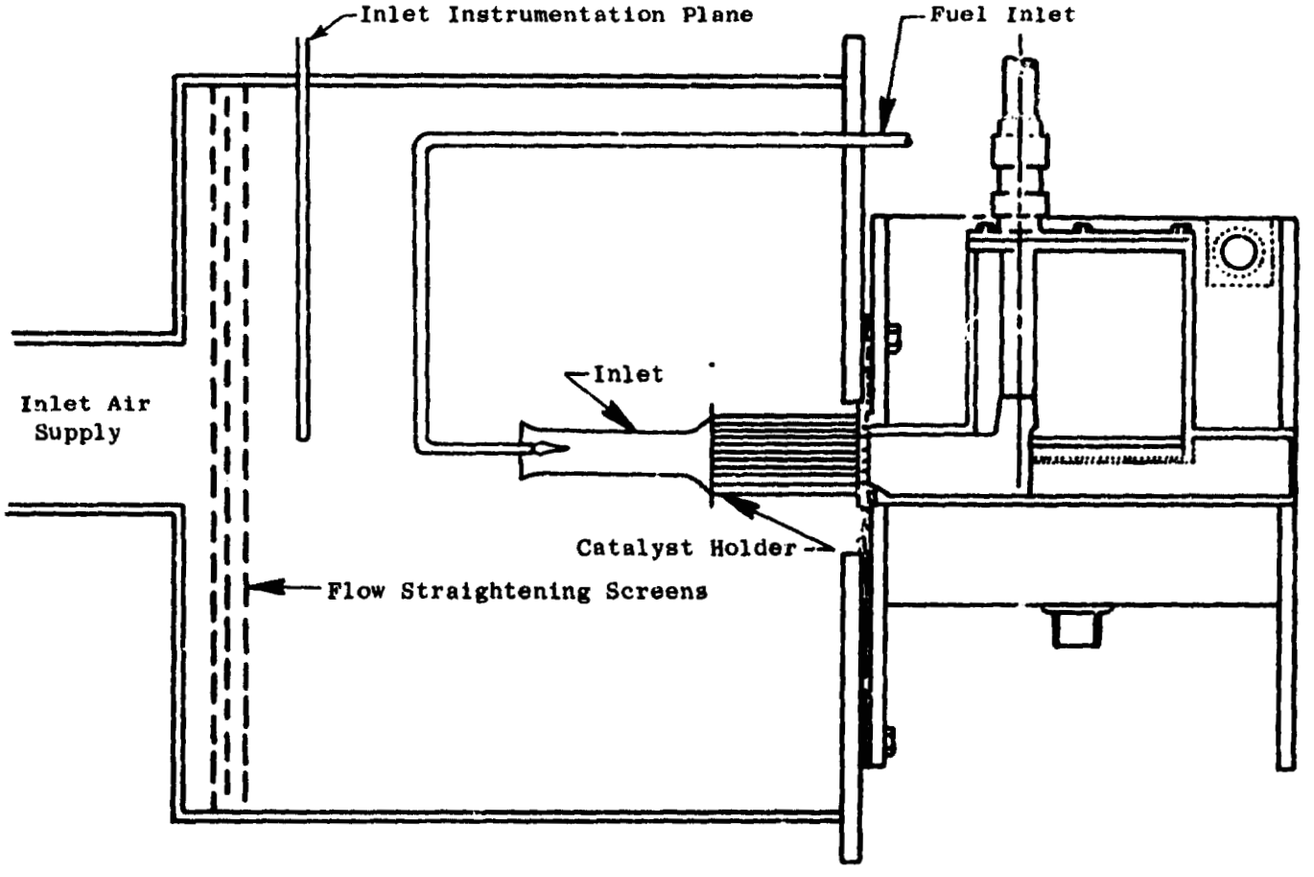

Figure 25. Test Rig for Fuel Distribution Tests of Parallel-Staged Combustor Premixing Duct.

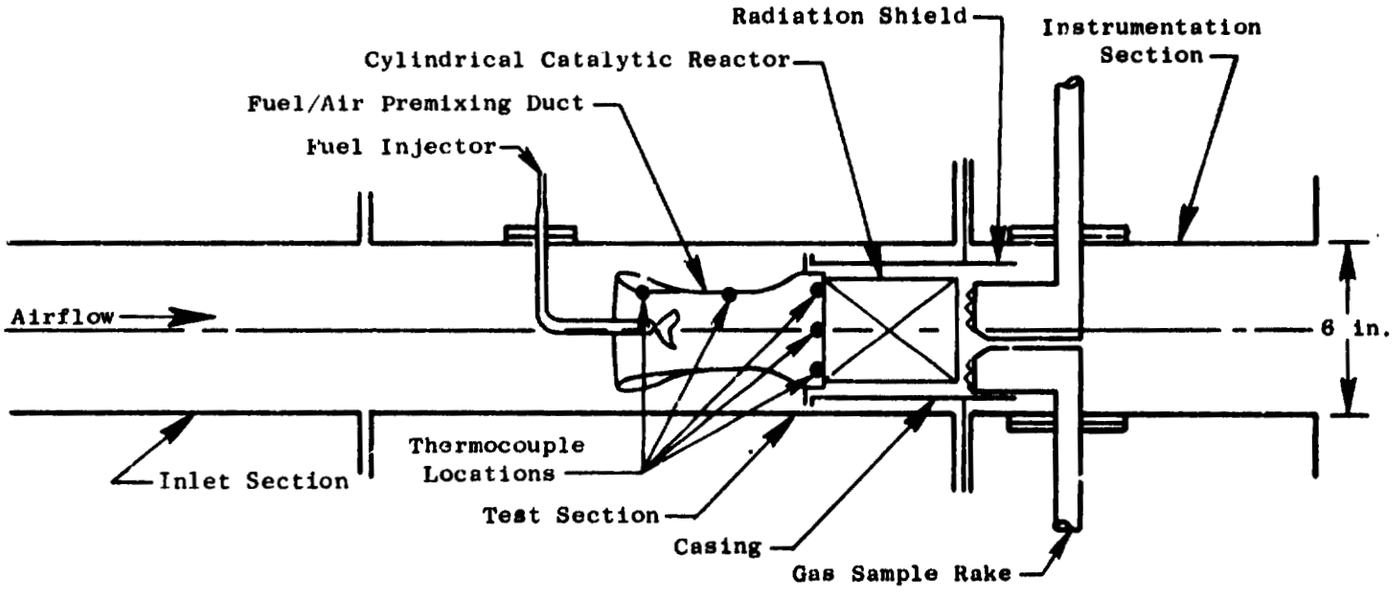

Figure 26. High Pressure Subcomponent Test Rig Assembly for Fuel Distribution and Catalytic Reactor Performance Tests.

catalytic reactor and premixing duct assembly were mounted in one of the test rig flanges. This 15 cm pipe rig was used for both fuel distribution tests for the reverse flow combustor and for performance tests of the catalytic reactors.

During the performance testing of the catalytic reactors (after the test of the second configuration), a shield was added to the test rig just aft of the catalytic reactor to reduce possible radiant heat loss from the catalytic reactor to the test rig wall. This shield was added in two increments of approximately 8 and 5 cm (total 13 cm). Also, both the test section and the instrumentation were insulated to reduce heat losses.

The candidate catalytic reactor configurations are listed in Table 7. All of the configurations used a precious metal catalyst applied on an alumina washcoat. The different configurations represent different substrate materials and different cell geometries in order to determine the effect of these parameters on performance. All of the configurations had two elements separated by a spacer except for Configuration 3. Configurations 1 and 3 used the same cell density. Configuration 2 used an increased cell density relative to 1 and 3. Configuration 4 used an increased cell density in the forward element and the same density as Configurations 1 and 3 in the aft element. The pressure drop for these catalytic reactors ranged from 3% to 4% of the inlet pressure with the single-cell, single-element Configuration 3 having the lowest pressure drop.

Two of the configurations utilized Torvex α-alumina substrates which have a recommended maximum continuous operating temperature level of 1770 K. Configuration 2 used a zircon composite substrate, which has a continuous operating temperature limit of 1700 K and a melting point on the order of 1920 K. Adequate supplies of this material were available for this program, however, this product is no longer commercially available. The forward section of the fourth configuration had a lower maximum continuous use temperature of 1623 K. However, substrate temperatures achieved in the forward sections of the catalytic reactors are expected to be lower than for the aft sections.

A photograph of one of the catalytic reactors installed in a housing is shown in Figure 27. The catalytic reactor housing used in the high pressure

Table 7. Catalytic Reactor* Configurations For High-Pressure, Single-Can Tests.

Configuration	Length, cm	Channel Density Channels/in^2	Substrate Material	Predicted Pressure Loss, Percent
1. Single-Cell Multielement				3.6
Inlet Segment	7.6	60	Torvex-α-alumina	
Space	1.3	-	-	
Downstream Segment	3.8	60	Torvex-α-alumina	
2. Single-Cell, Multielement				4.0
Inlet	5.1	96	Zircon Composite	
Space	0.6	-	-	
Downstream	7.0	96	Zircon Composite	
3. Single-Cell, Single-Element	12.7	60	Torvex-α-alumina	3.0
4. Multicell, Multielement				4.0
Inlet	6.4	120	Torvex-mullite	
Space	0.6	-	-	
Downstream	5.7	60	Torvex-α-alumina	

*All utilize Engelhard Proprietary Catalysts

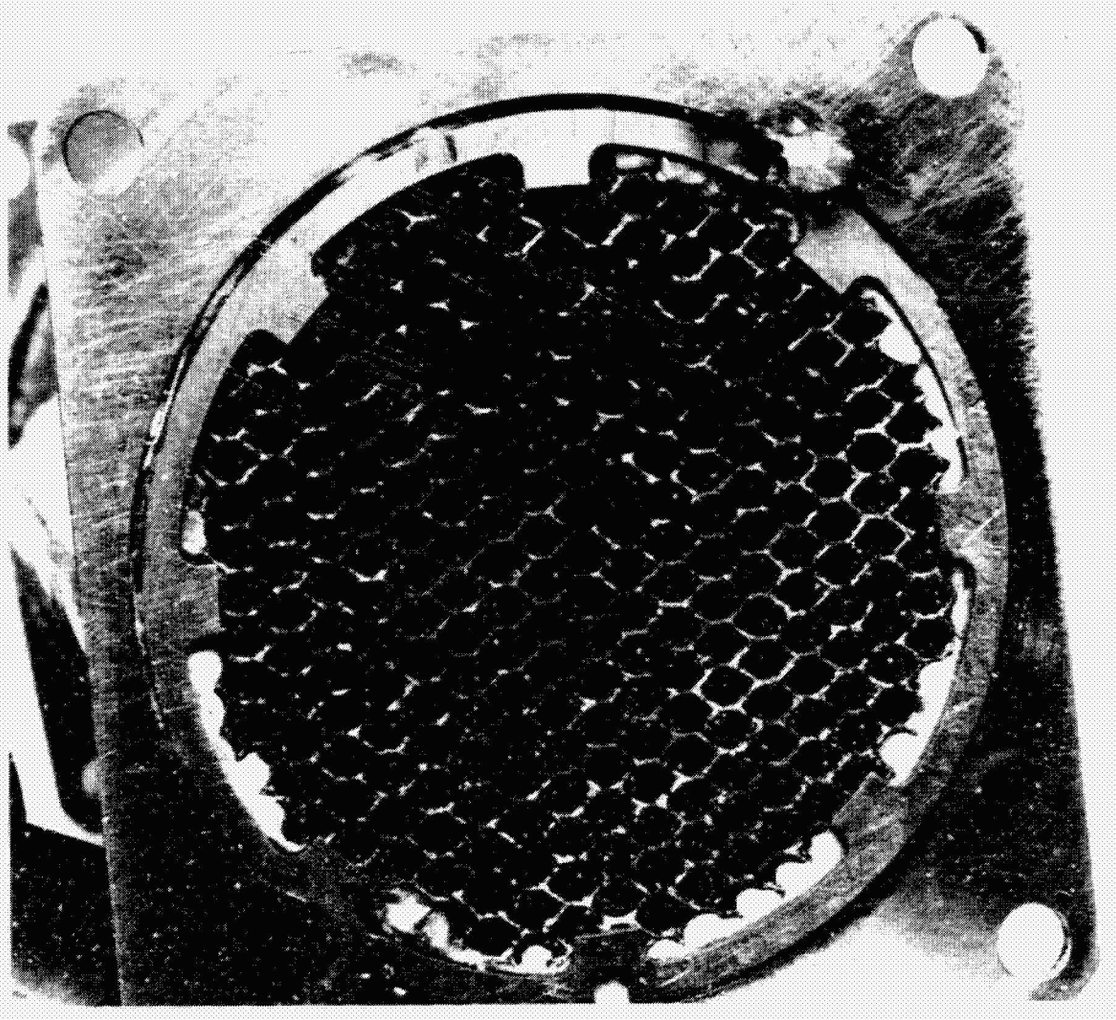

Figure 27. Front Face of Catalytic Reactor for Single-Can Catalytic Reactor Performance Tests.

catalytic reactor tests is identical to the housing used in the Reverse-Flow sector combustor (Figures 8 and 10).

High Pressure Rig Instrumentation

During some of the testing (fuel/air distribution tests), fuel/air ratio profiles were measured for a nonburning condition. During these tests, an uncooled gas sampling rake was used.

The system utilized for these measurements is shown in Figure 28. The samples were burned in a catalytic oxidizing cell and the fuel/air ratio then determined from the CO_2 concentration in the products. With the system used, dilution airflow could be added in the case of samples with very high fuel/air ratios. In these instances, the dilution air is carefully metered to accurately adjust the measured fuel/air ratio value to the actual value.

During the combustion tests with catalytic reactors in the high pressure 15 cm diameter rig, water cooled gas sample rakes were used and the same gas analysis equipment used for the sector combustor tests (Paragraph 5.1) was used to determine the performance. For the first catalytic reactor test, gas samples were extracted close to the catalytic reactor exit. For the remainder of the tests, the gas sample rake was moved aft to provide the same gas residence time aft of the reactor as was available between the catalytic reactor and the combustor exit in the engine configuration.

Catalytic reactor bed temperatures were measured during some of the tests. Figure 29 shows the thermocouple locations for the first catalytic reactor test which was typical. Thermocouples were located at the inlet and exit of the forward element, at the exit of the downstream element, and in the space between the two elements. Platinum thermocouples were used for the catalytic reactor bed temperature measurements.

The premixing ducts were instrumented to detect any signs of autoignition of the fuel/air mixture during the high pressure tests. Chromel-alumel thermocouples attached to the duct walls were used for this purpose and the locations are indicated in Figure 26.

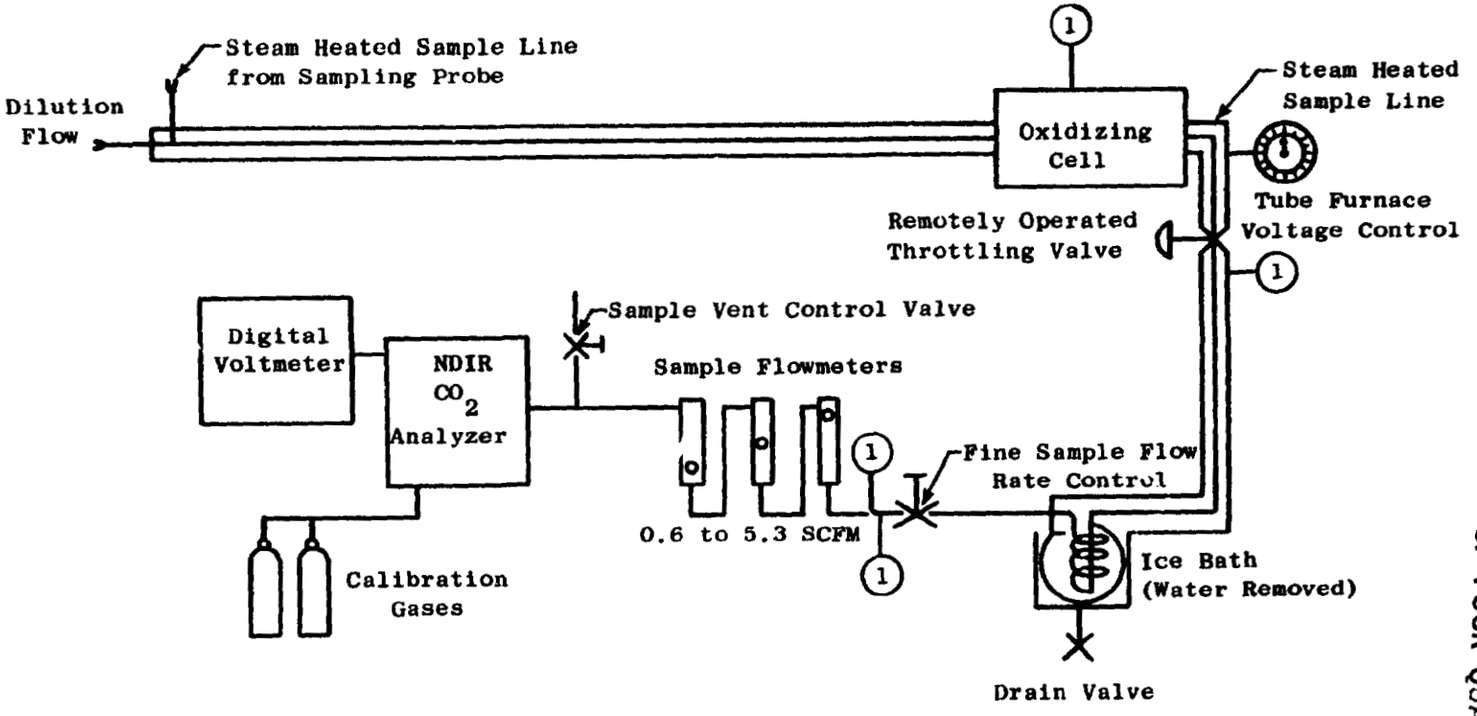

Figure 28. Fuel/Air Ratio Analysis System Diagram.

Figure 29. Typical Catalytic Reactor Thermocouple Locations.

High Pressure Rig Test Procedures

The initial tests conducted in the high pressure rigs (Figures 11 and 26) were fuel distribution measurements for various candidate fuel injectors and premixing duct configurations. These tests were conducted without combustion and an uncatalyzed substrate was used in the catalytic reactor housing to provide the proper system pressure loss. The fuel distribution at the catalytic reactor exit plane was determined by gas analysis. The fuel distribution tests for the parallel staged combustor were limited to 0.4 MPa pressure because of the sector test rig structural limitations. The tests for the reverse flow combustor were conducted in the 15 cm diameter pipe rig and were conducted at pressures up to 11 MPa. In both rigs, tests were conducted with inlet temperatures up to 810 K (combustor inlet temperature at takeoff conditions).

The subcomponent performance tests of the catalytic reactor configurations were all conducted in the 15 cm diameter pipe rig with the primary measurements being premixing duct wall temperatures (to detect autoignition), catalytic reactor bed temperatures, and gas samples at the reactor exit.

The major test operating conditions were approach, cruise, and takeoff conditions. Approach power conditions with low inlet temperatures were the most severe from the standpoint of achieving performance, while takeoff conditions presented the most severe conditions relative to operating temperatures because of the high inlet temperature and cycle fuel/air ratio.

The test conditions for these investigations are presented in Table 8. Most of the catalytic reactor performance evaluations were made at 0.41 MPa pressure since that would be the sector combustor condition. However, tests were also conducted up to 1.1 MPa to generate pressure corrections. Fuel flows were varied over a range for each configuration to determine the efficiency characteristics versus fuel/air ratio. Each configuration was run up to a fuel flow where the bed temperature limit was reached. During the testing, airflow rates were also varied (generally to lower values) to determine velocity effects. These parametric variations in test condition were selected during the tests depending on the catalytic reactor performance levels.

Table 8. Subcomponent High Pressure Rig (15 cm diameter) Test Point Schedule for Evaluation of Catalytic Reactors.

Cycle Condition	Pressure, MPa	Temperature, K	Airflow, kg/s	Fuel/Air Ratio
Approach	0.41	635	0.19	0.005 to Reactor Temperature Limit
	1.1	635	0.51	
60% Power	0.41	717	0.18	
	1.1	717	0.48	
Cruise	0.41	745	0.16	
	1.1	745	0.44	
SLTO	0.41	814	0.15	
	1.1	814	0.40	

6.0 RESULTS AND DISCUSSION

The initial task in this program involved the testing and development of fuel injection systems for uniform fuel distribution to the catalytic reactor. The second major effort was the evaluation of several candidate catalytic reactor systems to select the configuration for use in the combustion system tests which constituted the final program activity.

6.1 FUEL INJECTION SYSTEM TEST RESULTS

The need to achieve very uniform fuel distribution for the main stage (catalytic reactors) of the combustion system presented a major challenge during this program, and an extensive series of subcomponent tests of fuel injector systems was conducted. The catalytic reactor substrates utilized during the sector combustor tests have continuous operating temperature capabilities of approximately 1700 K, although somewhat higher temperatures are acceptable for short periods of time. Thus for a 1700 K reactor temperature limit, any maldistribution of fuel results in reduced total fuel flow (average temperature) within the reactor. A very challenging goal for the local fuel/air ratio (no more than 10% above the average fuel/air ratio) was established for this program based on the allowable continuous operating temperature of the catalytic reactors and the cycle takeoff average fuel/air ratio required.

Catalytic Reactor Continuous Operating Temperature Limit	1700 K
Air Inlet Temperature (Takeoff Conditions)	814
Allowable Peak Temperature Rise	886
Allowable Peak Fuel/Air Ratio (f) (From Temperature Rise and Inlet Temperature for Jet-A Fuel)	0.0267

$$f\ \text{uniformity} = \frac{f\ \text{peak}}{f\ \text{cycle at takeoff}} = \frac{0.0267}{0.0243} = 1.1$$

In addition, the length of the premixing ducts to achieve the uniformity indicated above were limited to approximately 13 cm because of the potential for autoignition of the fuel and air mixture at some operating conditions (Paragraph 4.2).

Preliminary screening tests of the fuel injector systems were conducted in the ambient pressure and temperature test rigs with water injection representing the fuel injection.

Prior to conducting the ambient distribution tests, an investigation of the velocity profiles at the exit of the simulated fuel/air premixing ducts was carried out to assure uniform airflow profiles. Any flow separation would result in long fuel/air resident times locally and could lead to autoignition. As shown in Figures 30 and 31, both the parallel duct and reverse flow ducts exhibit very uniform velocity at the duct exit. Although the center duct velocities were somewhat above the overall average, the velocities at the outermost measurement areas were between 80% and 90% of the average velocity.

Results of the water distribution tests for 10 parallel duct fuel injector configurations and 7 reverse flow duct fuel injector configurations are presented in Tables 9 and 10, respectively. Each of the evaluation parameters, σ, σ_R, σ_C and the kurtosis were given a rating on an arbitrary scale from one to five where the lowest number represented the best performance. The product of the individual ratings was used for the overall rating.

At this point in the fuel injector development, the most promising fuel injector configurations appeared to be the annular spray ring for the parallel-staged duct, Figure 23(a), and the pressure atomizing fuel injector for the reverse flow duct, Figure 24(c). However, the fluid profiles were generally center-peaked and little of the fluid (H_2O) followed the duct contours at the duct exit flare. It was likely that, at the high temperatures associated with the actual engine cycle, the fuel would evaporate and the vapor would follow the airstream which was known to follow the duct contour. Nevertheless, a conical premixing duct which would avoid the flow turning at the exit was designed for the reverse flow combustor. In order to maintain the residence

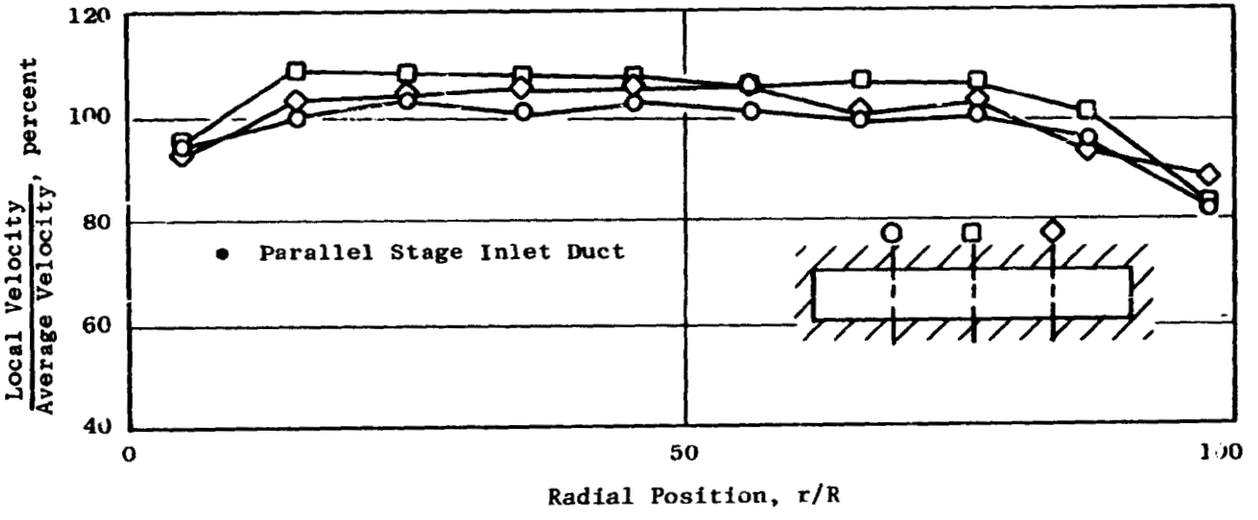

Figure 30. Exit Velocity Profile Downstream of Simulated Catalyst Face for Parallel-Staged Combustor Premixing Duct.

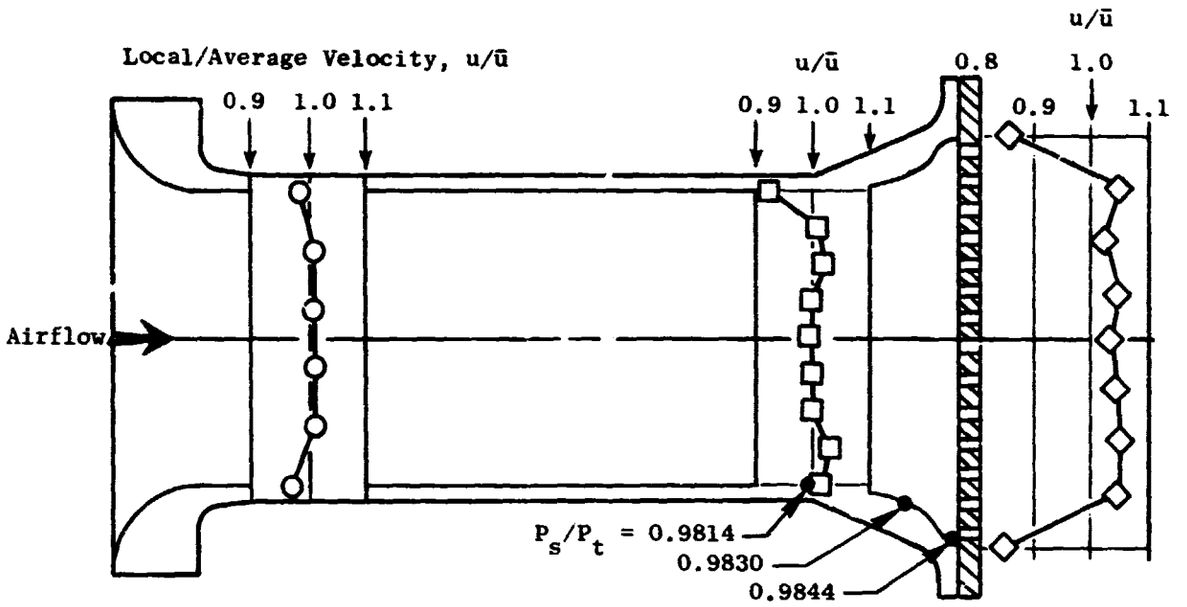

Figure 31. Reverse Flow Inlet Duct Airflow Test, Local Velocities, and Pressures.

Table 9. Parallel Flow Configuration - H_2O Distribution Test Summary.

Test	Configuration (Hole diam. and fluid ΔP)	Overall		Radial		Circumferential	
		Rating	σ	σ_R	Kurtosis	σ_c	Kurtosis
1	Carb. Tubes > 1 psiΔ	540	1.03 (3)	0.796 (3)	3.16 (5)	0.469 (3)	2.25 (4)
2	1 Spray Ring 0.5 mm Diameter, 35 KPa ΔP	128	1.25 (4)	0.893 (4)	2.72 (4)	0.414 (2)	1.76 (1)
3	1 Spray Ring 0.3 mm Diameter 35 KPa ΔP	60	1.01 (3)	0.853 (4)	3.00 (5)	0.238 (1)	1.75 (1)
4	1 Spray Ring 0.3 mm Diameter 172 KPa ΔP	24	0.841 (2)	0.762 (3)	2.77 (4)	0.199 (1)	1.69 (1)
5	1 Spray Ring 0.3 mm Diameter 414 KPa ΔP	8	0.877 (2)	0.500 (1)	1.77 (1)	0.375 (2)	1.87 (2)
6	2 Spray Rings 0.3 mm Diameter 172 KPa ΔP	48	0.784 (1)	0.700 (3)	2.60 (4)	0.333 (3)	1.91 (2)
7	2 Spray Rings 0.3 mm Diameter 172 KPa ΔP	240	1.494 (5)	0.730 (3)	1.53 (2)	0.620 (4)	1.61 (2)
8	2 Spray Rings 0.3 mm Diameter 172 KPa ΔP	72	1.205 (4)	0.498 (1)	1.51 (2)	0.522 (3)	2.07 (3)
9	2 Spray Rings 0.3 mm Diameter 172 KPa ΔP	12	0.686 (1)	0.600 (2)	2.27 (3)	0.250 (1)	1.90 (2)
10	5 Spray Bars 1.5 psiΔ	576	1.155 (4)	0.736 (2)	2.54 (4)	0.473 (3)	2.25 (4)

Notes:
1. Rating - Lowest number shows best performance.
2. Numbers in parentheses indicate ranking on a scale of 1 to 5 with the lowest number representing best performance.
3. Similar configurations (such as Tests 6, 7, 8, and 9) were run with different hole patterns in the spray ring(s).

Table 10. Reverse Flow Configuration - H_2O Distribution Test Summary.

Standard Duct

Test	Configuration	Overal Rating	σ	Kurtosis
1	Plain Jet Fuel Tube-Holes at 90° 0.5 mm diameter holes, 55 KPa ΔP	2	0.79 (2)	2.1 (1)
2	Plain Jet Tube with Baffle 0.5 mm diameter holes, 55 KPa ΔP	6	0.84 (3)	1.5 (2)
3	Venturi Nozzle 517 KPa ΔP	1	0.73 (1)	2.0 (1)
4	Plain Jet Tube - Holes at 45° 0.5 mm diameter holes, 55 KPa ΔP	8	1.02 (4)	2.5 (2)
5	Dual Spray Angle Nozzle 577 KPa ΔP	8	0.99 (4)	2.4 (2)
6	Single Spray Angle Nozzle (90°) Simplex Nozzle 73 psiΔ	15	1.17 (5)	3.1 (3)
7	Fuel Tube With Deflector Plate 41 KPa ΔP	10	1.16 (5)	2.4 (2)

Note: Rating value in parenthesis indicates ranking for parameter indicated on a scale of 1 to 5 with lowest number representing best performance. The overall rating is the product of the other two ratings.

time within the duct (2 ms at the design point), the length of the conical duct was only 7 versus 13 cm for the original duct configuration. It was felt that to achieve adequate fuel spreading in the very short length conical duct, some means of augmenting radial fuel spreading would be required. Therefore, vortex generators were used at the duct entrance. The pressure drop associated with the vortex generator drag was approximately 0.5% of the inlet pressure. The fuel nozzle tip was located axially in the duct entrance so that none of the fuel entered the separated flow regions at the vanes but did enter into the vortices downstream of the vanes. A series of tests was conducted to evaluate the conical duct with vortex generators and pressure atomizing nozzles for the reverse flow combustor. Considerable improvement relative to the standard duct was achieved. The standard deviation of the fluid samples at the duct exit was 0.34 versus 0.73 (Table 10) for the earlier tests. Figure 32 shows the resulting conical duct configuration which used three pairs of vortex generator blades at the duct entrance.

At this point in the program, the sector combustor rig and the high pressure pipe rig were available and premixing duct fuel distribution tests were continued with actual fuel at elevated pressures and temperatures.

The initial high pressure tests were carried out with both the original cylindrical duct design and the new conical duct configuration for the reverse flow combustor. Both ducts were equipped with the vortex generator blades and pressure atomizing nozzles.

The standard duct, when equipped with a simplex fuel nozzle and vortex generators, did not provide adequate spreading and mixing of the fuel as indicated by center-peaked profiles. Fuel nozzle flow characteristics, such as spray angle and nozzle pressure drop, had very little effect on the profile shape.

The conical inlet test results were also disappointing: when the inlet was equipped with a simplex fuel nozzle, center-peaked profiles were obtained.

Based on these initial results, the following conclusions were drawn relative to the current inlet duct premixing designs:

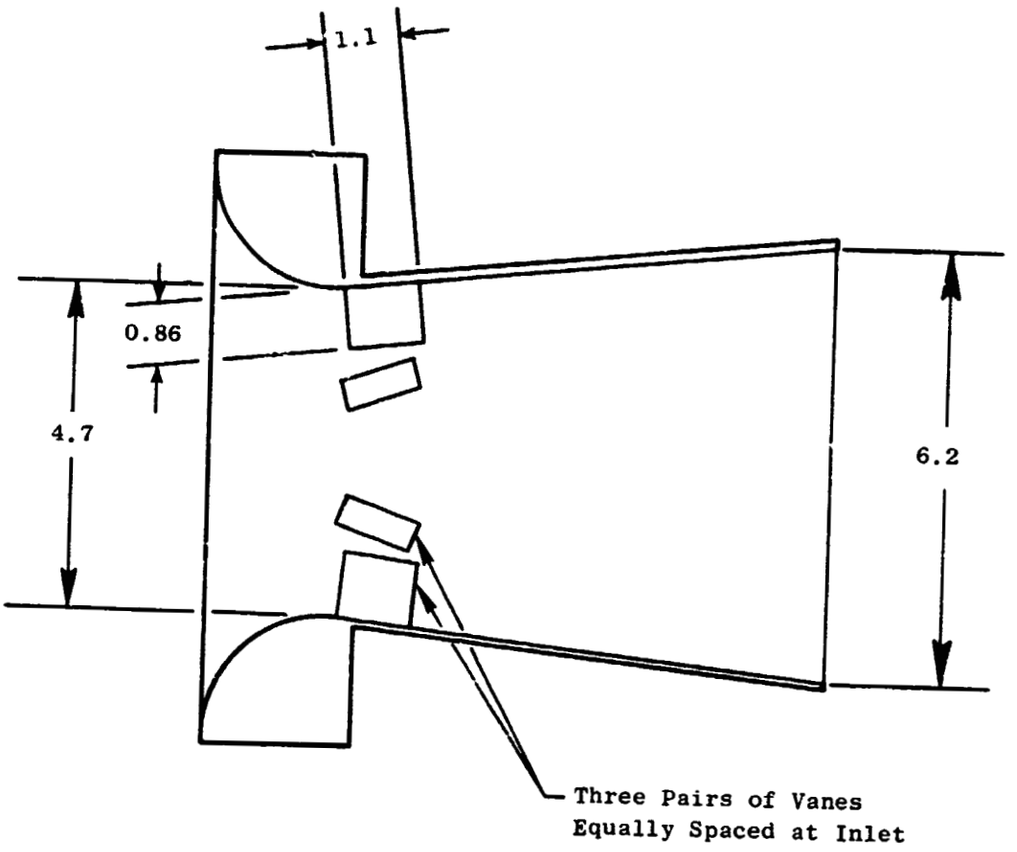

Figure 32. Conical Premixing Duct with Vortex Generators to Promote Fuel Spreading and Mixing.

The increased air density relative to the ambient tests suppresses the radial spreading of the fuel drops. The axial momentum of the air is at least 10 times greater than the radial momentum of the fuel drop. This lack of fuel droplet penetration at pressure was also indicated in premixing duct tests conducted at NASA (Reference 11).

In order to permit more fuel spreading, the standard duct was modified with an extension added to the inlet. The purpose of the larger-diameter inlet was to permit the fuel droplets to penetrate further across the duct in the lower velocity air in the forward section. However, the inlet extension increased the duct residence time from 2.0 to 6.6 ms. The vortex generators were removed from the throat of the duct to eliminate a possible flame-holding source with upstream fuel injection. The results of these tests are shown in Figure 33. Although the profiles were improved from the original standard duct, the peak fuel/air ratios were still above the desired level.

Based on the test results obtained in the one-atmosphere tests and the high-pressure subcomponent tests, it was concluded that the very challenging goal of obtaining a uniform fuel/air profile with a peak value within 10% of the average with only 2 ms residence time would require extensive additional development. Therefore, a longer conical duct with 11 ms residence time was constructed to determine if additional added mixing length would provide the desired profiles. The 11 ms time was selected based on autoignition and flashback criteria (Reference 12) for operation in the subcomponent and sector combustor tests. With this residence time, autoignition would not be expected below a pressure of 1.2 MPa as shown in Figure 34. Both the sector combustor tests and the high pressure pipe tests were to be conducted at pressures below this level. However, it is recognized that in an engine application where the pressure is much higher, the residence times would have to be reduced to avoid flashback and autoignition. As expected, much improved fuel/air profiles were obtained, approaching the target level. The results for the test with the long (41 cm) conical duct are shown in Figure 35. At the takeoff condition, the fuel distribution met the objective level. At approach conditions, the profile exceeded the goal somewhat, but with the lower inlet temperature and cycle fuel/air ratio this profile was fully adequate. The long conical duct was selected as the inlet design for the initial reverse flow sector combustor testing.

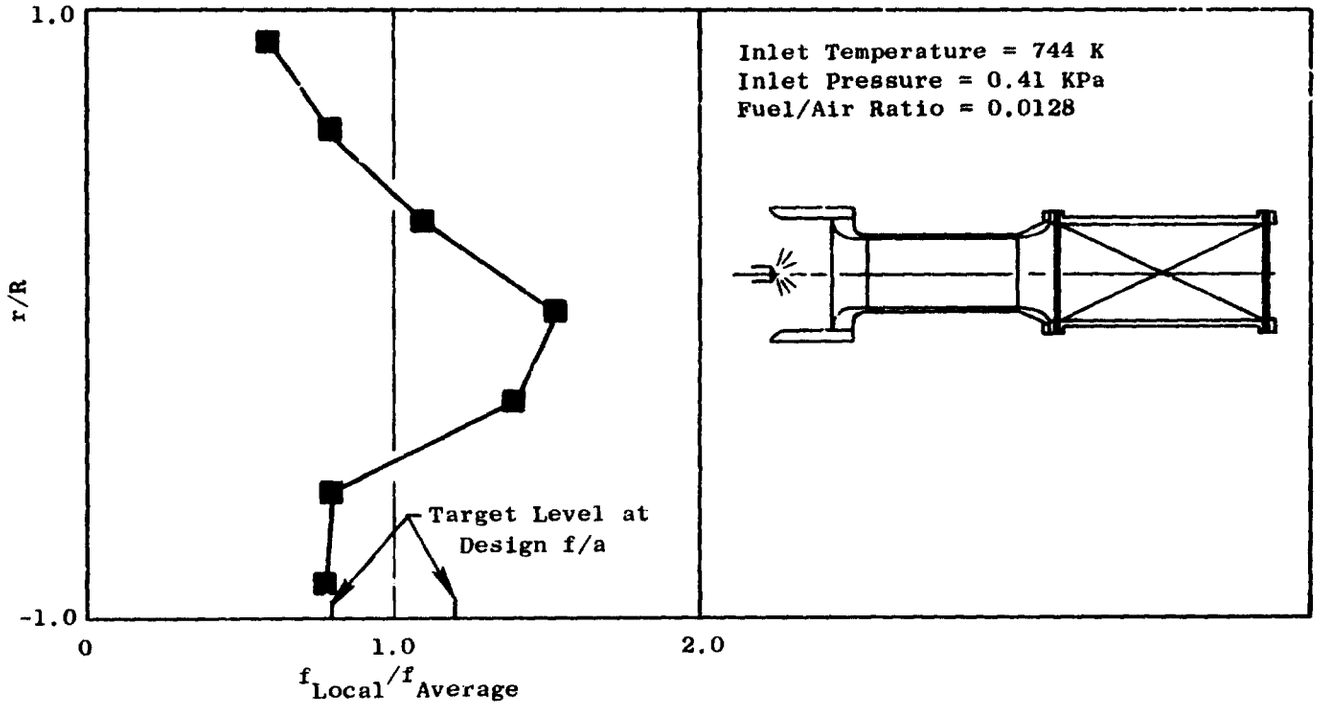

Figure 33. Premixing Duct Exit Fuel Distribution with Increased Length.

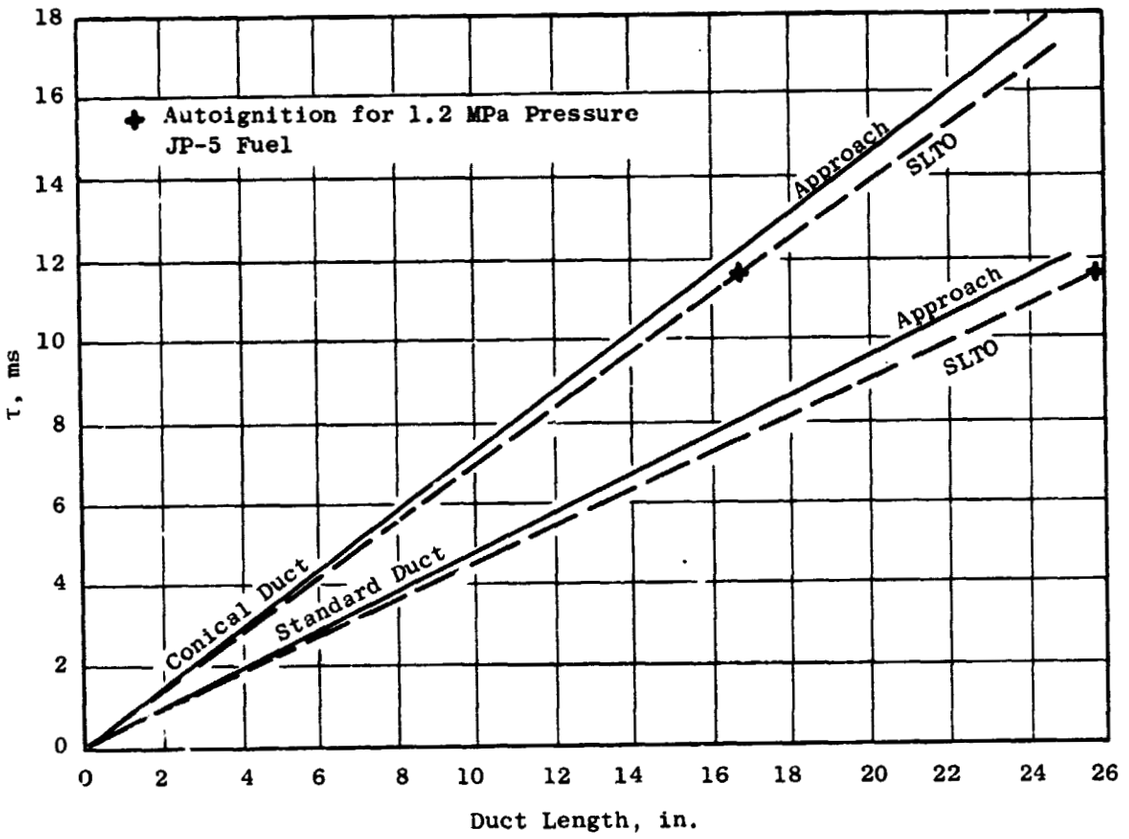

Figure 34. Effect of Duct Length on Autoignition Delay Time for Reverse Flow Combustor.

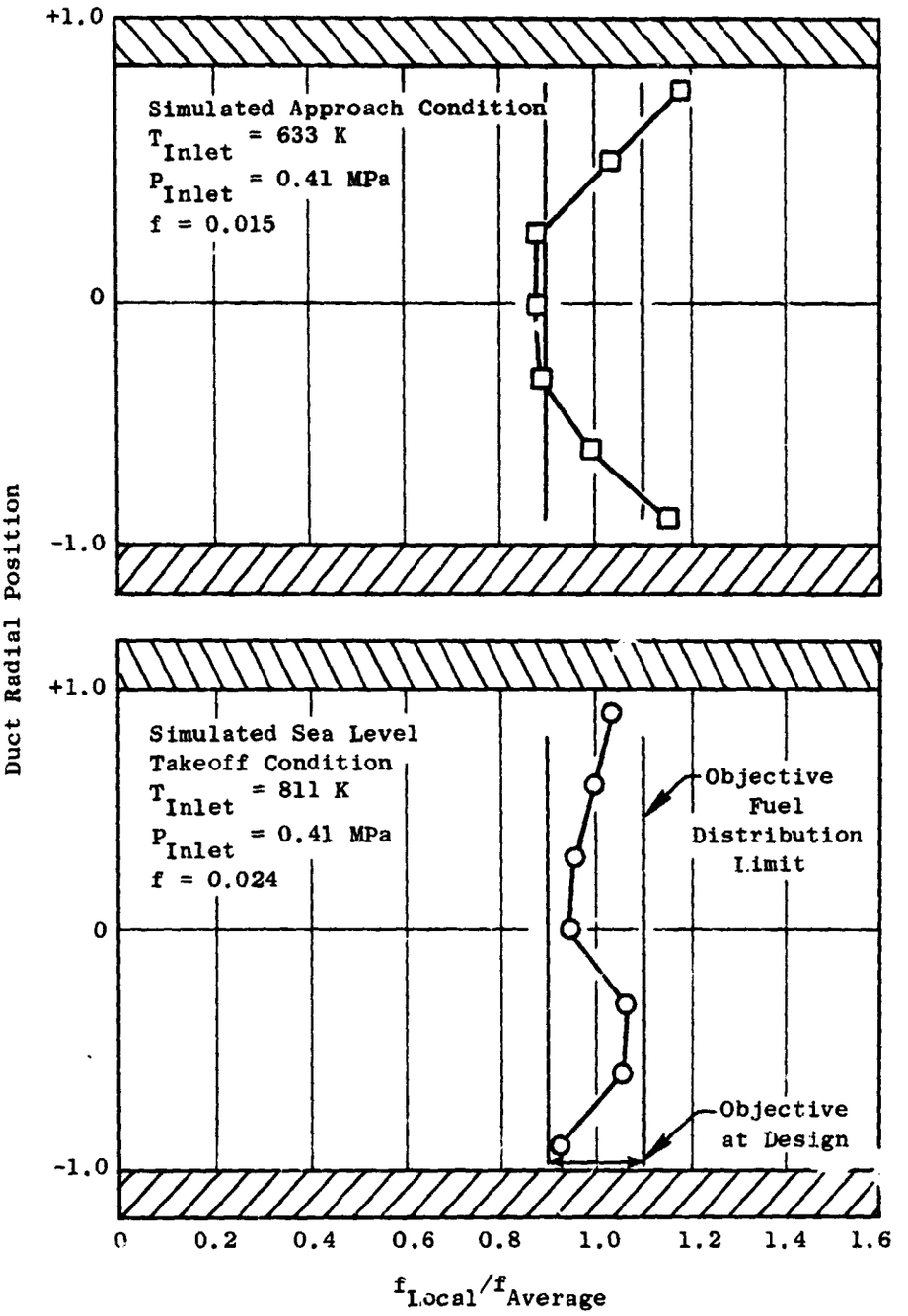

Figure 35. Fuel/Air Distribution - Long Conical Duct for Reverse Flow Combustor.

Next, the fuel/air distribution tests at elevated pressures and temperatures were carried out for the parallel duct system. The test was conducted in the sector combustor test rig, and the data was acquired with gas sample rakes at the catalytic reactor discharge plane. Typical results obtained are shown in Figure 36. The results were encouraging since the peak-to-metered values were significantly lower than those obtained in the ambient tests. However, further improvements would eventually be required to meet the goal level of 1.1 peak to average fuel distribution.

At this point, fuel injection/duct systems were selected for the combustion test phase. For the reverse flow combustor, the long conical duct with vortex generators and single pressure atomizing nozzle was selected even though the residence time was 11 ms. This configuration would be adequate for operation to approximately 1.24 MPa pressure operation without autoignition. This pressure level would be high enough for all of the planned high-pressure, catalytic reactor tests and would provide considerable margin for the 0.41 MPa sector-combustor tests.

The single ring fuel injector and the original length premixing duct (2 ms residence time) were selected for the parallel-staged combustor. Even though the objective fuel distribution had not yet been achieved, it was considered beyond the scope of the current program to redesign and build new ducts for the parallel-staged combustor. The ducts involve compound curvatures and would require long lead times for procurement.

As will be shown in a later section of this report (Section 6.3), efforts to improve fuel distribution were continued during the sector-combustor testing. The goal level of 1.1 peak to average fuel distribution was eventually achieved by the addition of perforated plates just upstream of the fuel nozzles. The perforated plates caused a marked improvement in fuel distribution because the inlet airflow pattern could be better matched to the fuel spray pattern by selecting the proper size and location of the perforations. The increased turbulence of the air jets also improved the mixing process.

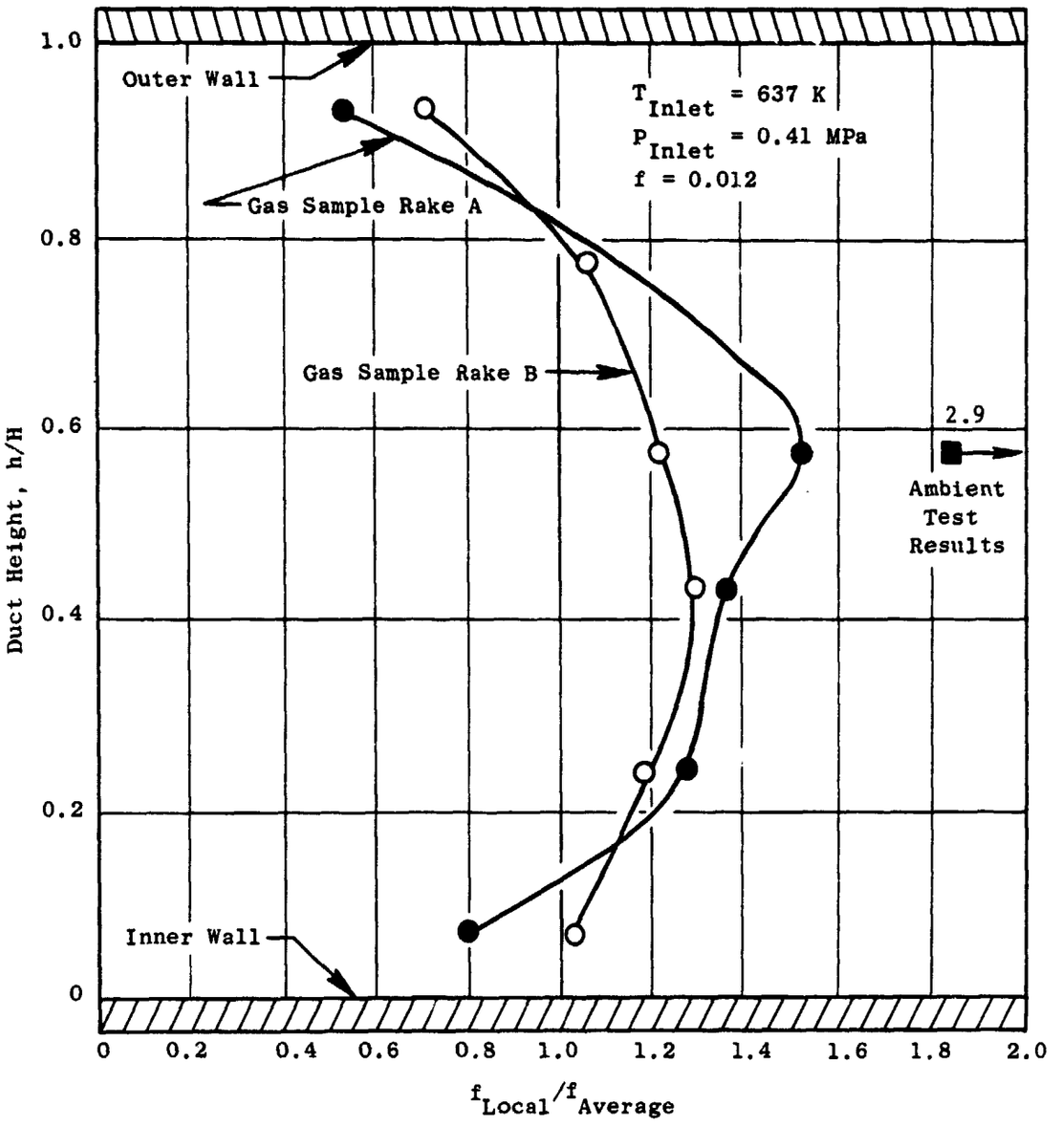

Figure 36. Parallel Duct Fuel Distribution at Simulated Approach Power Conditions.

6.2 SINGLE CAN CATALYTIC REACTOR PERFORMANCE TESTS

Single can catalytic reactor tests were conducted to select the catalytic reactor configuration for use in the sector-combustor tests and to investigate the effects of operating pressure on catalytic reactor performance. The pressure correlations generated during these tests would be used to correct the four-atmosphere, sector-combustor tests to engine pressure levels. The single can, catalytic reactor tests were conducted at pressure levels ranging from 0.41 to approximately 1.11 MPa in the test rig previously illustrated in Figure 26. This is the same test rig as used in the high pressure fuel distribution tests.

Four catalytic reactor configurations were evaluated during this test series and a repeat test on one of the configurations was conducted.

During the course of the single can catalytic reactor performance testing, a number of improvements were made to the test rig and instrumentation. Because of these changes and the fact that the second configuration did not exhibit results up to expectations, a repeat test of Configuration 2 was conducted. The results for Configuration 1 are probably not as reliable as for the other tests. Tests of Configurations 3, 4, and the repeat of Configuration 2 is, therefore, the primary basis for these discussions.

Light off in the catalytic reactors proved to be no problem at any of the test conditions. Activity in the catalytic reactors, as indicated by bed thermocouples, was observed almost as soon as fuel was introduced into the system. Although no steady-state readings were taken at the very low fuel/air ratios, the data in Figure 37 shows that even for the approach power conditions significant activity was present at fuel/air ratios down to at least 0.01 which was below the required steady-state operating conditions for the catalytic reactors (Reference, Table 2). Figure 37 also shows that at the approach power conditions (T inlet = 633 K) high combustion efficiencies were not achieved even at fuel/air ratios in excess of 0.020. It was apparent that light off would be no problem but combustion efficiency would need improvement. Although catalytic reactor operation is not required at approach conditions (T inlet = 633 K), it is required at 60% power (T inlet - 717 K). It appeared

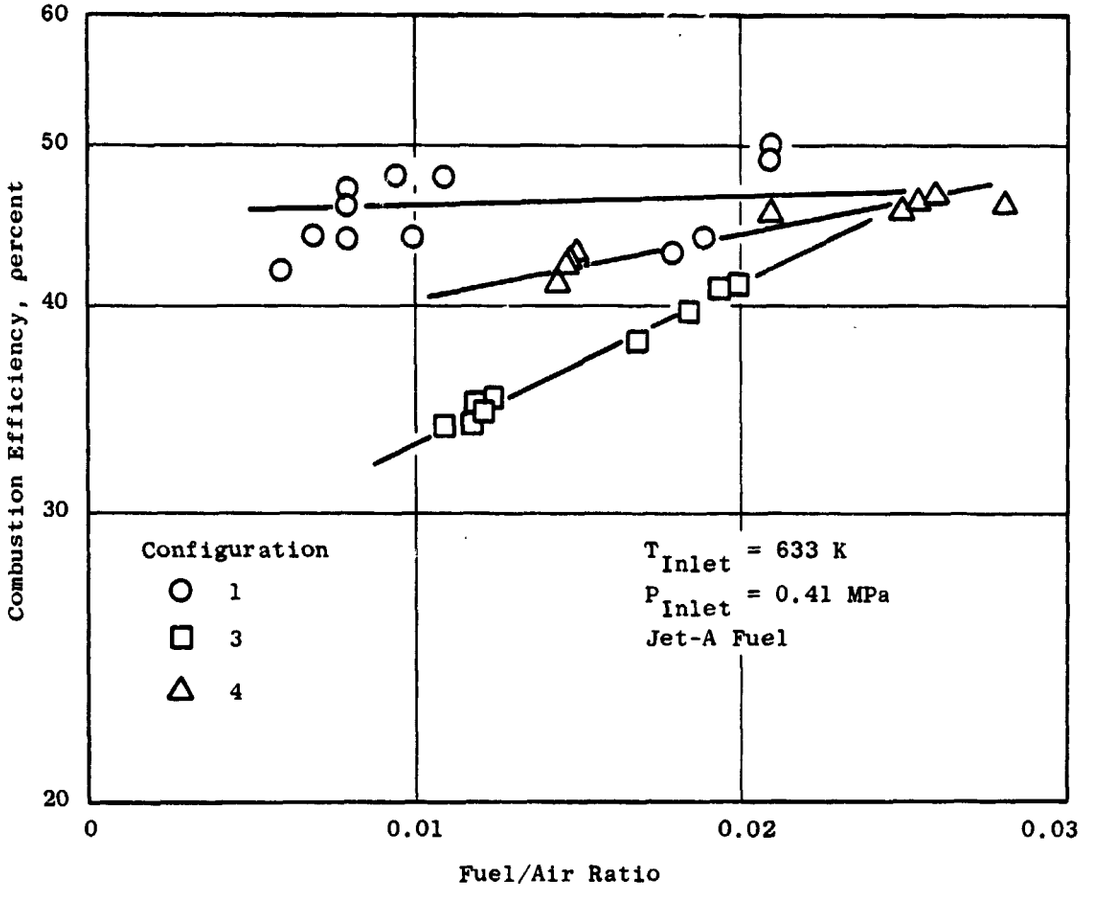

Figure 37. Catalytic Reactor Performance at Approach Power.

that at the low power condition the catalytic reactor bed temperatures did not reach the expected levels. As shown in Figure 38 at 633 K inlet temperature, the bed temperatures were below predictions, but were above predictions at 811 K inlet temperature.

Combustion efficiencies as a function of fuel/air ratio for the four configurations are shown at cruise conditions in Figure 39. The test data for the repeat test of Configuration 2 are presented in this figure. Configurations 2 and 4 were clearly superior and reached the target efficiency level of 99% within the bed temperature limits. Configuration 2 reached a level of 99.9% within the temperature limits and was selected as the choice for the sector combustor testing to follow. Configuration 2 also had the substrate material with the high melting point which was also considered a desirable feature.

The NO_x emissions levels were also measured during these tests and were well below the cruise objective level of 3.0 g/kg for the overall combustion system. As shown in Figure 40, the NO_x emissions as indicies were less than 1.0. Most of the test data were at 0.41 MPa, the sector combustor pressure level, but for one point at 1.1 MPa, the NO_x emission index did not increase from the levels measured at the lower pressures. Other investigators have also found that NO_x emissions levels were independent of operating pressures for premixed systems (Reference 13). Also, there was no apparent increase in NO_x with fuel/air ratio over the range tested.

Unburned hydrocarbons and carbon monoxide were also measured. The hydrocarbon emission indicies were quite high as expected when the combustion efficiencies were low, and decreased steadily as combustion efficiency was increased. The carbon monoxide emissions were low at the very low efficiency levels (below 50%), increased initially as efficiencies increased to about 70%, and then decreased again as the combustion efficiency levels approached 100%. Some results are presented in Figure 41 for cruise operating conditions.

The effects of pressure and reference velocity on catalytic reactor performance were also determined. The combined effects of flame temperature, reference velocity, and pressure on combustion efficiency were correlated using multiple-regression analyses. The following functional form was used for this analysis:

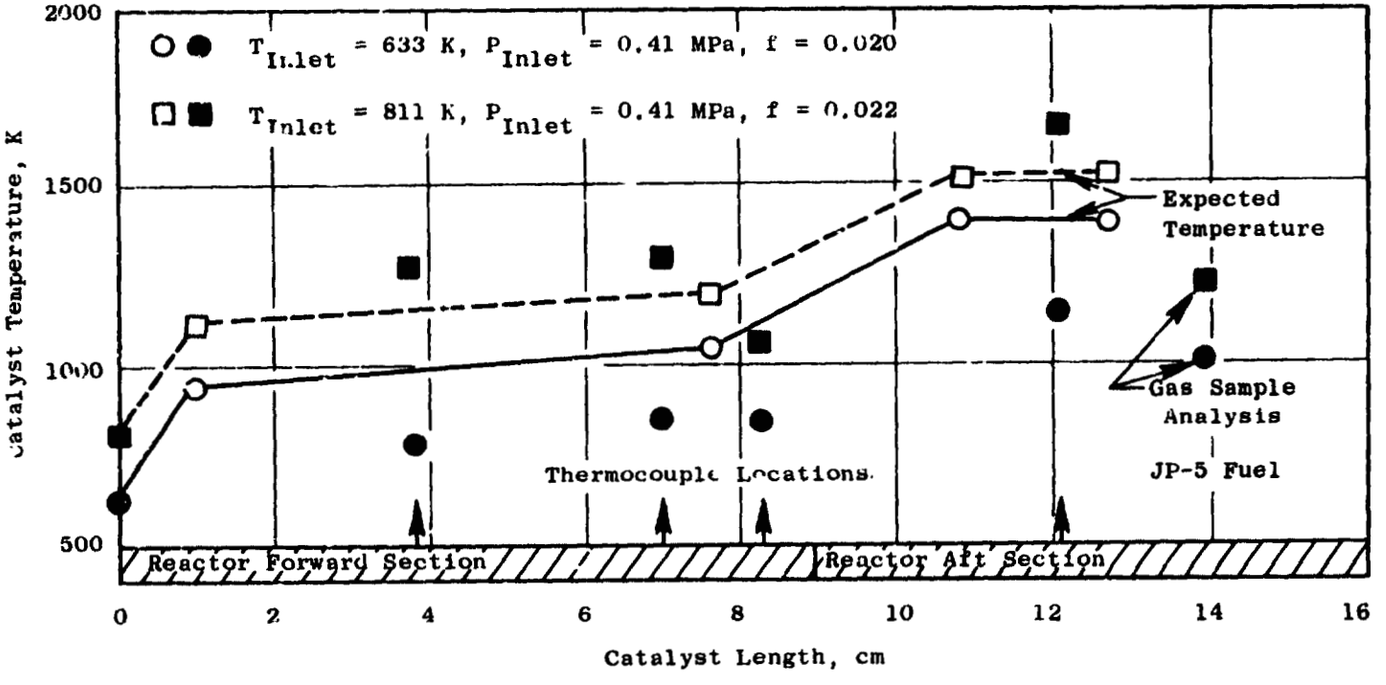

Figure 38. Comparison of Measured and Estimated Catalyst Bed Centerline Temperature.

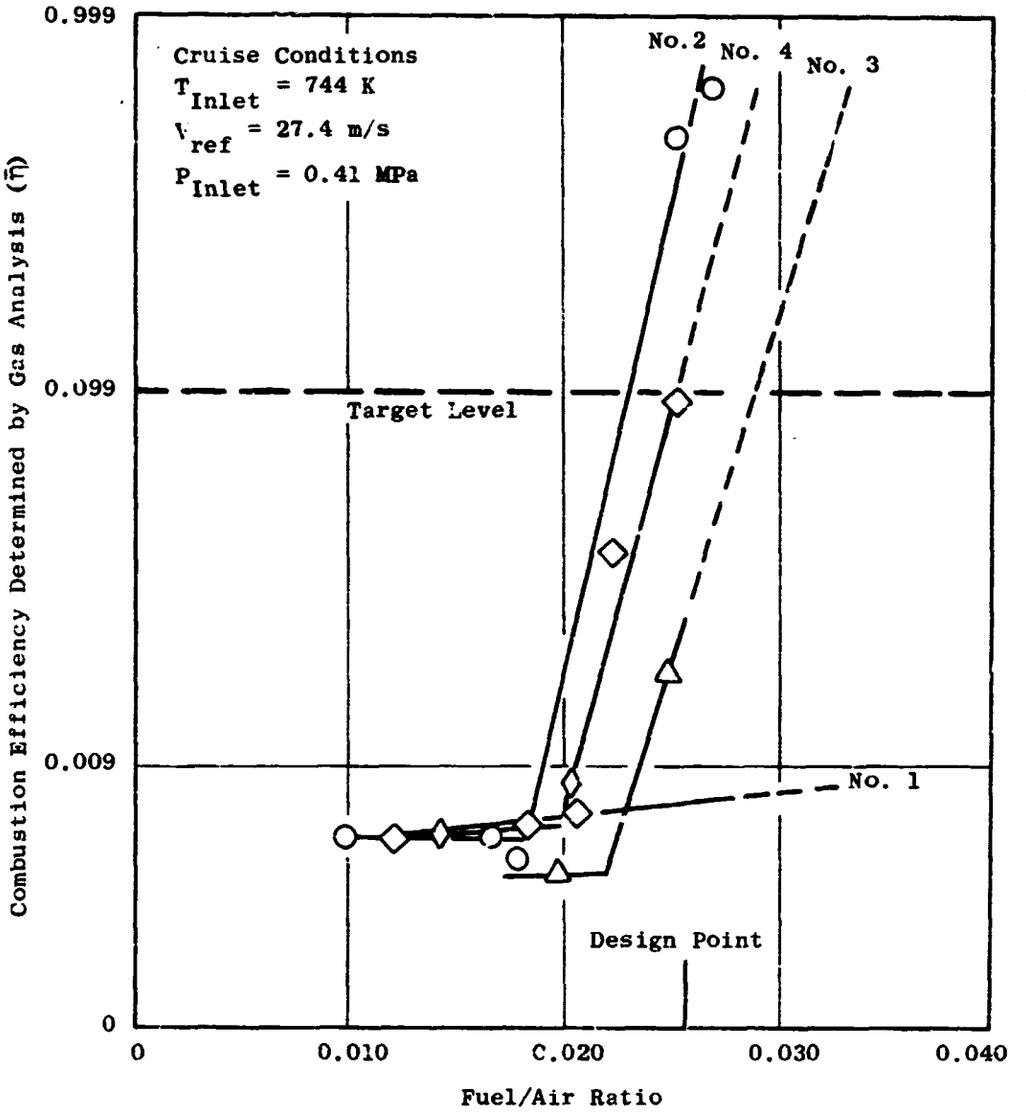

Figure 39. Combustion Efficiency Versus Fuel/Air Ratio from Catalytic Reactor Subcomponent Tests at Cruise Operating Conditions.

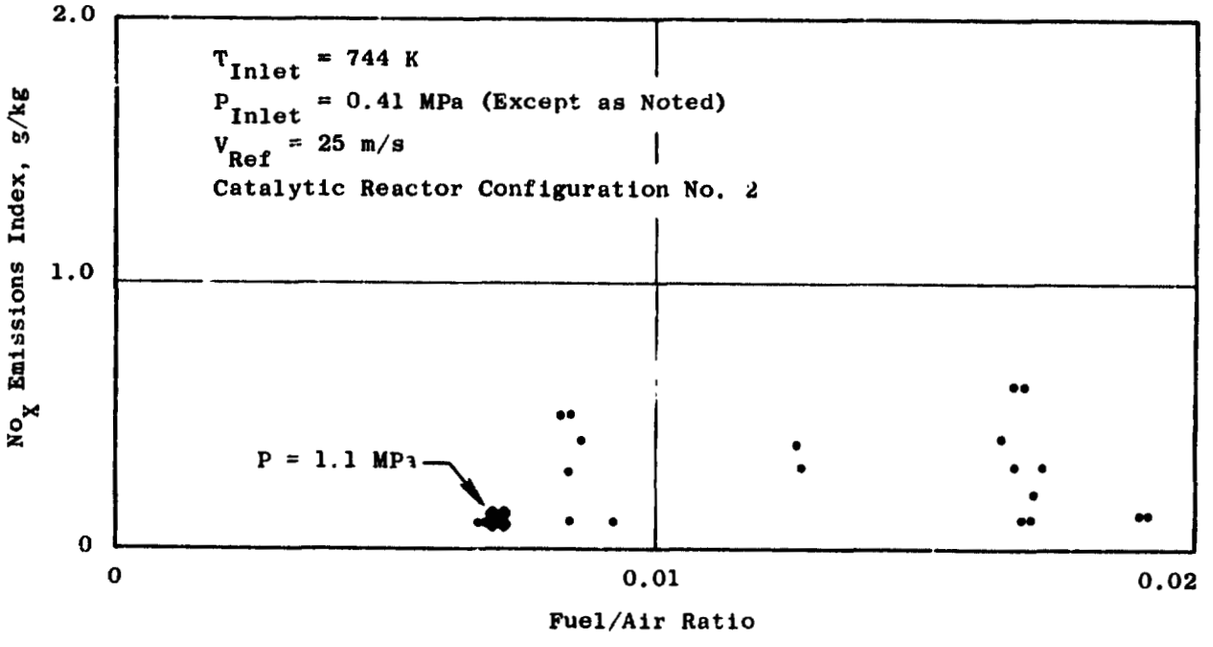

Figure 40. NO_X Emissions Indices as a Function of Fuel/Air Ratio for Catalytic Reactor Configuration 2 at Cruise Condition.

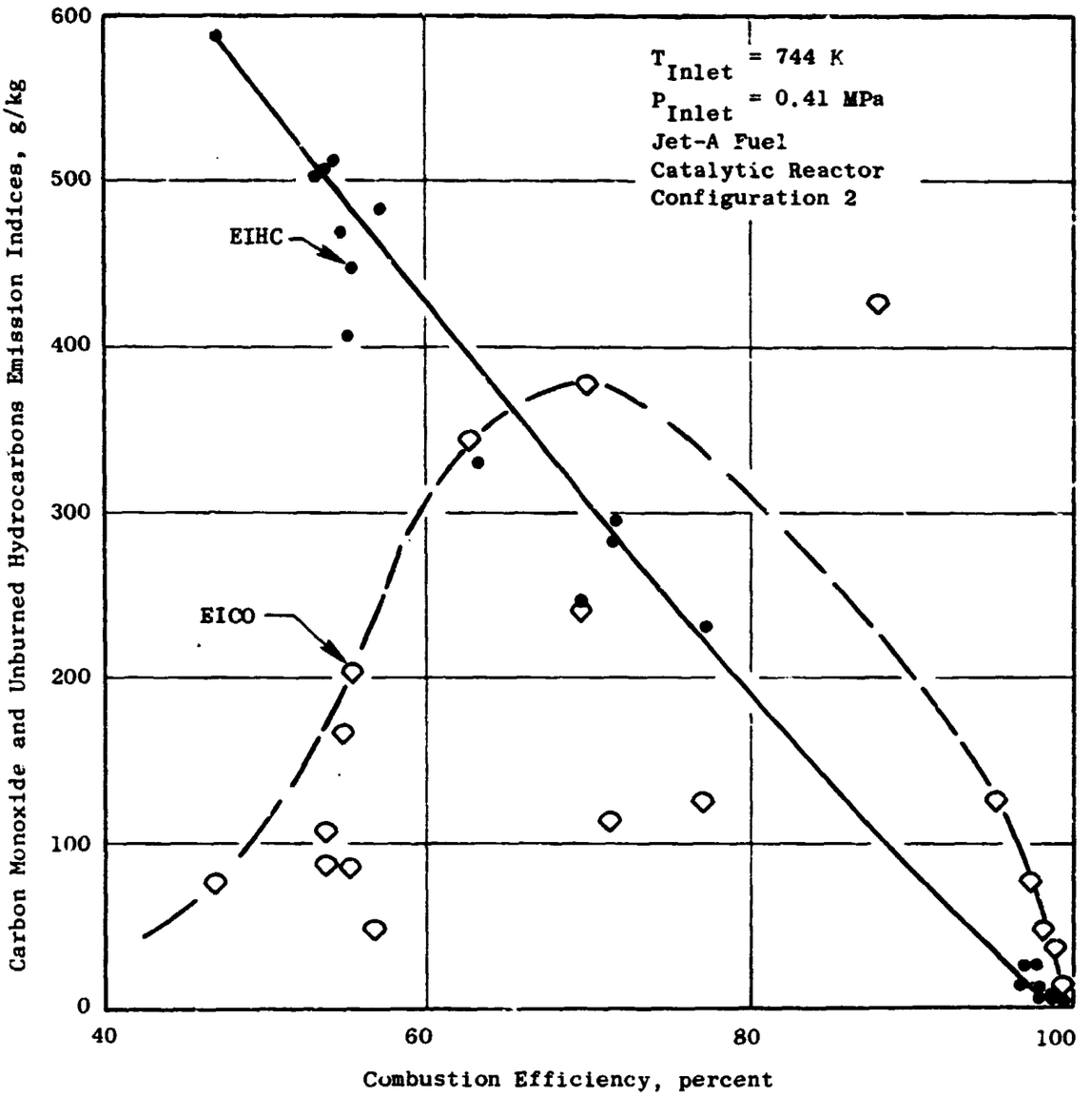

Figure 41. Carbon Monoxide and Unburned Hydrocarbons Emission Indices as a Function of Combustion Efficiency at Cruise Operating Conditions.

$$100 - \eta \propto P^{A} V_{ref}^{\ B} \exp\left(T_{adi}/C\right) \qquad (1)$$

where η, P, V_{ref}, and T_{adi}, are the efficiency (in percent), the operating pressure level (psia) the reference velocity (ft/s), and the adiabatic flame temperature (° F), respectivcly. A, B, and C are constants determined by the regression analysis. Functional forms similar to the above expression have been used in previous correlations of emissions from conventional combustors and catalytic reactors (References 5 and 14).

Results of the above regression analysis are presented in Table 11. The first catalytic reactor test and the initial test of Configuration 2 were not included in the correlation because the test techniques were not the same as for the last three tests. Also, not all of the variables were investigated for all of the catalytic reactors. Therefore, some blanks appear in the table. The correlations were done only for test data with combustion efficiencies of 70% or above so that only data of practical interest was used.

Table 11. Combustion Efficiency Correlation Constants.

Catalytic Reactor Configuration	Coefficient Values		
	A	B	C
2	-1.256	---	-95.95
3	---	2.976	-102.3
4	---	---	-105.9
Selected Constant	-1.25	3.0	-100

Coefficient B, for reference velocity, was based on only one test but is the same as determined during a previous catalytic combustion program (Reference 14). Coefficient C for adiabatic flame temperature was evaluated for all three of the tests in Table 11 and good agreement was obtained. The pressure coefficient, A, was based on only one of the tests.

The correlation for combustion efficiency can be used to correct from the 0.41 MPa pressure used in the sector-combustor tests to the higher pressures that would occur in an engine.

In summary, the single-can high pressure rig tests resulted in the selection of a catalytic reactor configuration which met the efficiency goal at the design fuel/air ratio and appeared to have NO_x emissions levels well within the range required to meet the program goals when used in a combustion system, which would include a pilot stage dome. The tests also provided the necessary relationships for effects of combustor inlet temperature, pressure, and reference velocity on catalyst performance to make adjustments to the subsequent sector combustor tests at 0.41 MPa to predict the performance at actual engine operating conditions.

6.3 FULL-SCALE SECTOR COMBUSTOR SYSTEM TESTS

The plan for the sector-combustor development phase involved conducting two baseline tests each on the basic parallel-staged combustor and the reverse-flow combustor followed by an additional six tests on the most promising of the two combustor systems.

6.3.1 Baseline Sector Combustor Tests

The reverse flow combustor, instrumented and ready for installation in the test rig, is shown in Figure 42. The parallel staged combustor installed on the test rig mounting plate is shown in Figure 43.

During the first test of each of these combustors, high combustion efficiencies (>99%) could not be achieved with the catalytic reactors without exceeding the safe operating temperature of 1700 K. When the combustors were operated at 60% power on the pilot stage only, the combustion efficiencies were in excess of 99.7% demonstrating the satisfactory performance of the pilot stage. However, when both the pilot and the catalytic reactor main stages were fueled, the combined system combustion efficiencies were less than 85%. This was the case regardless of the fuel split between the pilot

Figure 42. Reverse Flow Combustor Ready for Installation in the Test Rig.

Figure 43. Basic Parallel-Staged Combustor Mounted on Test Rig Aft Bulkhead.

and main stage and even when the residence time in the catalytic reactor was increased by reducing the combustion system airflow. Some of these test results are presented in Table 12.

Even with increased inlet temperature and reduced airflow rates, the efficiency of the system did not exceed 85%. These efficiencies were based on gas samples extracted at the combustor exit plane.

The basic parallel flow combustor was in good condition following the first test. Photographs of the hardware are shown in Figures 44 and 45. However, for the reverse flow combustor, the catalytic reactors experienced damage, shown in Figure 46, as the result of poor fuel distribution caused by blockage from insulation that was used on the fuel lines. A portion of the insulation blankets was torn loose by air turbulence and the debris lodged on the forward face of the catalytic reactors. Figure 47 shows one of the blocked reactors.

Based on the earlier single-can, catalytic-reactor tests, it was known that improved performance could be achieved by reducing the catalytic reactor reference velocity. The decision was made to reduce the reactor reference velocity for the sector-combustor from a nominal value of 30 to 15 m/s. With the reduced velocity, the catalytic reactor pressure drop would also be reduced. In order to maintain the overall combustion system pressure drop and maintain normal pilot airflow, it was necessary to introduce a pressure drop in series with the reactors. This was accomplished by the addition of perforated plates at the entrance to the premixing ducts. It was decided to use the existing hardware and accept the reduced reactor airflow associated with the reduced reference velocity in order to avoid a lengthy redesign and hardware procurement cycle. In effect. the test was conducted with and undersized main stage relative to the pilot stage. However, the combustor performance characteristics could still be determined with this approach.

Figures 48 and 49 show perforated plates mounted on the premixing duct inlets of the parallel staged and reverse flow combustors, respectively.

The addition of perforated plates (and pressure drop) at the premixing duct inlets provided another and very important benefit. The air profiles downstream of the perforated plates could be controlled by the hole pattern

Table 12. Combustion Efficiency for Initial Combustor Tests.

	Reverse-Flow Combustor			Basic Parallel-Staged Combustor						
	60% Power			60% Power				Cruise[3]	85%[3]	Takeoff[3]
T_3 Inlet Temperature, K	710	718	715	718	719	717	718	744	778	813
f - Overall Fuel/Air Ratio	0.016	0.0217	0.0258	0.0064	0.007	0.0162	0.0149	0.0172	0.0163	0.0164
f_p - Pilot Fuel/Air Ratio[1]	0.0376	0.045	0.0323	0.0171	0.0187	0.0184	0.0183	0.0192	0.0186	0.0186
f_R - Reactor Fuel/Air Ratio[2]	---	0.0226	0.0216	---	---	0.0178	0.0154	0.0199	0.0179	0.0180
Combustion Efficiency, percent	99.6	83.7	76.9	99.8	99.8	76.4	79.8	82.7	85	84.9

(1) Based on pilot stage airflow only

(2) Based on catalytic reactor airflow

(3) Combustion System reference velocity reduced 25%

Figure 44. Basic Parallel-Staged Combustor Posttest Condition.

Figure 45. Basic Parallel-Staged Combustor Catalytic Reactor Posttest Condition.

Figure 46. Reverse Flow Combustor Catalytic Reactor Damage from First Test.

Figure 4. Reverse Flow Catalytic Reactor Blockage by Foreign Material.

Figure 48. Parallel-Staged Combustor Premix Duct Inlet Perforated Plate.

Figure 19. Reverse Flow Combustor Premix Duct Perforated Plates.

configuration to match the fuel spray pattern. Also, the turbulence from the jet mixing probably contributed to the fuel and air mixing in the premixing ducts. Very uniform fuel/air distribution, meeting the program objective of a peak to average ratio of 1.1, was achieved. Figure 50 presents profiles measured with the reverse flow combustor in the sector combustor test rig. For this test, the long premixing ducts (11 m/s residence time) were used. The profiles were calculated from thermocouple readings taken in the catalytic reactor bed.

A significant improvement in reactor performance was achieved with the reduced reference velocity. Both of the combustor designs operated with high combustion efficiency for the first time and with no reactor damage or melting. Figure 51 shows the posttest discharge end of the catalytic reactor from the parallel-staged combustor.

At 60% power, the engine condition where the catalytic reactor is first fueled, the combustion efficiency was in excess of 99% for both the reverse flow and the basic parallel staged combustors. Data at the 60% power condition is presented in Figures 52 and 53.

Figure 52 shows radial gas sample data with fuel/air ratio (FAR), $EINO_x$, and combustion efficiency (η) plotted as a percentage of passage height for the reverse flow combustor. There were four, five-element gas sample rakes located in the instrumentation section as described in Paragraph 5.1. Two of the rakes were read individually and two were ganged. For the reverse flow combustor, one individually read and one ganged rake were located in line with the catalytic reactor and one each were between reactors and therefore in line with pilot dome swirl cups. The readings for the ganged rakes are indicated by arrows in Figure 52. The radial fuel/air ratio profiles, Figure 52(a), were uniform (very flat) in line with both the reactor and the pilot swirlers, with the reactor somewhat richer. The level of the two profiles is determined by the fuel split between the pilot and catalytic reactor. Note that a turbine rotor effectively integrates the temperature profiles in the circumferential direction and, therefore, would experience a flat profile corresponding to the average of the two individual profiles. The combustor pattern factor which is related to the turbine stator life and is defined as:

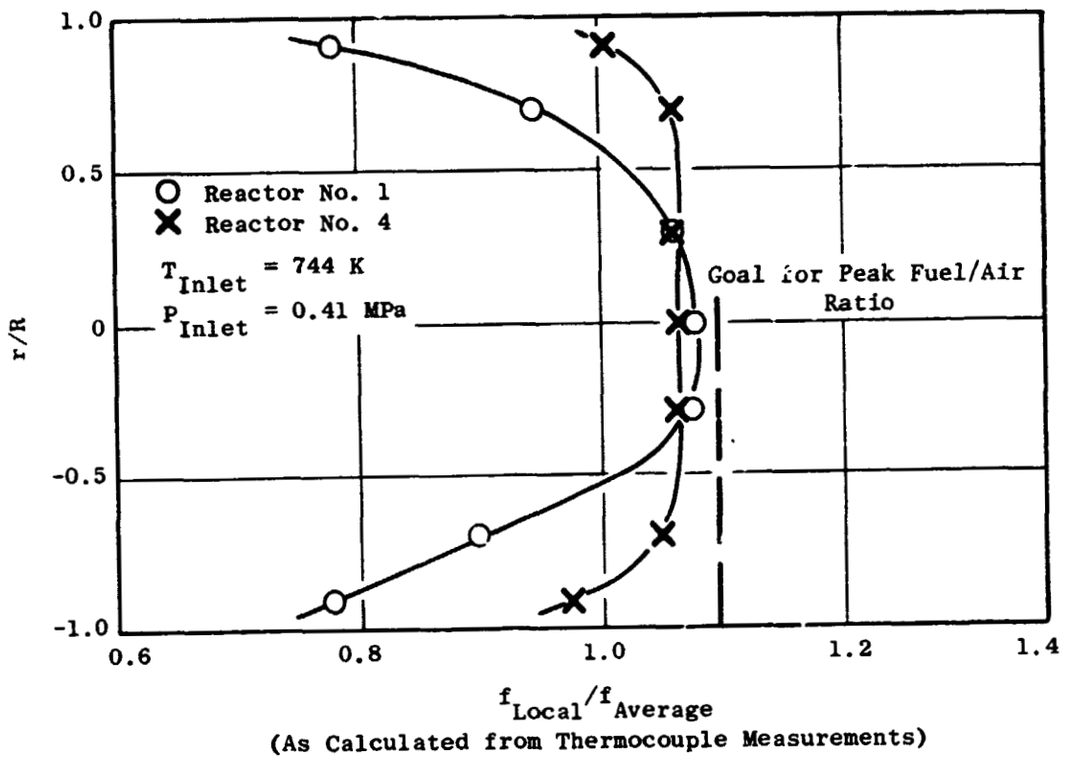

Figure 50. Fuel Distribution for Reverse-Flow Premixing Duct with Perforated Plate Inlet.

Figure 51. Parallel-Staged Combustor Posttest Condition After Test Demonstrating High Combustion System Efficiency.

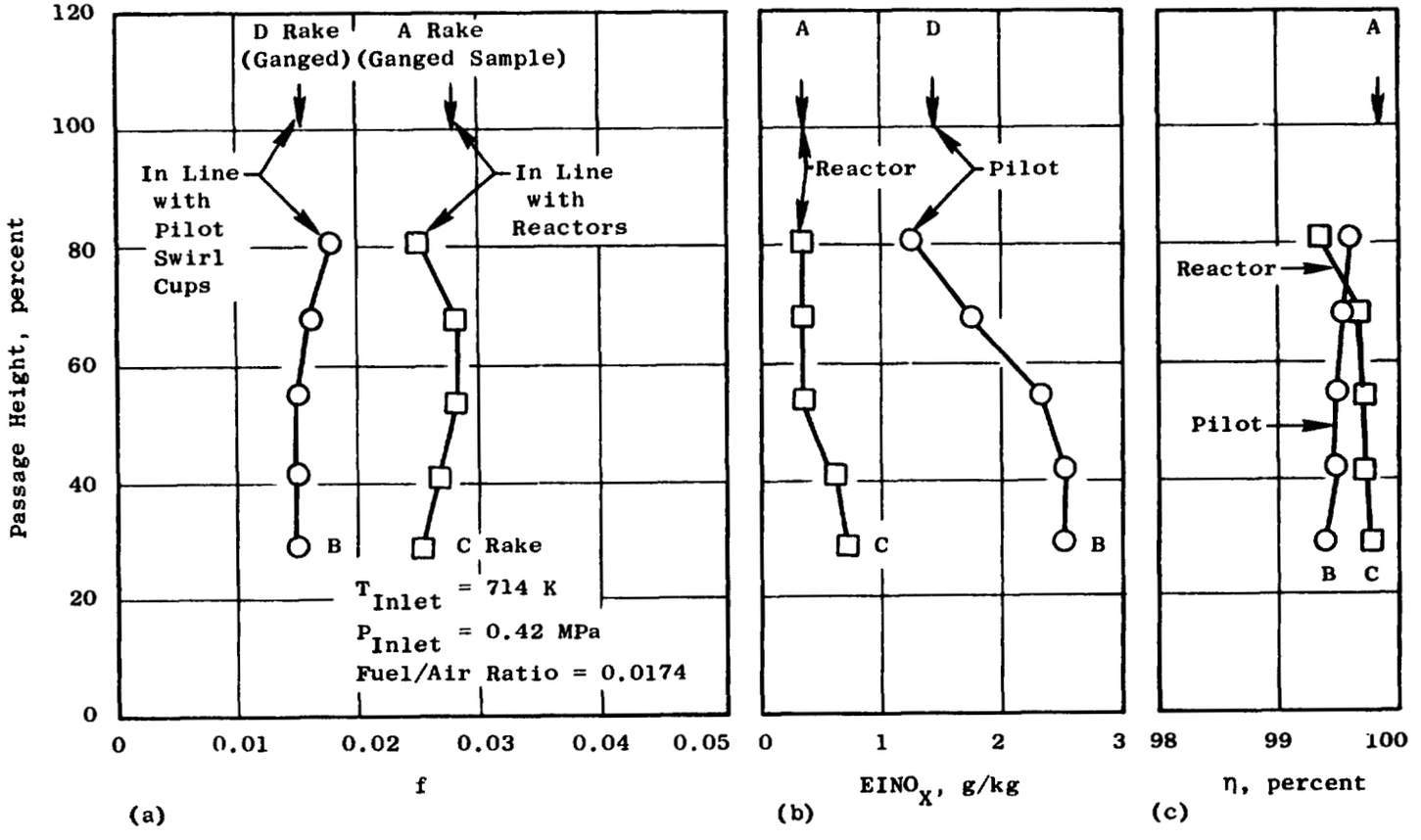

Figure 52. Radial Profiles of Fuel/Air Ratio (FAR), NO_x Emission Index ($EINO_x$), and Combustion Efficiency (η%) at 60% Power for the Reverse Flow Combustor.

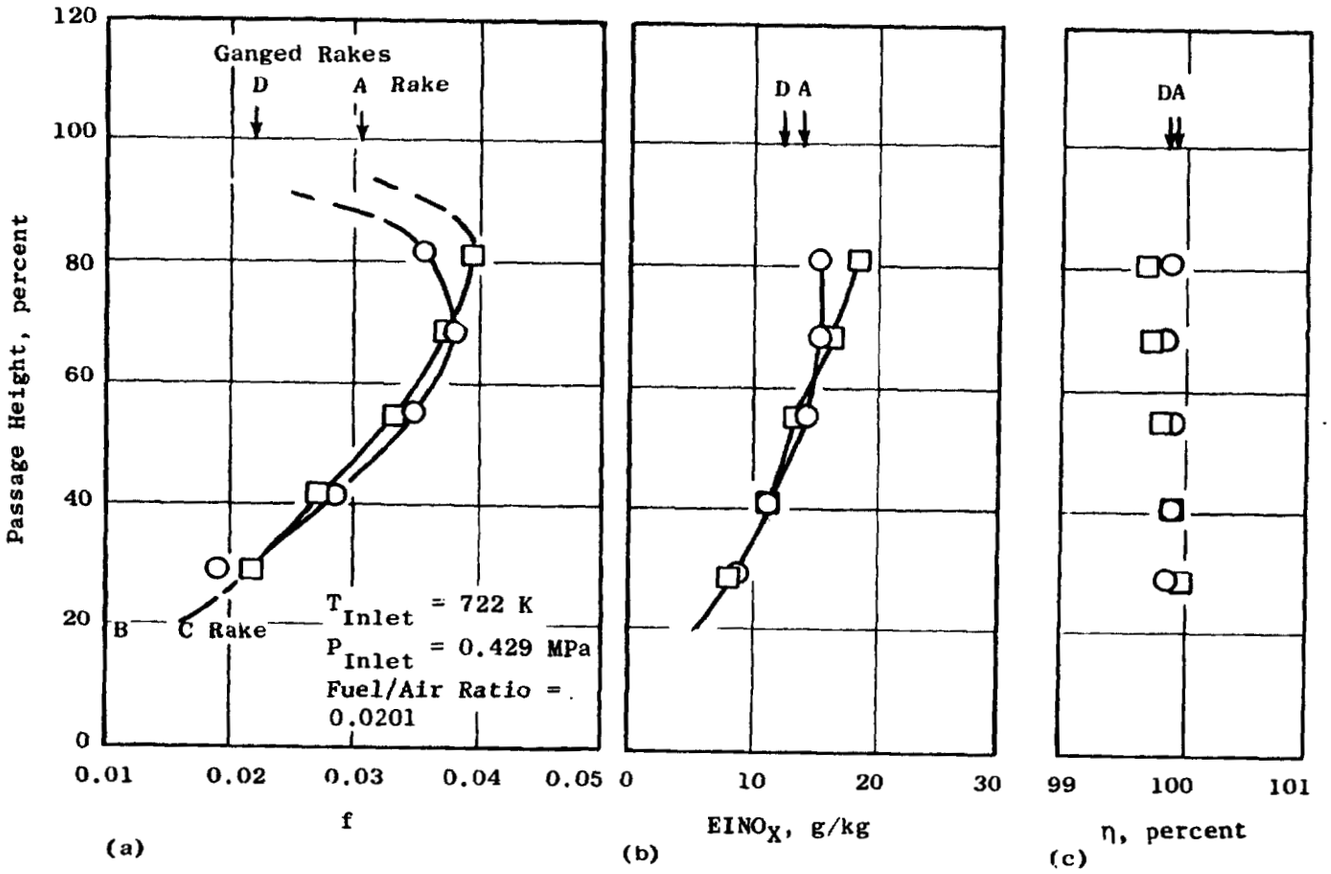

Figure 53. Radial Profiles of Fuel/Air Ratio (FAR), NO_X Emissions Index ($EINO_X$), and Combustion Efficiency (η%) at 60% Power for the Basic Parallel-Staged Combustor.

$$\text{Pattern Factor} = \frac{\text{Highest Local Temperature - Average Temperature}}{\text{Combustor Temperature Rise}},$$

is a function of the highest local temperature. Therefore, pattern factor would be a function of the fuel split between the pilot and the catalytic reactor and could be minimized by using equal fuel/air ratios in the two stages of the combustor.

The NO_x emission index, Figure 52(b), is ultra low (0.3 to 0.4) from the reactor and higher (2 to 3) for the pilot. It became rather obvious from the data in Figure 52 and other data collected during this program that the results from the outer three samples on Rake C are representative of the catalytic reactor while the inner two elements contain a mixture of gases from the catalytic reactor and the pilot. Also, the inner three elements from Rake B are most representative of the pilot, while the outer two have a mixture of gases.

Uniformly high combustion efficiencies were indicated for all of the gas samples whether in line with the pilot or catalytic reactor.

Figure 53 presents comparable data for the basic parallel-staged combustor. In this case, the inner elements of the rakes get samples from the annular catalytic reactor and the outer elements are dominated by combustion gases from the pilot. For the test point shown, the pilot fuel/air ratio is higher than that of the catalytic reactor and the radial fuel/air ratio (and temperature) profile is peaked outward. The turbine rotor would experience an outward peaked profile in this case.

The NO_x emissions were greater by an order of magnitude than was observed for the reverse flow combustor. This was determined to be the result of autoignition and, therefore, droplet burning in the premixing duct. The autoignition was promoted by a step in the premixing duct where the fuel injector penetrated the sidewall. Figure 54 shows the fuel injector mounting port and the heat stain on the premix duct sidewall. The 0.32 cm high step in the sidewall tripped the flow and resulted in the autoignition. Carbon deposits were found in the tripped region and on the fuel injector tube near the wall. No heat stains or carbon deposits were found on the other side of the duct.

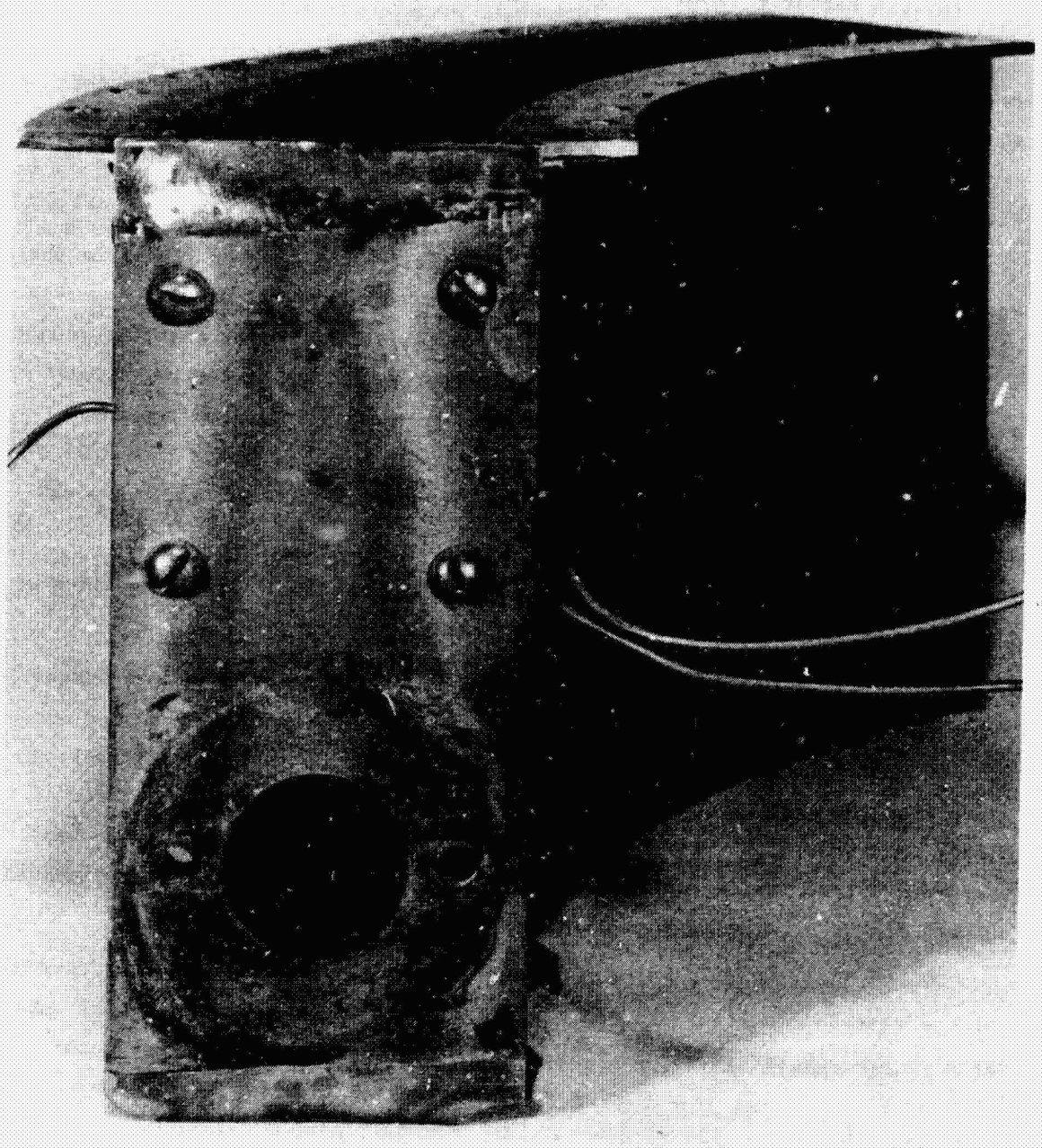

Figure 54. Parallel-Staged Combustor Premix Duct Showing Heat Stain from Autoignition which Initiated at the Fuel Injector Mounting Port in the Duct Sidewall.

The autoignition did not adversely effect the combustion efficiency and high efficiencies were indicated by all gas samples.

Based on these results, the reverse flow combustor was selected for the refinement tests. The reasons for this selection were:

- High efficiency combined with low NO_x had been demonstrated with the reverse-flow combustor without autoignition. Additional testing would be required to develop low NO_x and autoignition-free performance with the parallel-staged combustor.
- The cylindrical or conical premixing ducts of the reverse-flow combustor appeared to have more potential for achieving uniform fuel distribution than did the annular ducts of the parallel-staged combustors.
- Flat radial temperature profiles were measured for the reverse flow combustor.
- The length from compressor discharge to the turbine inlet was the same for the reverse flow combustor as for the E^3 combustor. The parallel-staged combustor required an engine length increase.
- Catalytic reactor removal from an engine system for maintenance purposes would be considerably easier for the reverse-flow system than for the annular arrangement of the basic parallel-staged combustor.

6.3.2 Reverse-Flow Combustor Refinement Tests

The refinement tests were used to further investigate the range of operation of the catalytic combustor, to investigate the use of a reduced length premixing duct, and to determine the effects of premixing duct perforated plate hole patterns.

6.3.2.1 Combustion Efficiency

Figure 55 shows combustion efficiencies obtained from sev 1 tests from gas samples taken directly in line with the catalytic reactor for a range of inlet temperature and 0.41 MPa pressure. The reactor efficiency is approximately 60% up to 0.015 fuel/air ratio and then rises rapidly as the fuel/air ratio is further increased. At fuel/air ratios of 0.022 and above, the efficiencies were in excess of 99.5%. It is clear from this plot that, for the reactor conditions of this test, local fuel/air ratios must be at least 0.022 in order to obtain combustion efficiency greater than 99.5%. This establishes

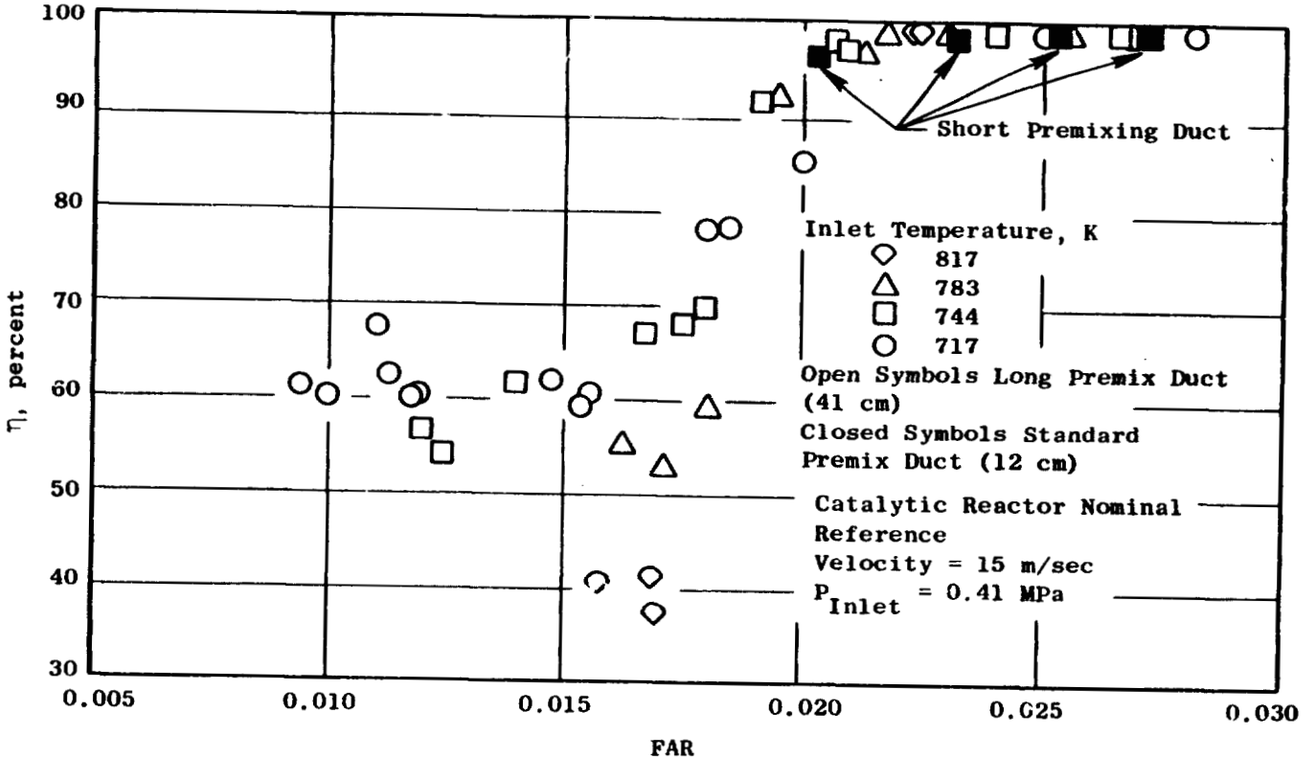

Figure 55. Combustion Efficiency Versus Fuel/Air Ratio for Reverse Flow Sector Combustor Test.

the minimum reactor temperature, depending on the inlet temperature. The maximum reactor temperature is 1700 K and these two limits establish the reactor operating range.

The initial reverse flow sector-combustor tests were conducted with fuel premixing ducts that were 41 cm long versus 12 cm for the original combustor design. The added length was to provide more uniform fuel distribution. The long length would be unacceptable for use at actual engine pressures. The last three of the four refinement tests of the sector-combustor were conducted with the original, short premixing ducts. Although the fuel distribution was somewhat poorer with the short duct (1.23 versus 1.1 peak to average fuel/air ratio), no significant change in combustion efficiency was observed, as shown in Figure 55.

The sector-combustor tests were conducted at four-atmosphere pressure with a nominal catalytic reactor reference velocity of 15 m/s. Actual engine pressures for the high-power conditions would be higher than in the component tests and would have a beneficial effect on combustion efficiency. As pressure is increased, reference velocity can also be increased with no change in combustion efficiency. The effects of increased pressure can be predicted using the results of the single-can, catalytic reactor tests. The allowable increase in reference velocity as a function of pressure was calculated for constant combustion efficiency using Equation 1 (Section 6.2) and the coefficients in Table 11.

For constant combustion efficiency, η, and adiabatic flame temperature, T_{adi}:

$$\frac{(P^A V_{ref}{}^B)\ 0.4\ \text{MPa Test}}{(P^A V_{ref}{}^B)\ \text{engine pressure}} = 1 \qquad (2)$$

and: $$V_{ref,\ \text{engine pressure}} = 0.561\ (P^{0.417})_{\text{engine}}\ (V_{ref})_{\text{Test}} \qquad (3)$$

where pressure is in atmospheres. The effect of pressure on allowable reference velocity, based on Equation (3), is presented in Figure 56. At true

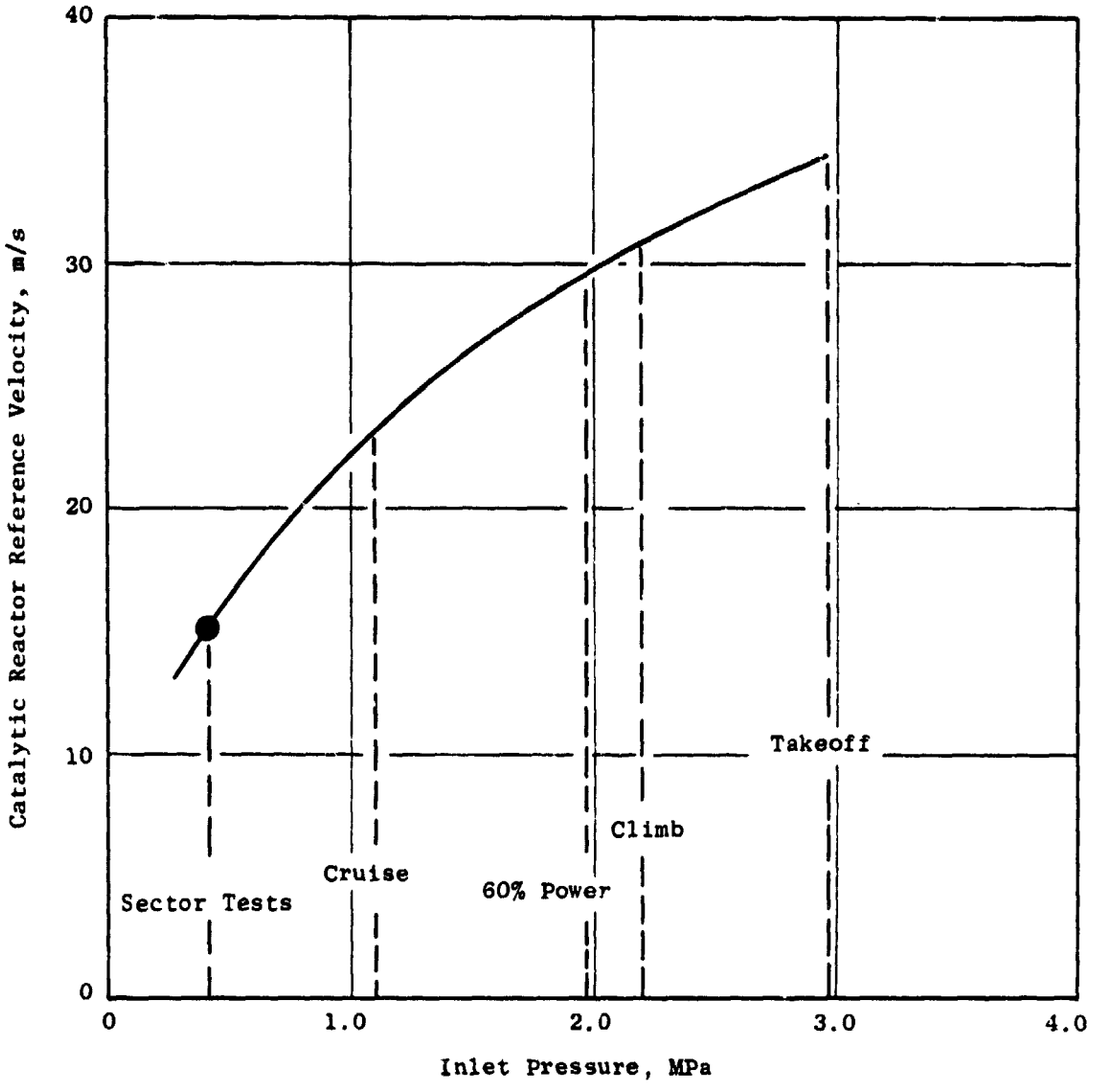

Figure 56. Reference Velocity Versus Operating Pressure for Constant Combustion Efficiency for Reverse Flow Combustor.

cruise conditions, the reference velocity could be increased to approximately 23 m/s for the same combustion efficiency (99.5%) as observed in the sector-combustor tests. Also, during the component test, there appeared to be some combustion efficiency margin. The reactor fuel/air ratio is approximately 0.026 at cruise conditions. The efficiency reaches 99.7% at a fuel/air ratio of 0.022 (Figure 55). Therefore, a design reference velocity for an actual engine, of between 24 and 27 m/s would be an appropriate compromise between the 30 m/s used in the original design and the 15 m/s used for most of the sector-combustor tests, which were conducted at four-atmospheres pressure.

6.3.2.2 NO_x Emissions

Some measured NO_x emission indicies from the reverse-flow sector combustor for cruise conditions are presented in Figure 57. For the gas sample rakes directly in line with the catalytic reactor, very low NO_x emissions were measured from the outer three elements. However, for the inner elements some of the pilot gases mix with the gases from the reactor and increase the NO_x levels. For the gas sample rakes located between catalytic reactor positions and in line with the pilot swirl cups, the NO_x levels are significantly higher, as expected, and the emissions levels are representative of the pilot stage.

The NO_x emission level for the catalytic reactor is shown as a function of fuel/air ratio in Figure 58. As in the single-can tests, there was no significant increase in NO_x level with reactor fuel/air ratio over the range tested. Also, there was no apparent effect of pressure on NO_x during the single-can catalytic reactor performance tests (Section 6.2). However, the pressure effect test data was not very extensive. Therefore, the NO_x emission indicies in Figure 58 were corrected to engine pressure level using a pressure ratio exponent of 0.37, which was determined during a previous NASA-sponsored program conducted by the General Electric Company (Reference 5). The corrections were made with the expression:

$$NO_{x\ corrected} = NO_{x\ test} \left(\frac{P_{engine}}{P_{test}}\right)^{0.37} \qquad (4)$$

Figure 59 shows NO_x levels measured in line with the pilot cups for several pilot fuel/air ratios. As would be expected, the NO_x varies significantly

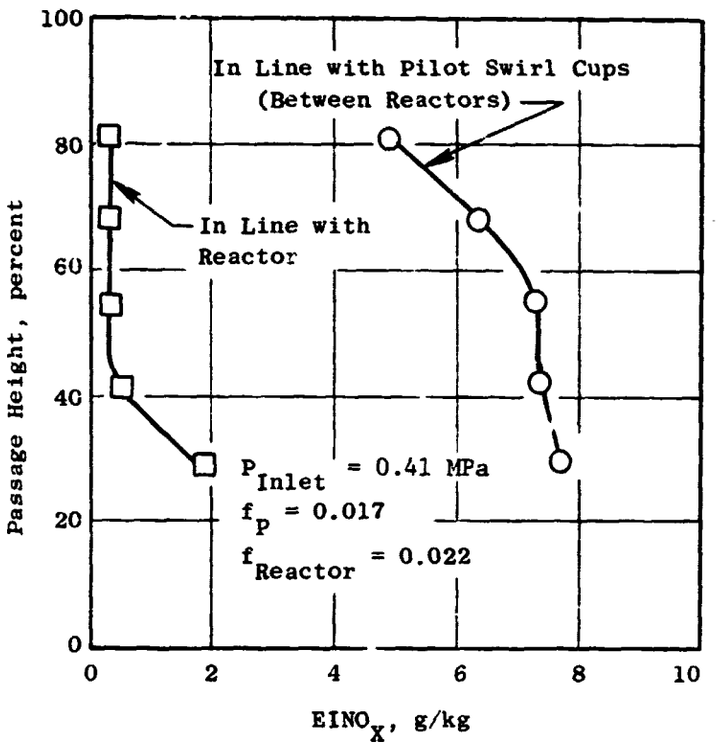

Figure 57. Radial Profile of NO_x Emissions Indices at Cruise Power for Reverse Flow Combustor.

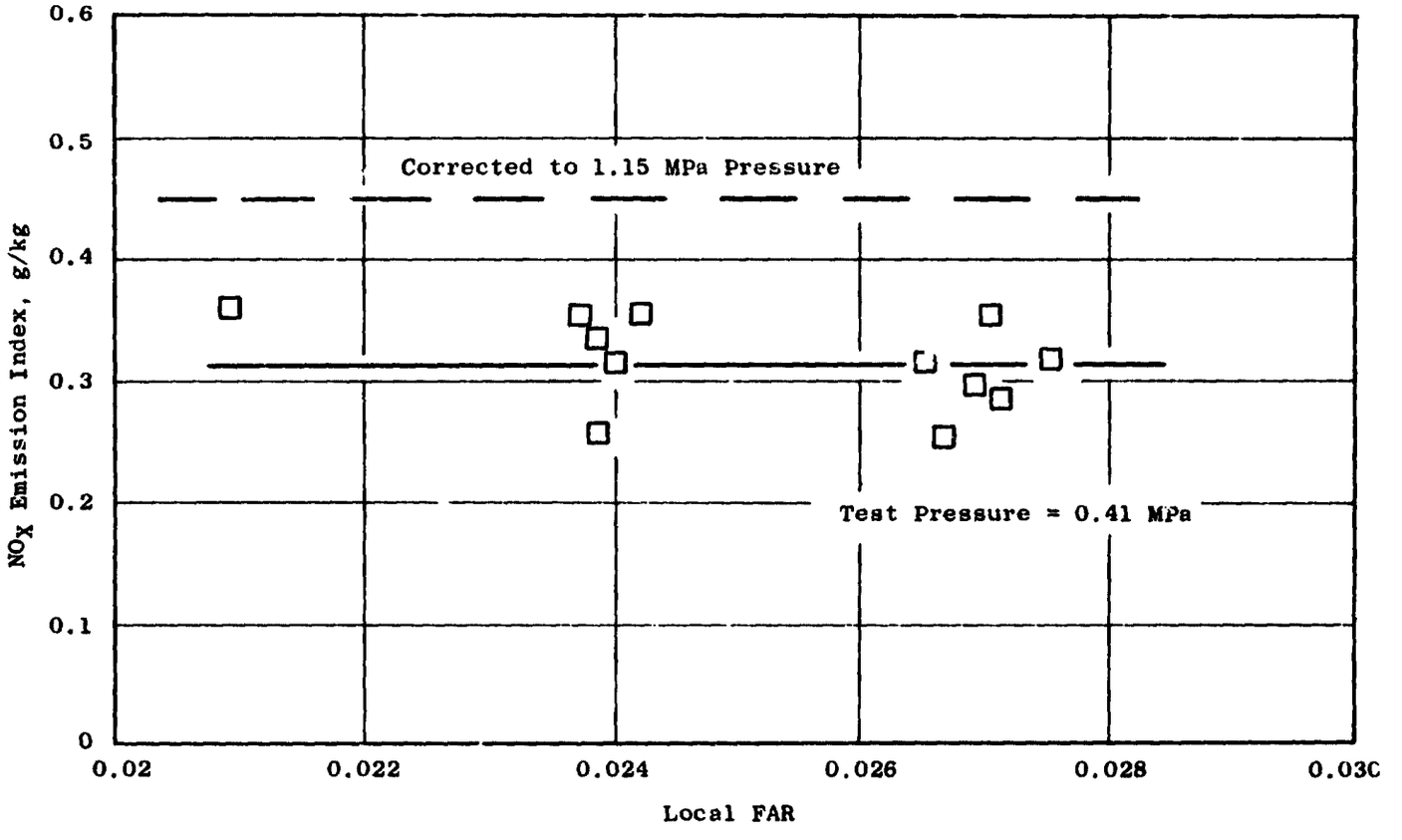

Figure 58. NO_x Emission Index as a Function of Fuel/Air Ratio for Catalytic Reactor of Reverse Flow Combustor at Cruise Power Conditions.

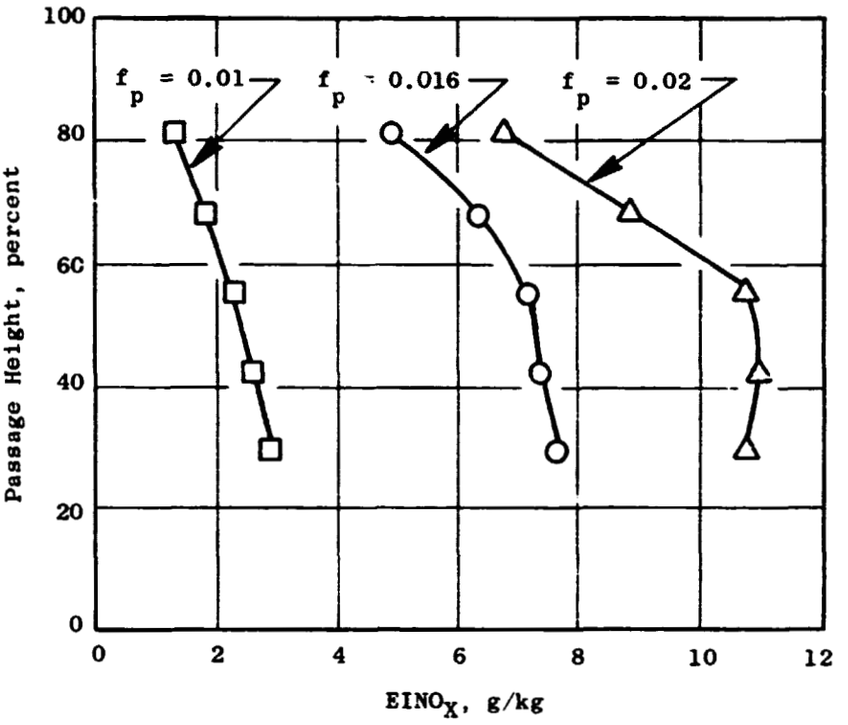

Figure 59. NO_X Emission Index Profile for Pilot Stage of Reverse-Flow Combustor.

with pilot fuel flow. Pilot NO_x is presented as a function of fuel/air ratio for the pilot stage in Figure 60. The data of Figure 60 is also shown adjusted to true engine cruise pressure using a pressure ratio exponent of 0.37. The combined data from Figures 58 and 60 can be used to predict combustion system NO_x as a function of fuel split between the pilot and catalytic reactor. The results are presented in Figure 61. The program goal of 3 g NO_x per kg of fuel can be achieved by using a pilot fuel/air ratio of 0.017 and a catalytic reactor stage average fuel/air ratio of 0.0265. At a cruise inlet temperature of 745 K and assuming a peak-to-average fuel distribution of 1.1, these conditions result in a peak temperature of 1707 K which is essentially at the continuous operating temperature limit of 1700 K for the catalytic reactor.

6.3.2.3 Emissions for EPA Landing - Takeoff Cycle

The same procedures to correct for pressure effects can be used to determine the emissions levels at climb and takeoff conditions to make a comparison with the EPA standards for the landing and takeoff cycle. The results are presented in Table 13. Because of the low idle emissions of the pilot stage and the low NO_x emissions of the catalytic reactor main stage, the EPA standard can be met with considerably more than the 25% margin that was chosen as a goal for this program. Because of this, the fuel/air ratios in the pilot and main stage would be the same at the high power conditions in order to reduce the combustor exit pattern factor. With equal fuel/air ratios in the pilot and main stage, the NO_x EPAP level for the landing and takeoff cycle would increase from 16 (Table 13) to only 16.7. This is still well below the program goal.

6.3.2.4 Smoke and Carbon

One concern at the outset of this program was the possibility of high smoke levels from the pilot stage of the combustor below and at the 60% power condition. Only the pilot is fueled between light off and 60% power. At 60% power, the overall fuel/air ratio is 0.0192 and the pilot primary zone equivalence ratio reaches 1.1 before the switch over to a combined operation with the catalytic reactor and main stage. At 60% power, with pilot-only operation, the measured smoke number was less than 1.0 as compared to a program goal of 15. However, combustor smoking tendency is known to be sensitive to operating

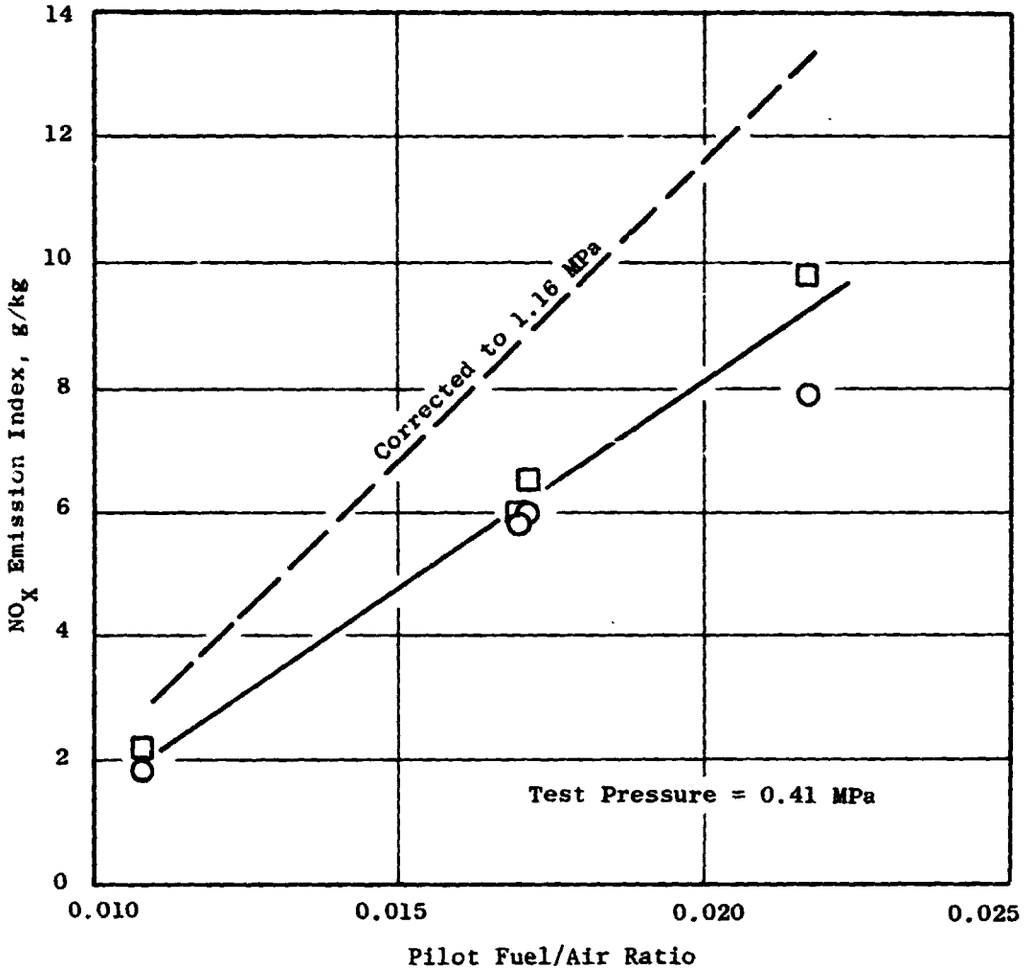

Figure 60. NO_x Emission Index as a Function of Fuel/Air Ratio for Reverse Flow Combustor Pilot at Cruise Conditions.

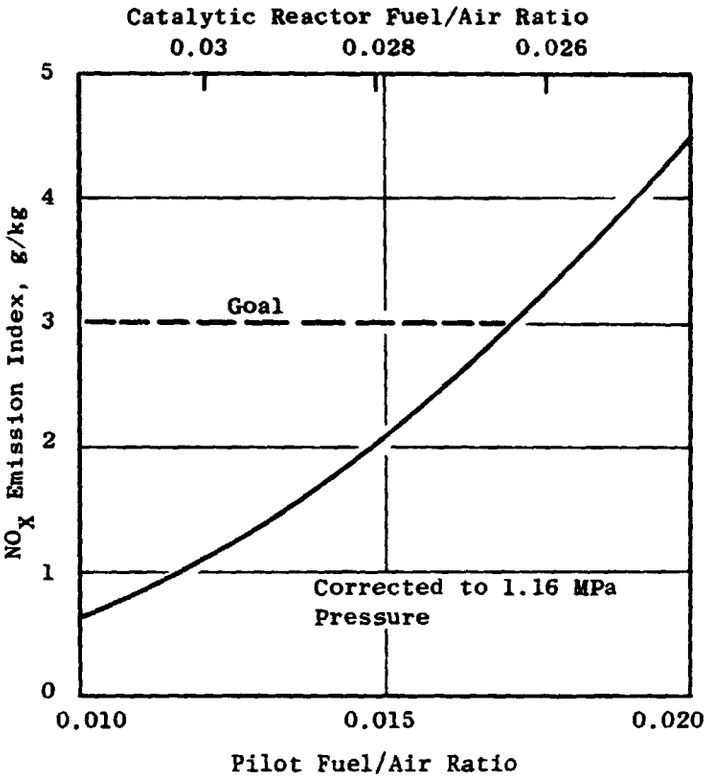

Figure 61. Emission Index as a Function of Pilot and Catalytic Reactor Fuel/Air Ratio for Reverse Flow Combustor at Cruise Conditions.

Table 13. Estimated Emissions for EPA Landing/Takeoff Cycle Based on 4 atm Sector Combustor Tests.

Operational Mode	% Thrust	Time Minutes	Emissions Index g/kg(1)		
			CO	HC	NO_x
Idle	6	26	5.3	0.6	4.8
Approach	30	4	2.6	0.5	11.6
Climb	85	2.2	3.8	0.3	2.9
Takeoff	100	0.7	2.9	0.4	6.0
Measured EPAP (g/kN)			11.5	1.7	16.0
EPAP Goal: 25% Below March 24, 1978 NPRM (g/kN)			19	2.5	25

(1) Test data above idle power level adjusted for pressure.

pressure and the sector tests were conducted at only 0.41 versus 1.9 MPa pressure for the true 60% power condition. Therefore, the smoking tendency of the combustion system should be tested at higher pressure in any future work. However, the ultra-low values measured at 0.41 MPa are very encouraging.

No significant carbon buildup in either the pilot or the main stage of the combustor was observed during the program. Figures 62 and 63 show the pilot dome and the catalytic reactor discharge end, respectively, after an extensive test including a wide range of operation from pilot only operation up to high power operation with both the pilot and main stage fueled. The catalytic reactors had no carbon deposit, as expected, since all continuous operation is at high power and the catalytic elements are swept with hot air (up to 717 K) during the time when the main stage is not fueled. The pilot, which was based on a previously successful design, was also free of carbon.

6.3.2.5 Turbine Inlet Temperature Profiles

Temperature and fuel/air ratio profiles at the turbine inlet (combustor exit) were quite flat for the reverse-flow combustor. Fuel/air profiles for the cruise condition are shown in Figure 64. More fuel was burned in the reactor than in the pilot in order to minimize NO_x emissions; as a result, the fuel/air ratios in line with the reactor are higher than for the pilot. However, both profiles are flat. The average profile, in terms of peak-to-average fuel/air ratio which is important to the turbine, was 1.2 at cruise versus a goal of 1.15.

At higher power conditions, the pilot fuel/air ratio could be set equal to the fuel/air ratio in the reactor, since the NO_x emissions were met with margin and the pilot did not have to be operated in a lean condition. Figure 65 shows profile measurements for climb conditions with the pilot and catalytic reactor at comparable fuel/air ratios. The average profile peak-to-metered overall average fuel/air ratio was 1.15 which was the goal.

No dilution hole pattern adjustments were made during this program. It is likely that some profile improvement could be realized and that improved profiles could be achieved at cruise as well as at high power.

Figure 62. Posttest Condition of Reverse-Flow Combustor Dome Showing No Significant Carbon Deposits.

Figure 63. Posttest Condition of Reverse-Flow Combustor Catalytic Reactors.

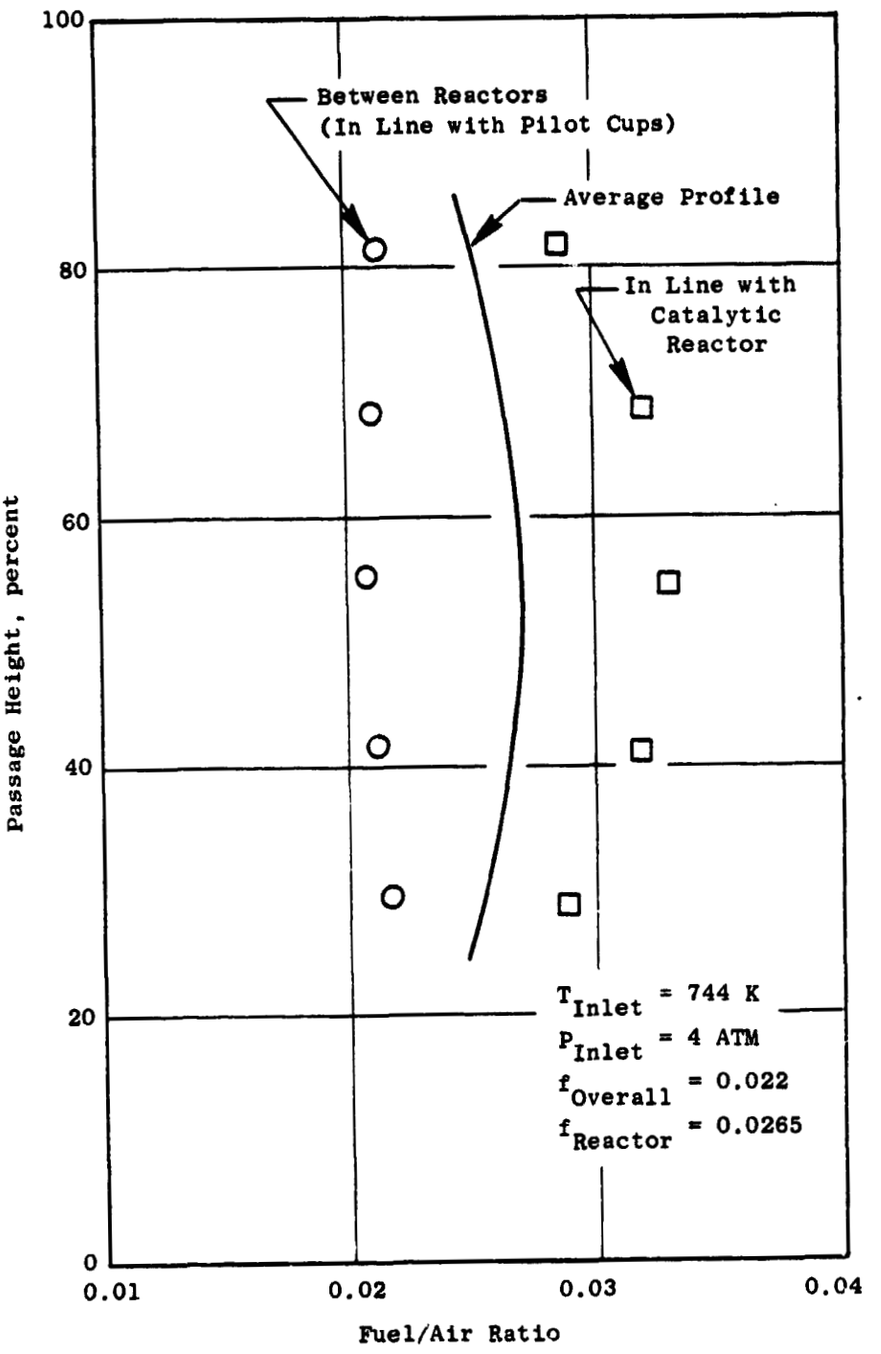

Figure 64. Radial Fuel/Air Ratio Profile for Reverse Flow Combustor at Cruise Conditions.

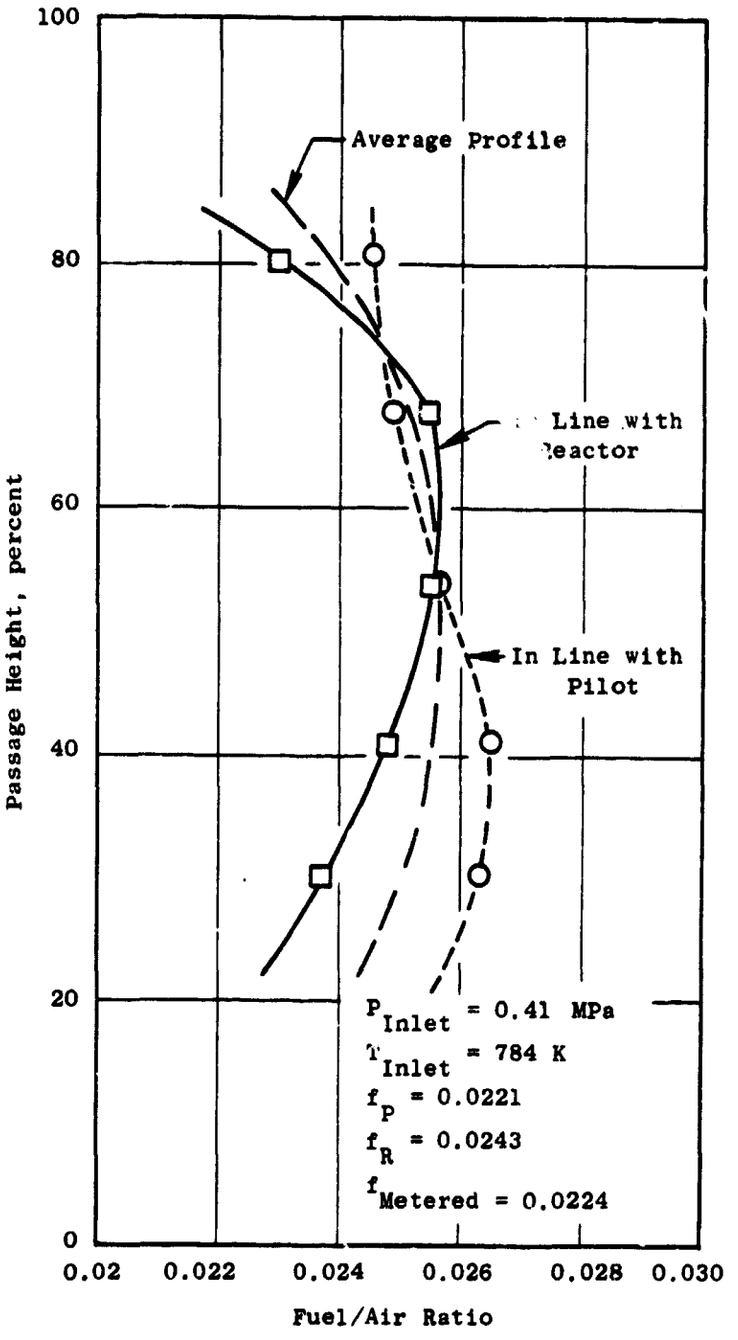

Figure 65. Combustion Discharge Fuel/Air Profile at Climb Power Conditions.

6.3.2.6 Ignition and Lean Blowout

Since the emphasis during this program was on catalytic combustion, only limited pilot stage ignition testing was conducted. Initially, the tests were conducted with an igniter installed through the pilot stage inner liner in the primary zone. This resulted in the igniter being in an inverted position with the tip facing upward. With this arrangement, the igniter tip was subjected to continual fuel wetting and puddling which prevented reliable spark ignition. Subsequent ignition was accomplished with a torch igniter. Two nozzle fuel flow sizes were tested to investigate the effects of fuel spray atomization over a range of airflows. As shown in Figure 66, little difference between the ignition performance of the two fuel nozzles was noted. As airflow and dome velocity increased, the combustor pressure drop increased and mixing and fuel atomization in the swirl cup improved. The results indicate that the pilot light off and lean blowout performance did not quite achieve the target levels at ground start ignition. No pilot ignition capability development was conducted under this program. However, since the pilot is designed specifically for low power operation (rich fuel/air ratios and low velocities) no problem would be anticipated in achieving the desired ignition capability.

No formal ignition tests were conducted with the catalytic reactors, however, in tests with inlet temperatures between 636 and 814 K, activity in the catalytic reactors was observed as soon as fuel was introduced. These observations were made from the thermocouples mounted at the exit plane of the catalytic reactors. The lowest design point inlet temperature is 717 K which is at the 50% engine power condition and well above those where rapid ignition was observed. Also, as expected, no catalytic reactor lean blowout problems were ever encountered during the program at any of the test conditions.

6.3.2.7 Combustor Resonance

During the program, some resonance of the pilot burner was observed at idle conditions. Analysis of acoustic signals taken during resonance showed that the wave length of the signal corresponded to the length of the test rig plenum chamber. The frequency ranged from 620 to 750 Hz and was proportional to the square root of the inlet temperature. The pilot design was based on

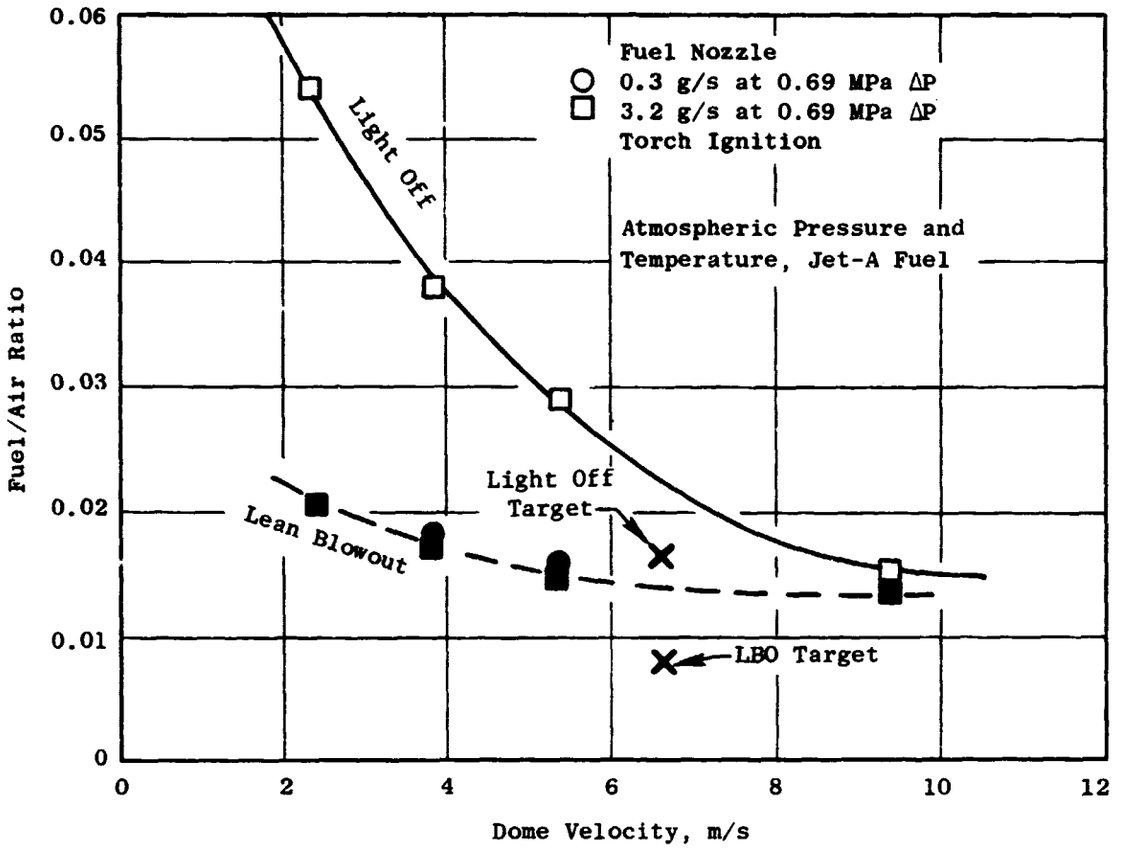

Figure 66. Reverse Flow Combustor Pilot Ground Start Ignition and Lean Blowout Characteristics.

the Energy Efficient Engine combustion system. The E^3 pilot does not have resonance when tested with engine casings. Therefore, it is likely that the resonance of the E^3 pilot would cease to be a problem with engine casings which would have significantly different acoustic characteristics than the test rig plenum chamber. No resonance suppression efforts, such as testing with contoured combustion casings, was undertaken since no damage was attributed to the resonance of the pilot and no resonance was encountered at the higher inlet temperatures where the catalytic reactors were in operation.

6.3.2.8 Liner Temperature and Hardware Durability

Liner temperatures presented no significant problem during this program although some of the temperatures did exceed the goal of 1144 K. The warmest spot on the reverse-flow combustor was on the duct, aft of the catalytic reactor, which reached 1214 K at the takeoff conditions as shown in Figure 67. No distress of the hardware was observed and no attempt was made to reduce the duct operating temperature. In the proposed engine design (Figure 4), this duct would have backside convection cooling which would result in lower operating temperatures. The component test combustor had only film cooling on the hot gas side. The premixing ducts generally operated at or just below the inlet temperature. The catalytic reactor housings operated at 65 to 158 K above the inlet temperature. The peak temperature was at the space between the catalytic reactor elements, possibly due to hot gas leakage.

Durability of the combustor hardware was generally good. The major difficulty was in overtemperaturing and damaging the catalytic reactors. Much of the testing involved operation at very close to the catalytic reactor temperature limit. Several times during the program, the temperature limit of the catalyst was exceeded and damage occurred. When one or more of the reactors for the reverse-flow combustor were damaged, the entire set was replaced to assure consistency among the reactors for subsequent testing. Even so, the individual reactors appeared to increase from the 60% efficiency level to a very high efficiency level at different times during the combustor start up. This magnified the problem of operating close to the catalytic reactor temperature limits. When the efficiency for the first reactor started to rise, pressure drop for that reactor increased, reducing its airflow and further

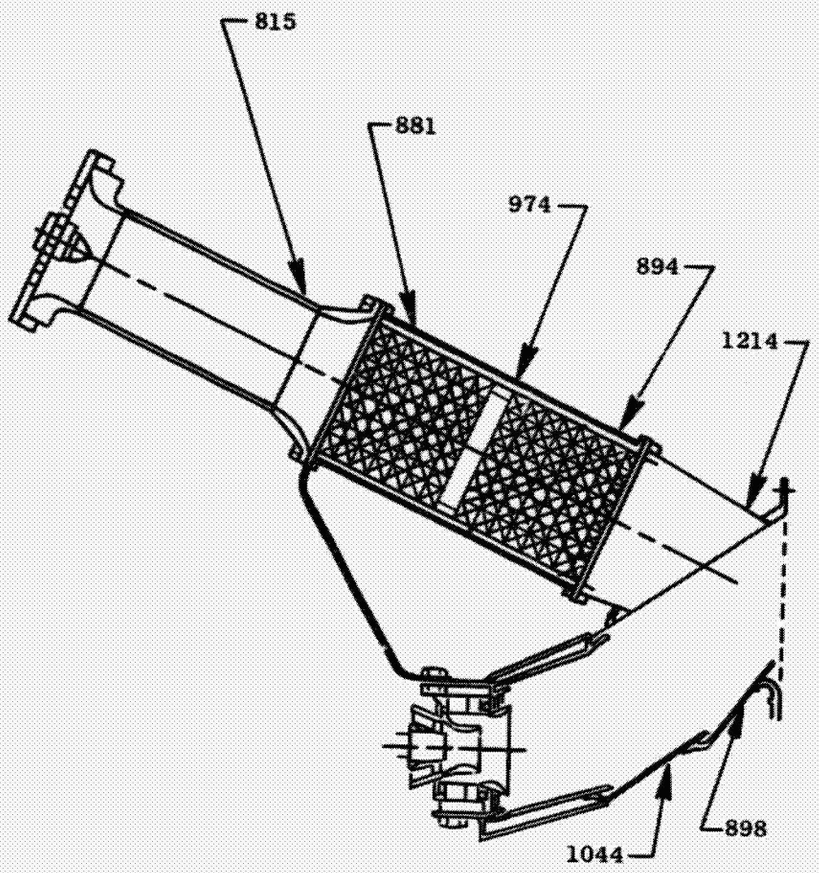

Inlet Temperature = 816 K
Inlet Pressure = 0.41 MPa

Figure 67. Combustor Metal Temperatures at Simulated Takeoff Conditions at 0.41 MPa Pressure.

increasing the fuel/air ratio. This increase in fuel/air ratio resulted in a corresponding increase in efficiency. The slight shift in airflow to the other reactors tended to retard their rise to high combustion efficiency. In order to provide better control in setting test points and reduce hardware damage, individual fuel control valves were added to the fuel supply to each of the reactors. For catalytic reactors with higher operating temperature capabilities, the complexity of individual fuel controls would not be required.

7.0 CONCLUDING REMARKS

During this program, the ultra-low NO_x emissions levels which were expected with catalytic combustion were demonstrated with an actual aircraft gas turbine combustion system. However, it does not appear likely that catalytic combustion will be utilized in modern high pressure ratio, high temperature aircraft gas turbines in the foreseeable future. Considerable advancement in catalytic reactor temperature capability would be required before catalytic combustors would become practical. Also, the concern about NO_x emissions from aircraft engines has subsided and the proposed EPA regulations for NO_x have not been promulgated. Catalytic combustion systems for aircraft turbine engines will, however, continue to look attractive because of their potential for improved hot section durability through improved combustor exit pattern factor and profile.

The use of a catalytic combustion system in stationary power engines would seem to be more practical since cycle pressures and temperatures are generally lower and NO_x emissions levels are much more stringent. For the overall catalytic combustion system tested during this program, NO_x emission indices of 3 g/kg appear possible. This level translates to approximately 40 ppm reference 15% oxygen. This represents a reduction of about 85% from typical uncontrolled levels for aircraft derivative engines burning liquid fuels. For the main stage catalytic reactor alone, the emissions index was less than 0.5 g/kg or approximately 7 ppm reference 15% oxygen, which would be a 98% reduction from the uncontrolled levels. Furthermore, in stationary power systems, small combustor length and size are not of critical importance. Relaxation of the reference velocity constraint imposed in the current program would improve the range of operation of the reactor.

The development of any future catalytic combustion system will require a significant portion of development effort to achieve uniform fuel distribution. One very successful method to achieve uniform fuel distribution was developed on this program and that was to use a flow restriction ahead of the fuel injector to match the airflow pattern to the fuel spray pattern and to increase turbulence.

Several areas that were not investigated during this program were long time durability of the catalysts and catalytic reactor substrates, effects of transients on the catalytic reactor life, and transient operational characteristics of the overall system. These areas will require evaluation in any future development of catalytic combustion systems.

8.0 SUMMARY OF RESULTS

A combustor program was conducted to evolve and to identify the technology needed for, and to establish the credibility of, using combustors with catalytic reactors in modern high-pressure-ratio aircraft turbine engines.

Two catalytic combustor concepts were designed, fabricated, and evaluated. The combustors were sized for use in the NASA/General Electric Energy Efficient Engine. One of the combustor designs was a basic parallel-staged double-annular combustor. The second design was also a parallel-staged combustor but employed reverse flow cannular catalytic reactors.

Subcomponent tests of fuel injection systems and of catalytic reactors for use in the combustion system were also conducted.

Major conclusions of this program were:

- Successful operation with high combustion efficiency has been achieved with an aircraft gas turbine combustion system using a state-of-the-art catalytic reactor as the main stage along with a conventional pilot stage for low-power operation.

- Ultra-low NO_x emissions levels that met the goals of the program were achieved.

- The catalytic reactor maximum operating temperature limit was the major constraint on the operation of the two catalytic combustion systems evaluated. At the cruise operating condition, in order to meet the ultra-low NO_x emissions goal, it was necessary to operate the catalytic reactor at the continuous operating temperature limit even when a very uniform fuel distribution was achieved. Considerable advancement in the operating temperature capability of catalytic reactor materials will be required for successful application of catalytic combustors to very high-pressure-ratio, high temperature engines of the type considered in this study.

- A considerable effort will be required to develop reliable short-length, fuel/air preparation systems to provide uniform fuel/air distribution into the catalytic reactors.

- One very promising method for achieving a uniform fuel distribution in the premixing process is to use a pressure drop device (perforated plate) in series with the premixing duct to provide a means to adjust the inlet air profile.

- A maximum design reference velocity of 24 to 27 m/s for the catalytic reactor has been determined for high performance levels at the actual engine pressure conditions studied on this program.

9.0 REFERENCES

1. Dodds, W.J., "Advanced Catalytic Combustors for Low Pollutant Emissions, Phase I Final Report," NASA CR-159535, December 1978.

2. Lyon, T.F., Dodds, W.J., and Bahr, D.W., "Determination of Pollutant Emissions Characteristics of General Electric CF6-6 and CF6-50 Model Engines," FAA-EE-80-27, March 1980.

3. Control of Air Pollution from Aircraft and Aircraft Engines - Proposed Amendments to Standards, U.S. Environmental Protection Agency, Federal Register, Volume 43, Number 58, March 1978.

4. "Energy Efficient Engine - Preliminary Design and Integration Studies, Final Report," NASA CR-135444, September 1978.

5. Gleason, C.C., Rogers, D.W., and Bahr, D.W., "Experimental Clean Combustor Program, Phase II Final Report," NASA CR-134981, July 1976.

6. Gleason, C.C. and Bahr, D.W., "Experimental Clean Combustor Program, Phase III Final Report," NASA CR-135384, June 1979.

7. Dodds, W.J., Gleason, C.C., and Bahr, D.W., "Aircraft Gas Turbine Low Power Emissions Reduction Technology Program - Final Report," NASA CR-135434, October 1978.

8. Marek, C.J., Papthakos, L.C., and Verbulecz, P.W., "Preliminary Studies of Autoignition and Flashback in a Premixing-Prevaporizing Flame Tube Using Jet-A Fuel at Lean Equivalence Ratios," NASA TM X-3526, May 1977.

9. "Procedure for the Continuous Sampling and Measurement of Gaseous Emissions from Aircraft Turbine Engines," Society of Automotive Engineers, Aerospace Recommended Practice, ARP1256A, Revised October 1, 1980.

10. "Aircraft Gas Turbine Engine Exhaust Smoke Measurement," Society of Automotive Engineers, Aerospace Recommended Practice ARP1179A, Revised June 15, 1980.

11. Tacina, R., "Experimental Evaluation of Premixing-Prevaporizing Fuel Injection Concepts for a Gas Turbine Catalytic Combustor," NASA TM-73755, August 1977.

12. Spadaccini, L.J., "Autoignition Characteristics of Hydrocarbon Fuels at Elevated Temperatures and Pressures," ASME Paper 76-GT-3, March 1973.

13. Roffe, G. and Venkataramani, K.S., "Emission Measurements for a Lean Premixed Propane/Air System at Pressures up to 30 Atmospheres," NASA CR-159421, August 1978.

14. Dodds, W.J. and Ekstedt, E.E., "Demonstration of Catalytic Combustion with Residual Fuel," Final Report, NASA CR-165369, August 1981.

APPENDIX A - NOMENCLATURE

EICO	CO Emission Index, g/kg
EIHC	HC Emission Index, g/kg
$EINO_x$	NO_x Emission Index, g/kg
f	Total fuel/air ratio
f_P	Pilot fuel/air ratio
f_R	Reactor fuel/air ratio
fs	Fuel/air ratio sample (from gas analysis)
P_{inlet}, P_3	Combustor inlet pressure, kPa
PTF	Pattern factor
R	Radius, cm
SN	Smoke number
T_{inlet}, T_3	Combustor inlet temperature, K
T_{Pmax}	Maximum pilot liner temperature, K
T_R	Average reactor exit temperature, K
T_{R1}	Reactor exit temperature No. 1, K
T_{R2}	Reactor exit temperature No. 2, K
T_{R3}	Reactor exit temperature No. 3, K
T_{R4}	Reactor exit temperature No. 4, K
TR_{max}	Maximum reactor shell temperature, K
T4	Average combustor exit temperature, K
V	Velocity, m/s
W_A	Combustor Airflow, kg/s
W_f	Total combustor fuel flow, g/s
W_{fP}	Pilot fuel flow, g/s
W_{fR}	Reactor fuel flow, g/s
ΔP_{fP}	Pilot fuel injection pressure drop, kPa
ΔP_{fR}	Reactor fuel injection pressure drop, kPa
$\Delta P/P$	Total pressure loss, %
η_s	Combustion efficiency (from gas analysis), %
σ	Standard deviation
τ	Premixing duct residence time, ms

APPENDIX B - CATALYTIC COMBUSTOR SECTOR TEST DATA

The two catalytic combustors, the parallel-staged and the reverse flow, were tested in a one-sixth sector (60°) portion of the full scale combustors. A total of eight separate tests were run, two with the parallel staged combustor and six with the reverse flow combustor. A summary of the combustor test data is given in the following tables, along with a brief description of the configuration tested and the results of the test. The reverse flow combustor results are first presented, followed by results of the two tests of the parallel-staged combustor.

Table B-1 summarizes the results of the first test of the reverse flow combustor (baseline test). Some plugging of the inlet to the reactors occurred during this test and some reactor damage was sustained.

Table B-2 summarizes the results of the second test of the reverse flow combustor (Modification Number 1). A perforated plate was added to reduce the reference velocity and valves were added to control flow to the individual reactor fuel nozzles. Good results (high combustion efficiency with low NO_x) were obtained. No significant reactor damage occurred.

Table B-3 summarizes the results of the third test of the reverse flow combustor (Modification Number 2). The combustor configuration was essentially the same as for the previous test but thermocouples were added at the reactor exit to obtain the exit temperature distribution. In an attempt to run the system at lower pressures, some large temperature excursions occurred and significant reactor damage was sustained.

Table B-4 summarizes the results of the fourth test of the reverse flow combustor. The major combustor change was the use of the short premixing duct ahead of the reactors. As on the previous test, exit temperature distribution was measured. As expected, profiles were not as uniform with the short duct as with the long duct previously used.

Table B-5 summarizies the results of the fifth test of the reverse flow combustor. A redesigned perforated plate was used which resulted in more uniform temperature distribution. In addition, a spectrum analyzer (Schlumberger

Table B-1. Clean Catalytic Combustor - Sector Test Data Summary.

Combustor Configuration: Reverse Flow Baseline

Run: 8 Date: November 17-19, 1981

Reading Number	2	3	4	5	6	7	8
Nominal Power Setting, %	Idle	30	30	60	60	60	60
Combustor Inlet Data							
Fuel Split, Pilot/Total	1.0	1.0	1.0	0.456	0.544	1.0	0
T_3 - Inlet Temperature, K	492	616	619	718	715	710	712
P_3 - Inlet Pressure, kPa	414	415	[illegible]	414	412	418	403
WA - Airflow, kg/s	1.606	1.402	[illegible]02	1.297	1.329	1.306	1.320
W_f - Fuel Flow, g/s	15.31	14.87	20.79	28.10	34.27	21.34	14.93
W_{fP} - Pilot Fuel Flow, g/s	15.31	14.87	20.79	12.12	18.65	21.34	0
W_{fR} - Reactor Fuel Flow, g/s	0	0	0	15.96	15.62	0	14.93
f - Total Fuel/Air Ratio	0.0095	0.0106	0.0148	0.0217	0.0258	0.0163	0.0113
f_P - Pilot Fuel/Air Ratio*	0.0220	0.0244	0.0342	0.0215	0.0323	0.0376	0
f_R - Reactor Fuel/Air Ratio*	0	0	0	0.0226	0.0216	0	0.0208
ΔP_{fP} - Pilot Fuel Injector Pressure Drop, kPa	614	593	1172	545	931	1234	0
ΔP_{fR} - Reactor Fuel Injector Pressure Drop, kPa	0	0	0	1855	1855	0	1834
Combustion Exit Data							
$\Delta P/P$ - Total Pressure Loss, %	4.83	5.57	4.[illegible]9	6.99	6.86	4.95	6.84
T_{R1} - Reactor Exit Temperature No. 1, K				1213	1475		---
T_{R2} - Reactor Exit Temperature No. 2, K				1202	1291		1695
T_{R3} - Reactor Exit Temperature No. 3, K				1513	---		
T_{R4} - Reactor Exit Temperature No. 4, K				---	---		---
T_R - Average Reactor Exit Temperature, K							
T_4 - Average Combustor Exit Temperature, K	693	784	866	1309	1211	906	1103
PTF - Pattern Factor	2.31	2.92	2.63	0.38	0.84	3.11	1.18
Gas Analysis Data							
EICO - CO Emission Index, g/kg	28.5	5.2	8.9	79.6	108.2	7.8	20.9
EIHC - HC Emission Index, g/kg	8.3	3.5	1.9	165.8	236.7	3.0	369.9
$EINO_x$ - NO_x Emission Index, g/kg	3.7	7.1	10.3	0.7	2.9	6.1	0.2
f_g - Fuel/Air Ratio (From Gas Sample)	0.0056	0.0061	0.0099	0.0243	0.0212	0.0110	0.0135
η_g - Combustor Efficiency (From Gas Sample), %	98.6	99.6	99.6	83.7	76.9	99.6	67.4
SN - Smoke Number	---	---	0	---	---	---	---
Metal Temperatures							
$T_{P,Max}$ - Maximum Pilot Liner Temperature, K	783	974	1060	996	1096	1193	798
$T_{R,Max}$ - Maximum Reactor Shell Temperature, K	503	631	644	1015	1142	710	713

*Based on Pilot Airflow = 0.434 * WA
Reactor Airflow = 0.545 * WA

Table B-2. Clean Catalytic Combustor - Sector Test Data Summary.

Combustor Configuration: Reverse Flow Modification 1/7

Run: 12 Date: January 27, 1982

Reading Number	2	3	4	5	7	8	9
Nominal Power Setting, %	Idle	30	60	60	60	60	60
Combustor Inlet Data							
Fuel Split, Pilot/Total	1.0	1.0	1.0	0.738	1.0	0.668	0.557
T_3 - Inlet Temperature, K	498	635	720	719	721	716	720
P_3 - Inlet Pressure, kPa	403	416	411	416	414	419	417
WA - Airflow, kg/s	1.13	1.01	0.93	0.93	0.93	0.93	0.93
W_f - Fuel Flow, g/s	18.0	18.9	24.5	18.4	24.3	18.6	16.8
W_{fP} - Pilot Fuel Flow, g/s	18.0	18.9	24.5	13.6	24.3	12.4	9.4
W_{fR} - Reactor Fuel Flow, g/s	0	0	0	4.8	0	6.2	7.4
f - Total Fuel/Air Ratio	0.0159	0.0188	0.0263	0 0199	0.0260	0.0199	0.0180
f_P - Pilot Fuel/Air Ratio*	0.0277	0.0328	0.0460	0.0257	0.0454	0.0233	0.0175
f_R - Reactor Fuel/Air Ratio*	0	0	0	0.0131	0	0.0166	0.0201
ΔP_{fP} - Pilot Fuel Injector Pressure Drop, kPa	0.848	938	1.503	0.407	---	0.441	0.255
ΔP_{fR} - Reactor Fuel Injector Pressure Drop, kPa	0	0	0	2.785	0	4.612	6578
Combustion Exit Data							
$\Delta P/P$ - Total Pressure Loss, %	4.5	4.6	4.7	5.0	6.5	5.8	5.5
T_{R1} - Reactor Exit Temperature No. 1, K				---		1021	1133
T_{R2} - Reactor Exit Temperature No. 2, K				1213		1304	1473
T_{R3} - Reactor Exit Temperature No. 3, K				954		1063	1166
T_{R4} - Reactor Exit Temperature No. 4, K				1066		1218	1421
T_R - Average Reactor Exit Temperature, K				1078		1151	1298
T_4 - Average Combustor Exit Temperature, K	844	1026	1266	1079	1209	1180	1098
PTF - Pattern Factor	0.89	0.64	0.51	0.67	0.87	0.32	0.39
Gas Analysis Data							
EICO - CO Emission Index, g/kg	4	4	9	54	10	89	92
EIHC - HC Emission Index, g/kg	2	1	0	78	1	81	69
$EINO_x$ - NO_x Emission Index, g/kg	4.4	8.9	13.9	5.9	12.9	4.2	3.2
f_g - Fuel/Air Ratio (From Gas Sample)	0.0146	0.0166	0.0245	0.0179	0.0273	0.0190	0.0201
η_b - Combustor Efficiency (From Gas Sample), %	99.7	99.8	99.8	92.0	99.7	90.9	91.9
SN - Smoke Number	---	---	0	---	---	---	---
Metal Temperatures							
$T_{P,Max}$ - Maximum Pilot Liner Temperature, K	774	976	1157	1011	1152	1003	949
$T_{R,Max}$ - Maximum Reactor Shell Temperature, K	543	696	813	954	814	1020	1091

*Based on Pilot Airflow = 0.434 * WA
Reactor Airflow = 0.545 * WA

Table B-2. Clean Catalytic Combustor - Sector Test Data Summary. (Continued)

Combustor Configuration: Reverse Flow Modification 1/7

Run: 12 Date: January 27, 1982

Reading Number	10	11	12	13	14	15
Nominal Power Setting, %	Cruise	Cruise	Climb	Climb	T/O	T/O
Combustor Inlet Data						
Fuel Split, Pilot/Total	0.736	0.651	0.747	0.652	0.770	0.676
T_3 - Inlet Temperature, K	744	744	780	781	816	815
P_3 - Inlet Pressure, kPa	415	417	419	415	413	418
WA - Airflow, kg/s	0.87	0.87	0.85	0.85	0.83	0.83
W_f - Fuel Flow, g/s	22.2	21.5	22.5	21.1	24.2	22.5
W_{fP} - Pilot Fuel Flow, g/s	16.3	14.0	16.8	13.8	18.6	15.2
W_{fR} - Reactor Fuel Flow, g/s	5.9	7.5	5.7	7.3	5.6	7.3
f - Total Fuel/Air Ratio	0.0255	0.0247	0.0265	0.0249	0.0292	0.0270
f_P - Pilot Fuel/Air Ratio*	0.0327	0.0280	0.0345	0.0283	0.0392	0.0319
f_R - Reactor Fuel/Air Ratio*	0.0169	0.0216	0.0168	0.0217	0.0169	0.0220
ΔP_{fP} - Pilot Fuel Injector Pressure Drop, kPa	0.752	0.545	0.786	0.490	0.958	0.662
ΔP_{fR} - Reactor Fuel Injector Pressure Drop, kPa	4.413	6.578+	4.302	6.578+	4.509	6.578+
Combustion Exit Data						
$\Delta P/P$ - Total Pressure Loss, %	4.5	5.0	5.1	4.7	4.8	5.6
T_{R1} - Reactor Exit Temperature No. 1, K	1055	1219	1061	1230	1050	1230
T_{R2} - Reactor Exit Temperature No. 2, K	1332	1565	1329	1579	1285	1596
T_{R3} - Reactor Exit Temperature No. 3, K	1082	1259	1095	1224	1048	1155
T_{R4} - Reactor Exit Temperature No. 4, K	1270	1515	1264	1541	1229	1560
T_R - Average Reactor Exit Temperature, K	1185	1390	1187	1394	1153	1385
T_4 - Average Combustor Exit Temperature, K	1194	1190	1214	1274	1241	1383
PTF - Pattern Factor	0.62	0.55	0.75	0.40	0.45	0.38
Gas Analysis Data						
EICO - CO Emission Index, g/kg	92	108	96	61	85	19
EIHC - HC Emission Index, g/kg	54	39	59	52	52	71
$EINO_x$ - NO_x Emission Index, g/kg	9.5	6.5	12.0	7.0	14.7	10.7
f_g - Fuel/Air Ratio (From Gas Sample)	0.0247	0.0246	0.0262	0.0242	0.0271	0.0262
η_g - Combustor Efficiency (From Gas Sample), %	93.2	94.1	92.7	94.0	90.1	93.4
SN - Smoke Number						
Metal Temperatures						
$T_{P,max}$ - Maximum Pilot Liner Temperature, K	1092	1060	1150	1104	1214	1179
$T_{R,max}$ - Maximum Reactor Shell Temperature, K	1055	1153	1050	1175	1051	1214

*Based on Pilot Airflow = 0.434 * WA
Reactor Airflow = 0.565 * WA

Table B-2. Clean Catalytic Combustor - Sector Test Data Summary. (Concluded)

Combustor Configuration: Reverse Flow Modification 1/23

Run: 13 Date: January 1982

Reading Number	2	3	4	5	6	7	8
Nominal Power Setting, %	60	60	Cruise	Cruise	Climb	Climb	T/O
Combustor Inlet Data							
Fuel Split, Pilot/Total	0.540	0.406	0.647	0.549	0.655	0.566	0.684
T_3 - Inlet Temperature, K	713	714	747	749	784	784	814
P_3 - Inlet Pressure, kPa	412	416	415	409	408	414	413
WA - Airflow, kg/s	0.93	0.93	0.86	0.87	0.83	0.84	0.83
W_f - Fuel Flow, g/s	16.8	16.2	20.8	19.2	20.8	18.8	23.5
W_{fP} - Pilot Fuel Flow, g/s	9.1	6.6	13.4	10.6	13.6	10.6	16.1
W_{fR} - Reactor Fuel Flow, g/s	7.7	9.6	7.3	8.7	7 2	8.2	7.4
f - Total Fuel/Air Ratio	0.0181	0.0174	0.0240	0.0222	0.0249	0.0224	0.0283
f_p - Pilot Fuel/Air Ratio*	0.0171	0.0123	0.0272	0.0213	0.0285	0.0221	0.0338
f_R - Reactor Fuel/Air Ratio*	0.0210	0.0259	0.0213	0.0252	0.0216	0.0244	0.0225
ΔP_{fP} - Pilot Fuel Injector Pressure Drop, kPa	0.241	0.131	0.524	0.331	0.538	0.338	0.724
ΔP_{fR} - Reactor Fuel Injector Pressure Drop, kPa	1.627	2.413	1.455	1.999	1.427	1.820	1.544
Combustion Exit Data							
$\Delta P/P$ - Total Pressure Loss, %	6.7	4.5	5.3	6.2	4.4	3.5	4.5
T_{R1} - Reactor Exit Temperature No. 1, K	1416	1653	1437	1644	1436	1660	1520
T_{R2} - Reactor Exit Temperature No. 2, K	1389	1666	1425	1669	1460	1665	1513
T_{R3} - Reactor Exit Temperature No. 3, K	1407	1684	1425	1663	1440	1646	1499
T_{R4} - Reactor Exit Temperature No. 4, K	1368	1660	1421	1661	1449	1668	1540
T_R - Average Reactor Exit Temperature, K	1395	1666	1427	1659	1446	1660	1518
T_4 - Average Combustor Exit Temperature, K	1086	1091	1129	1173	1224	1196	1294
PTF - Pattern Factor	0.38	0.60	0.83	0.58	0.56	0.60	0.65
Gas Analysis Data							
EICO - CO Emission Index, g/kg	165	17	39	3	25	3	12
EIHC - HC Emission Index, g/kg	11	2	4	0	3	1	2
$EINO_x$ - NO_x Emission Index, g/kg	3.1	1.1	8.4	4.9	10.1	7.0	13.8
f_g - Fuel/Air Ratio (From Gas Sample)	0.0192	0.0195	0.0245	0.0244	0.0261	0.0244	0.0293
η_g - Combustor Efficiency (From Gas Sample), %	95.2	99.5	98.7	99.9	99.2	99.9	99.6
SN - Smoke Number							
Metal Temperatures							
$T_{P,Max}$ - Maximum Pilot Liner Temperature, K	773	744	888	851	912	876	942
$T_{R,Max}$ - Maximum Reactor Shell Temperature, K	1028	1184	1121	1219	1155	1225	1208

*Based on Pilot Airflow = 0.434 * WA
Reactor Airflow = 0.545 * WA

Table B-3. Clean Catalytic Combustor - Sector Test Data Summary.

Combustor Configuration: Reverse Flow Modification 2

Run: 14 Date: February 12, 22, 24, 1982

Reading Number	2	3	4	7	8	9	10	11	12
Nominal Power Setting, %	Idle	30	60	60	60	60	Cruise	Cruise	Cruise
Combustor Inlet Data									
Fuel Split, Pilot/Total	1.0	1.0	1.0	0.583	0.542	0.528	0.535	0.523	0.409
T_3 - Inlet Temperature, K	494	636	719	717	718	715	744	743	745
P_3 - Inlet Pressure, kPa	401	416	412	412	410	414	413	416	416
WA - Airflow, kg/s	1.19	0.98	0.91	0.86	0.86	0.86	0.84	0.84	0.84
W_f - Fuel Flow, g/s	17.2	13.8	24.0	15.4	15.9	16.5	15.2	15.6	12.7
W_{fp} - Pilot Fuel Flow, g/s	17.2	13.8	24.0	8.8	8.6	8.7	8.1	8.2	5.2
W_{fR} - Reactor Fuel Flow, g/s	0	0	0	6.6	7.3	7.8	7.1	7.4	7.5
f - Total Fuel/Air Ratio	0.0144	0.0140	0.0264	0.0179	0.0185	0.0192	0.0180	0.0186	0.0150
f_p - Pilot Fuel/Air Ratio*	0.0255	0.0247	0.0466	0.0181	0.0176	0.0179	0.0170	0.0171	0.0108
f_R - Reactor Fuel/Air Ratio*	0	0	0	0.0191	0.0212	0.0227	0.0210	0.0222	0.0223
ΔP_{fp} - Pilot Fuel Injector Pressure Drop, kPa	114	75	213	32	23	30	27	29	10
ΔP_{fR} - Reactor Fuel Injector Pressure Drop, kPa	0	0	0	160	194	217	182	202	202
Combustion Exit Data									
$\Delta P/P$ - Total Pressure Loss, %	4.7	4.2	5.4	4.5	3.5	4.3	3.3	3.8	3.8
T_{R1} - Reactor Exit Temperature No. 1, K				1410	1580	1596	1587	1577	1600
T_{R2} - Reactor Exit Temperature No. 2, K				1424	1594	1695	1581	1690	1685
T_{R3} - Reactor Exit Temperature No. 3, K				1423	1587	1694	1575	1681	1688
T_{R4} - Reactor Exit Temperature No. 4, K				1411	1585	1589	1581	1570	1606
T_R - Average Reactor Exit Temperature, K				1417	1587	1644	1581	1630	1645
T_4 - Average Combustor Exit Temperature, K									
PTF - Pattern Factor									
Gas Analysis Data									
EICO - CO Emission Index, g/kg	5	3	13	32	10	3	13	3	7
EIHC - HC Emission Index, g/kg	1	1	0	2	1	0	1	0	0
$EINO_x$ - NO_x Emission Index, g/kg	4.8	7.8	14.3	5.6	4.6	4.2	4.4	4.1	1.2
f_s - Fuel/Air Ratio (From Gas Sample)	0.0135	0.0137	0.0252	0.0212	0.0220	0.0243	0.0213	0.0231	0.0188
n_s - Combustor Efficiency (From Gas Sample)	99.8	99.9	99.7	99.1	99.7	99.9	99.6	99.9	99.8
SN - Smoke Number									
Metal Temperatures									
$T_{P,Max}$ - Maximum Pilot Liner Temperature, K	761	941	1083	955	956	956	970	970	915
$T_{R,Max}$ - Maximum Reactor Shell Temperature, K	494	639	720	958	1023	1073	1026	1084	1071

*Based on Pilot Airflow = 0.566 * WA
Reactor Airflow = 0.399 * WA

Table B-3. Clean Catalytic Combustor - Sector Test Data Summary. (Concluded)

Combustor Configuration: Reverse Flow Modification 2

Run: 14 Date: February 12, 22, 24, 1982

Reading Number	13	14	15	16	17	18	19	20
Nominal Power Setting, %	Cruise	85	85	100	100	Cruise	Cruise	Cruise
Combustor Inlet Data								
Fuel Split, Pilot/Total	0.578	0.537	0.497	0.532	0.515	0.497	0.501	0.493
T_3 - Inlet Temperature, K	743	783	781	808	813	748	748	747
P_3 - Inlet Pressure, kPa	416	410	414	412	413	307	412	410
WA - Airflow, kg/s	0.84	0.84	0.86	0.82	0.82	0.64	1.01	1.12
W_f - Fuel Flow, g/s	17.8	15.2	15.7	15.4	15.3	12.3	18.8	21.7
W_{fp} - Pilot Fuel Flow, g/s	10.3	8.2	7.8	8.2	7.9	6.1	9.4	10.7
W_{fR} - Reactor Fuel Flow, g/s	7.5	7.0	7.9	7.2	7.4	6.2	9.4	11.0
f - Total Fuel/Air Ratio	0.0212	0.0182	0.0185	0.0188	0.0187	0.0193	0.0187	0.0193
f_p - Pilot Fuel/Air Ratio*	0.0217	0.0172	0.0162	0.0177	0.0170	0.0169	0.0166	0.0168
f_R - Reactor Fuel/Air Ratio*	0.0224	0.0210	0.0232	0.0221	0.0227	0.0242	0.0234	0.0245
ΔP_{fp} - Pilot Fuel Injector Pressure Drop, kPa	44	27	29	30	30	15	37	45
ΔP_{fR} - Reactor Fuel Injector Pressure Drop, kPa	209	184	211	196	206	140	313	420
Combustion Exit Data								
$\Delta P/P$ - Total Pressure Loss, %	5.1	3.5	6.0	5.0	4.0	5.2	6.4	8.2
T_{R1} - Reactor Exit Temperature No. 1, K	1601	1583	1647	1320	1659	1685	1648	1285
T_{R2} - Reactor Exit Temperature No 2, K	1685	1580	1689	1476	1685	1693	1614	1659
T_{R3} - Reactor Exit Temperature No. 3, K	1687	1572	1669	1589	1666	1698	1658	1695
T_{R4} - Reactor Exit Temperature No. 4, K	1605	1581	1718	1585	1643	1712	1427	1443
TR - Average Reactor Exit Temperature, K	1645	1579	1681	1493	1663	1697	1587	1521
T_4 - Average Combustor Exit Temperature, K								
PTF - Pattern Factor								
Gas Analysis Data								
EICO - CO Emission Index, g/kg	2	7	4	4	3	2	12	9
EIHC - HC Emission Index, g/kg	0	0	0	1	0	2	1	1
$EINO_x$ - NO_x Emission Index, g/kg	6.4	4.9	4.2	5.4	4.2	2.2	3.1	2.5
f_g - Fuel/Air Ratio (From Gas Sample)	0.0257	0.0210	0.0220	0.0219	0.0207	0.0225	0.0217	0.0227
η_g - Combustor Efficiency (From Gas Sample)	99.9	99.8	99.9	99.9	99.9	99.8	97.0	99.7
SN - Smoke Number								
Metal Temperatures								
$T_{P,Max}$ - Maximum Pilot Liner Temperature, K	1007	1009	985	1026	1029	961	970	980
$T_{R,Max}$ - Maximum Reactor Shell Temperature, K	1084	1065	1029	1067	1076	1048	1019	1051

*Based on Pilot Airflow = 0.566 * WA
Reactor Airflow = 0.399 * WA

Table B-4. Clean Catalytic Combustor - Sector Test Data Summary.

Combustor Configuration: Reverse Flow Modification 3, Short Inlet

Run: 15 Date: March 15-16, 1982

Reading Number	2	3	4	5	6	7	8
Nominal Power Setting, %	Idle	Idle	30	60	60	60	60
Combustor Inlet Data							
Fuel Split, Pilot/Total	1.0	1.0	1.0	1.0	0.585	0.550	0.550
T_3 - Inlet Temperature, K	496	496	636	716	729	714	721
P_3 - Inlet Pressure, kPa	400	400	414	412	412	411	412
W_A - Airflow, kg/s	1.10	1.10	0.95	0.87	0.86	0.85	0.85
W_f - Fuel Flow, g/s	37.7	41.3	37.1	38.9	30.4	30.7	31.4
W_{fp} - Pilot Fuel Flow, g/s	37.7	41.3	37.1	38.9	17.8	16.9	17.3
W_{fR} - Reactor Fuel Flow, g/s	0	0	0	0	12.6	13.3	14.1
f - Total Fuel/Air Ratio	0.071	0.0188	0.0196	0.0225	0.0177	0.0181	0.0183
f_p - Pilot Fuel/Air Ratio*	0.0301	0.0329	0.0344	0.0395	0.0182	0.0175	0.0181
f_R - Reactor Fuel/Air Ratio*	0	0	0	0	0.0186	0.0206	0.0213
ΔP_{fp} - Pilot Fuel Injector Pressure Drop, kPa	0.965	1.144	0.958	1.055	0.234	0.207	0.200
ΔP_{fR} - Reactor Fuel Injector Pressure Drop, kPa	0	0	0	0	1.069	---	---
Combustion Exit Data							
$\Delta P/P$ - Total Pressure Loss, %	4.31	4.66	4.33	3.69	3.35	3.36	4.01
T_{R1} - Reactor Exit Temperature No. 1, K					---	---	---
T_{R2} - Reactor Exit Temperature No. 2, K					1693	1639	1685
T_{R3} - Reactor Exit Temperature No. 3, K					1655	1616	1702
T_{R4} - Reactor Exit Temperature No. 4, K					1624	1589	1624
T_R - Average Reactor Exit Temperature, K					1637	1615	1670
T_4 - Average Combustor Exit Temperature, K							
PTF - Pattern Factor							
Gas Analysis Data							
EICO - CO Emission Index, g/kg	14	13	4	5	36	43	44
EIHC - HC Emission Index, g/kg	32	9	5	4	14	40	20
$EINO_x$ - NO_x Emission Index, g/kg	4.3	4.3	8.1	12.6	3.3	2.7	2.8
f_s - Fuel/Air Ratio (From Gas Sample)	0.0179	0.0194	0.0197	0.0218	0.0199	0.0193	0.0203
η_s - Combustor Efficiency (From Gas Sample)	96.9	98.9	99.5	99.6	97.9	95.6	97.3
SN - Smoke Number							
Metal Temperatures							
$T_{P,Max}$ - Maximum Pilot Liner Temperature, K	726	624	940	1045	939	924	932
$T_{R,Max}$ - Maximum Reactor Shell Temperature, K	548	554	710	799	980	928	950

*Based on Pilot Airflow = 0.569 W_A
Reactor Airflow = 0.396 W_A

Table B-4. Clean Catalytic Combustor - Sector Test Data Summary. (Concluded)

Combustor Configuration: Reverse Flow Modification 3, Short Inlet

Run: 15 Date: March 15-16, 1982

Reading Number	9	10	11	12	13	14	15
Nominal Power Setting, %	Cruise	Cruise	Cruise	Cruise	Climb	T/O	T/O
Combustor Inlet Data							
Fuel Split, Pilot/Total	0.556	0.519	0.407	0.581	0.527	0.531	0.539
T_3 - Inlet Temperature, K	744	749	743	746	783	813	814
P_3 - Inlet Pressure, kPa	413	410	410	414	413	414	412
W_A - Airflow, kg/s	0.82	0.81	0.80	0.80	0.81	0.80	0.80
W_f - Fuel Flow, g/s	29.5	31.1	25.1	35.3	30.5	29.5	28.9
W_{fp} - Pilot Fuel Flow, g/s	16.4	16.2	10.2	20.5	16.1	15.7	15.6
W_{fR} - Reactor Fuel Flow, g/s	13.1	14.9	14.9	14.8	14.4	13.8	13.3
f - Total Fuel/Air Ratio	0.0179	0.0192	0.0157	0.0220	0.0190	0.0185	0.0181
f_p - Pilot Fuel/Air Ratio*	0.0176	0.0175	0.0112	0.0225	0.0175	0.0173	0.0171
f_R - Reactor Fuel/Air Ratio*	0.0201	0.0232	0.0234	0.0233	0.0226	0.0219	0.0211
ΔP_{fP} - Pilot Fuel Injector Pressure Drop, kPa	0.200	0.200	0.069	0.290	0.186	0.186	0.193
ΔP_{fR} - Reactor Injector Pressure Drop, kPa	---	---	---	---	---	---	---
Combustion Exit Data							
$\Delta P/P$ - Total Pressure Loss, %	3.51	1.68	3.20	3.99	4.34	3.66	4.36
T_{R1} - Reactor Exit Temperature No. 1, K	---	---	---	---	---	---	---
T_{R2} - Reactor Exit Temperature No. 2, K	1618	1709	1724	1594	1650	1664	1620
T_{R3} - Reactor Exit Temperature No. 3, K	1600	1688	1684	1681	1679	1674	1556
T_{R4} - Reactor Exit Temperature No. 4, K	1588	1706	1698	1650	1689	1692	1613
T_R - Average Reactor Exit Temperature, K	1602	1701	1702	1642	1673	1677	1596
T_4 - Average Combustor Exit Temperature, K							
PTF - Pattern Factor							
Gas Analysis Data							
EICO - CO Emission Index, g/kg	47	28	39	25	27	28	36
EIHC - HC Emission Index, g/kg	28	11	9	9	11	5	11
$EINO_x$ - No_x Emission index, g/kg	2.8	2.8	2.0	4.4	3.3	3.4	3.3
f_a - Fuel/Air Ratio (From Gas Sample)	0.0187	0.0198	0.0170	0.0225	0.0197	0.0191	0.0180
η_a - Combustor Efficiency (From Gas Sample)	96.4	98.4	98.4	98.6	98.4	98.9	98.2
SN - Smoke Number							
Metal Temperatures							
$TP_{,Max}$ - Maximum Pilot Liner Temperature, K	950	951	883	982	986	1013	1013
$TP_{,Max}$ - Maximum Reactor Shell Temperature, K	951	1101	1083	1094	1104	1107	1088

*Based on Pilot Airflow = 0.569 WA
Reactor Airflow = 0.396 WA

Table B-5. Clean Catalytic Combustor - Sector Test Data Summary.

Combustor Configuration: Reverse Flow - Modification 4

Run: 16 Date: June 15, 1982

Reading Number	2	3	4	5	6
Nominal Power Setting, %	Idle	30	60	60	60
Combustor Inlet Data					
Fuel Split, Pilot/Total	1.00	1.00	1.00	0.545	0.536
T_3 - Inlet Temperature, K	492	639	719	720	721
P_3 - Inlet Pressure, kPa	399	412	415	414	413
W_A - Airflow, kg/s	1.06	0.91	0.86	0.85	0.86
W_f - Fuel Flow, g/s	15.0	11.5	8.7	16.0	16.2
W_{fP} - Pilot Fuel Flow, g/s	15.0	11.5	8.7	8.7	8.7
W_{fR} - Reactor Fuel Flow, g/s	0	0	0	7.3	7.5
f - Total Fuel/Air Ratio	0.0142	0.0126	0.0101	0.0187	0.0189
f_P - Pilot Fuel/Air Ratio*	0.0243	0.0216	0.0172	0.0175	0.0174
f_R - Reactor Fuel/Air Ratio*	---	---	---	0.0223	0.0230
ΔP_{fP} - Pilot Fuel Injector Pressure Drop, kPa	0.707	0.418	0.240	0.238	0.235
ΔP_{fR} - Reactor Fuel Injector Pressure Drop, kPa	---	---	---	1.181	1.258
Combustion Exit Data					
$\Delta P/P$ - Total Pressure Loss, %	4.66	4.52	4.65	5.32	4.51
T_{R1} - Reactor Exit Temperature No. 1, K				1588	1588
T_{R2} - Reactor Exit Temperature No. 2, K				1597	1701
T_{R3} - Reactor Exit Temperature No. 3, K				1585	1693
T_{R4} - Reactor Exit Temperature No. 4, K				1584	1610
T_R - Average Reactor Exit Temperature, K				1589	1648
T_4 - Average Combustor Exit Temperature, K					
PTF - Pattern Factor					
Gas Analysis Data					
EICO - CO Emission Index, g/kg	19	6	2	7	3
EIHC - HC Emission Index, g/kg	3	0	0	0	0
$EINO_x$ - NO_x Emission Index, g/kg	5.7	7.6	9.0	4.9	5.0
f_g - Fuel/Air Ratio (From Gas Sample)	0.0155	0.0150	0.0134	0.0216	0.0216
η_g - Combustor Efficiency (From Gas Sample)	99.3	99.9	99.9	99.8	99.9
SN - Smoke Number					
Metal Temperatures					
$T_{P,Max}$ - Maximum Pilot Liner Temperature, K	878	964	1033	1012	1013
$T_{R,Max}$ - Maximum Reactor Shell Temperature, K	525	670	756	1030	1059

*Based on Pilot Airflow = 0.583 * W_A
Reactor Airflow = 0.381 * W_A

Table B-5. Clean Catalytic Combustor - Sector Test Data Summary. (Concluded)

Combustor Configuration: Reverse Flow Modification 5

Run: 17 Date: June 21, 1982

Reading Number	2	3	4	5	6	7	8	9
Nominal Power Setting, %	Idle	30	60	60	60	Cruise	Cruise	85
Combustor Inlet Data								
Fuel Split, Pilot/Total	1.00	1.00	1.00	1.00	0.524	0.540	0.518	0.540
T_3 - Inlet Temperature, K	495	634	716	713	713	741	743	778
P_3 - Inlet Pressure, kPa	400	414	413	400	412	412	414	412
W_A - Airflow, kg/s	1.04	0.91	0.84	0.84	0.84	0.80	0.80	0.78
W_f - Fuel Flow, g/s	15.6	15.6	17.5	24.2	16.4	15.4	15.9	16.1
W_{fP} - Pilot Fuel Flow, g/s	15.6	15.6	17.5	24.2	8.6	8.3	8.2	8.7
W_{fR} - Reactor Fuel Flow, g/s	0	0	0	0	7.8	7.1	7.7	7.4
f - Total Fuel/Air Ratio	0.0150	0.0172	0.0208	0.0289	0.0195	0.0193	0.0200	0.0206
f_p - Pilot Fuel/Air Ratio*	0.0257	0.0294	0.0356	0.0494	0.0175	0.0178	0.0178	0.0191
f_R - Reactor Fuel/Air Ratio*	---	---	---	---	0.0244	0.0232	0.0254	0.0249
ΔP_{fP} - Pilot Fuel Injector Pressure Drop, kPa	1.288	1.342	1.701	3.289	0.394	0.375	0.372	0.420
ΔP_{fR} - Reactor Fuel Injector Pressure Drop, kPa	---	---	---	---	1.307	1.122	1.298	1.239
Combustion Exit Data								
$\Delta P/P$ - Total Pressure Loss, %	4.31	3.50	3.84	4.98	4.01	4.36	3.99	3.69
T_{R1} - Reactor Exit Temperature No. 1, K					1606	1601	1694	1701
T_{R2} - Reactor Exit Temperature No. 2, K					1608	1535	1692	1698
T_{R3} - Reactor Exit Temperature No. 3, K					1574	1574	1694	1698
T_{R4} - Reactor Exit Temperature No. 4, K					1609	1583	1695	1697
T_R - Average Reactor Exit Temperature, K					1599	1586	1695	1699
T_4 - Average Combustor Exit Temperature, K								
PTF - Pattern Factor								
Gas Analysis Data								
EICO - CO Emission Index, g/kg	14	10	32	134	11	7	2	2
EIHC - HC Emission Index, g/kg	1	0	0	0	0	0	0	0
$EINO_x$ - NO_x Emission Index, g/kg	5.6	8.8	13.1	10.8	3.6	4.1	4.0	5.8
f_g - Fuel/Air Ratio (From Gas Sample)	0.0184	0.0225	0.0278	0.0364	0.0255	0.0254	0.0230	0.0236
η_g - Combustor Efficiency (From Gas Sample)	99.6	99.8	99.3	99.9	99.7	99.8	100	100
SN - Smoke Number								
Metal Temperatures								
$T_{P,Max}$ - Maximum Pilot Liner Temperature, K	960	1105	1169	1198	1024	1043	1045	1087
$T_{R,Max}$ - Maximum Reactor Shell Temperature, K	545	704	811	841	1025	1035	1070	1087

*Based on Pilot Airflow = 0.583 * W_A
Reactor Airflow = 0.381 * W_A

Model 1510) was used for acoustic analysis of pilot burner resoanance. The major single frequency was in the 620 to 750 Hz range.

Table B-6 summarizes the results of the sixth test of the reverse flow combustor. Modifications were made to the perforated plate to increase the reference velocity by about 25%. Poor pilot burner efficiency was obtained in this test.

Table B-7 summarizes the results of the first test of the parallel-staged combustor (baseline test). Overall poor reactor performance was obtained due to poor fuel distribution and no method of controlling distribution. Decreasing reference velocity improved reactor performance.

Table B-8 summarizes the results of the second test of the parallel-staged combustor. For this run, the reference velocity was reduced by the addition of a perforated plate. There was evidence of burning in the duct ahead of the reactor.

Table B-6. Clean Catalytic Combustor - Sector Test Data Sun_ ary.

Combustor Configuration: Reverse Flow - Modification 6

Run: 18 Date: July 13, 1982

Reading Number	2	3	4	5	6
Nominal Power Setting, %	Idle	30	60	60	60
Combustor Inlet Data					
Fuel Split, Pilot/Total	1.0	1.0	1.0	0.506	0.497
T_3 - Inlet Temperature, K	494	630	713	716	714
P_3 - Inlet Pressure, kPa	401	410	414	414	415
WA - Airflow, kg/s	1.11	0.96	0.90	0.90	0.90
W_f - Fuel Flow, g/s	15.9	16.5	24.3	17.2	17.5
W_{fP} - Pilot Fuel Flow, g/s	15.9	16.5	24.3	8.7	8.7
W_{fR} - Reactor Fuel Flow, g/s	---	---	---	8.5	8.8
f - Total Fuel/Air Ratio	0.0144	0.0171	0.0269	0.0191	0.0194
f_P - Pilot Fuel/Air Ratio*	0.0268	0.0320	0.0502	0.0181	0.0180
f_R - Reactor Fuel/Air Ratio*	---	---	---	0.0219	0.0225
ΔP_{fP} - Pilot Fuel Injector Pressure Drop, kPa	0.844	1.074	2.085	0.347	0.347
ΔP_{fR} - Reactor Fuel Injector Pressure Drop, kPa	---	---	---	1.333	1.429
Combustion Exit Data					
$\Delta P/P$ - Total Pressure Loss, %	4.5	4.2	4.0	4.0	3.5
T_{R1} - Reactor Exit Temperature No. 1, K				1590	1684
T_{R2} - Reactor Exit Temperature No. 2, K				1546	1650
T_{R3} - Reactor Exit Temperature No. 3, K				1558	1682
T_{R4} - Reactor Exit Temperature No. 4, K				1533	1688
T_R - Average Reactor Exit Temperature, K				1557	1676
T_4 - Average Combustor Exit Temperature, K					
PTF - Pattern Factor					
Gas Analysis Data					
EICO - CO Emission Index, g/kg	4	5	83	100	116
EIHC - HC Emission Index, g/kg	57	8	1	81	63
$EINO_x$ - NO_x Emission Index, g/kg	4.3	7.9	12.5	1.7	1.9
f_s - Fuel/Air Ratio (From Gas Sample)	0.0142	0.0164	0.0231	0.0195	0.0197
η_s - Combustor Efficiency (From Gas Sample), %	94.9	99.2	98.0	90.6	91.8
SN - Smoke Number					
Metal Temperatures					
$T_{P,Max}$ - Maximum Pilot Liner Temperature, K	916	1084	1223	1016	1013
$T_{R,Max}$ - Maximum Reactor Shell Temperature, K	573	736	876	1026	1044

*Based on Pilot Airflow = 0.569 WA
Reactor Airflow = 0.369 WA

Table B-6. Clean Catalytic Combustor - Sector Test Data Summary. (Concluded)

Combustor Configuration: Reverse Flow - Modification 7

Run: 19 Date: July 19, 1982

Reading Number	2	3	4	5	6	7	8	9
Nominal Power Setting, %	Idle	30	60	60	60	Cruise	85	T/O
Combustor Inlet Data								
Fuel Split, Pilot/Total	1.0	1.0	1.0	0.496	0.496	0.503	0.602	0.626
T_3 - Inlet Temperature, K	498	635	716	719	718	744	)	810
P_3 - Inlet Pressure, kPa	401	412	406	404	415	418	415	410
WA - Airflow, kg/s	1.14	0.99	0.91	0.90	0.89	0.86	0.85	0.82
W_f - Fuel Flow, g/s	16.7	19.0	24.3	17.8	17.8	16.4	19.8	20.1
W_{fP} - Pilot Fuel Flow, g/s	16.7	19.0	24.3	8.8	8.8	8.3	11.9	12.6
W_{fR} - Reactor Fuel Flow, g/s	---	---	---	9.0	9.0	8.1	7.9	7.5
f - Total Fuel/Air Ratio	0.0147	0.0191	0.0269	0.0197	0.0200	0.0191	0.0234	0.0246
f_P - Pilot Fuel/Air Ratio*	0.0274	0.0357	0.0500	0.0182	0.0185	0.0180	0.0262	0.0288
f_R - Reactor Fuel/Air Ratio*	---	---	---	0.0230	0.0234	0.0220	0.0215	0.0213
ΔP_{fP} - Pilot Fuel Injector Pressure Drop, kPa	1.150	1.390	2.114	0.294	0.286	0.253	0.543	0.608
ΔP_{fR} - Reactor Fuel Injector Pressure Drop, kPa	---	---	---	1.736	1.760	1.488	1.429	1.337
Combustion Exit Data								
$\Delta P/P$ - Total Pressure Loss, %	4.5	4.2	2.9	3.9	3.2	3.5	3.5	3.7
T_{R1} - Reactor Exit Temperature No. 1, K				1538	1641	1693	1694	1709
T_{R2} - Reactor Exit Temperature No. 2, K				1609	1534	1703	1731	1730
T_{R3} - Reactor Exit Temperature No. 3, K				1566	1594	1650	1681	1686
T_{R4} - Reactor Exit Temperature No. 4, K				1627	1616	1650	1703	1714
T_R - Average Reactor Exit Temperature, K				1585	1596	1674	1702	1710
T_4 - Average Combustor Exit Temperature, K								
PTF - Pattern Factor								
Gas Analysis Data								
EICO - CO Emission Index, g/kg	6	22	119	172	149	145	60	85
EIHC - HC Emission Index, g/kg	4	2	1	54	24	15	3	17
$EINO_x$ - NO_x Emission Index, g/kg	5.2	9.2	12.5	2.1	2.2	2.8	5.8	7.3
f_s - Fuel/Air Ratio (From Gas Sample)	0.0089	0.0132	0.0246	0.0200	0.0213	0.0200	0.0233	0.0240
η_s - Combustor Efficiency (From Gas Sample), %	99.5	99.4	97.2	91.3	94.5	95.3	98.3	96.5
SN - Smoke Number								
Metal Temperatures								
$T_{P,Max}$ - Maximum Pilot Liner Temperature, K	941	1118	1200	1008	1011	1023	1138	1183
$T_{R,Max}$ - Maximum Reactor Shell Temperature, K	569	739	851	1055	1078	1056	1112	1123

*Based on Pilot Airflow = 0.569 WA
Reactor Airflow = 0.369 WA

Table B-7. Clean Catalytic Combustor - Sector Test Data Summary.

Combustor Configuration: Parallel Staged Baseline

Run: 9 Date: December 3-8, 1981

Reading Number	2	3	4	5	6	7	8
Nominal Power Setting, %	Idle	30	60	Idle	30	60	60
Combustor Inlet Data							
Fuel Split, Pilot/Total	1.0	1.0	1.0	1.0	1.0	1.0	0.425
T_3 - Inlet Temperature, K	500	638	718	498	635	719	717
P_3 - Inlet Pressure, kPa	430	419	417	432	416	414	417
WA - Airflow, kg/s	1.60	1.42	1.24	1.60	1.42	1.32	1.30
W_f - Fuel Flow, g/s	10.5	9.6	7.9	11.4	10.1	9.2	21.0
W_{fP} - Pilot Fuel Flow, g/s	10.5	9.6	7.9	11.4	10.1	9.2	8.9
W_{fR} - Reactor Fuel Flow, g/s	0	0	0	0	0	0	12.1
f - Total Fuel/Air Ratio	0.0066	0.0068	0.0064	0.0072	0.0072	0.0070	0.0162
f_P - Pilot Fuel/Air Ratio*	0.0176	0.0182	0.0171	0.0192	0.0190	0.0187	0.0184
f_R - Reactor Fuel/Air Ratio*	0	0	0	0	0	0	0.0178
ΔP_{fP} - Pilot Fuel Injector Pressure Drop, kPa	290	255	193	359	283	248	200
ΔP_{fR} - Reactor Fuel Injector Pressure Drop, kPa	0	0	0	0	0	0	234
Combustion Exit Data							
$\Delta P/P$ - Total Pressure Loss, %	5.8	2.0	1.5	1.4	1.7		1.5
T_{R1} - Reactor Exit Temperature No. 1, K							1606
T_{R2} - Reactor Exit Temperature No. 2, K							1039
T_{R3} - Reactor Exit Temperature No. 3, K							1118
T_{R4} - Reactor Exit Temperature No. 4, K							
T_R - Average Reactor Exit Temperature, K							1254
T_4 - Average Combustor Exit Temperature, K	1038	1108	1149	1034	1103	1156	1165
PTF - Pattern Factor	0.95	0.87	0.86	0.94	0.94	0.88	0.69
Gas Analysis Data							
EICO - CO Emission Index, g/kg	10	3	2	8	2	1	26
EIHC - HC Emission Index, g/kg	4	2	2	3	2	2	264
$EINO_x$ - NO_x Emission Index, g/kg	6.8	12.2	17.9	5.9	11.1	17.3	7.0
f_s - Fuel/Air Ratio (From Gas Sample)	0.0112	0.0109	0.0102	0.0123	0.0114	0.0116	0.0174
n_s - Combustor Efficiency (From Gas Sample), %	99.4	99.7	99.8	99.5	99.3	99.8	76.4
SN - Smoke Number							
Metal Temperatures							
$T_{P,Max}$ - Maximum Pilot Liner Temperature, K	620	762	835	653	776	848	842
$T_{R,Max}$ - Maximum Reactor Shell Temperature, K	499	639	720	496	633	718	758

*Based on Pilot Airflow = 0.374 * WA
Reactor Airflow = 0.523 * WA

Table B-7. Clean Catalytic Combustor - Sector Test Data Summary. (Concluded)

Combustor Configuration: Parallel Staged Baseline

Run: 9 Date: December 3-8, 1981

Reading Number	9	10	11	12	13	14	15
Nominal Power Setting, %	Cruise	60	85	Cruise	Cruise	85	100
Combustor Inlet Data							
Fuel Split, Pilot/Total	0.448	0.459	0.397	1.0	0.396	0.426	0.425
T_3 - Inlet Temperature, K	746	718	776	745	744	778	813
P_3 - Inlet Pressure, kPa	419	421	413	416	410	423	421
WA - Airflow, kg/s	1.22	0.99	1.23	0.94	0.94	0.93	0.93
W_f - Fuel Flow, g/s	20.3	14.7	21.5	6.4	16.2	15.1	15.1
W_{fP} - Pilot Fuel Flow, g/s	9.1	6.8	8.5	6.4	6.4	6.4	6.4
W_{fR} - Reactor Fuel Flow, g/s	11.2	8.0	13.0	0	9.8	8.7	8.7
f - Total Fuel/Air Ratio	0.0167	0.0149	0.0175	0.0063	0.0172	0.0163	0.0164
f_P - Pilot Fuel/Air Ratio*	0.0200	0.0183	0.0186	0.0182	0.0182	0.0186	0.0186
f_R - Reactor Fuel/Air Ratio*	0.0176	0.0154	0.0202	0	0.0199	0.0179	0.0180
ΔP_{fP} - Pilot Fuel Injector Pressure Drop, kPa	248	159	200	145	186	172	165
ΔP_{fR} - Reactor Fuel Injector Pressure Drop, kPa	200	110	269	0	138	124	124
Combustor Exit Data							
$\Delta P/P$ - Total Pressure Loss, %	1.6	2.0	1.8	1.3	0.7	1.6	0.8
T_{R1} - Reactor Exit Temperature No. 1, K	1651	1660	1026		1704	1704	1669
T_{R2} - Reactor Exit Temperature No. 2, K	1130	1105	1092		1118	1166	1130
T_{R3} - Reactor Exit Temperature No. 3, K	1154	1105	1202		1259	1271	1324
T_{R4} - Reactor Exit Temperature No. 4, K							
T_R - Average Reactor Exit Temperature, K	1312	1290	1106		1360	1380	1374
T_4 - Average Combustor Exit Temperature, K	1215	1183	1201	1120	1259	1281	1273
PTF - Pattern Factor	0.64	0.72	0.68	0.90	0.70	0.60	0.47
Gas Analysis Data							
EICO - CO Emission Index, g/kg	33	22	55	1	36	61	66
EIHC - HC Emission Index, g/kg	250	226	269	9	189	156	156
$EINO_x$ - NO_x Emission Index, g/kg	10.8	12.8	7.1	24.5	12.2	14.1	16.0
f_g - Fuel/Air Ratio (From Gas Sample)	0.0181	0.0167	0.0176	0.0118	0.0181	0.0181	0.0184
η_g - Combustor Efficiency (From Gas Sample), %	77.5	79.8	75.3	99.2	82.7	85.0	84.9
SN - Smoke Number							
Metal Temperatures							
$T_{P,Max}$ - Maximum Pilot Liner Temperature, K	878	854	900	882	875	920	953
$T_{R,Max}$ - Maximum Reactor Shell Temperature, K	789	748	826	747	791	822	853

*Based on Pilot Airflow = 0.374 * WA
Reactor Airflow = 0.523 * WA

Table B-8. Clean Catalytic Combustor - Sector Test Data Summary.

Combustor Configuration: Parallel Flow With Reduced V_{REF}.

Run: 1C Date: December 17, 1981

Reading Number	2	3	4	5	6	7	8	9
Nominal Power Setting, %	Idle	30	60	60	60	60	60	60
Combustor Inlet Data								
Fuel Split, Pilot/Total	1.0	1.0	1.0	0.715	0.703	0	0	0.663
T3 - Inlet Temperature, K	497	638	718	715	722	716	720	720
P3 - Inlet Pressure, kPa	414	414	412	414	419	419	423	417
WA - Airflow, kg/s	1.20	1.07	0.97	0.98	0.98	0.98	0.98	0.98
W_f - Fuel Flow, g/s	14.4	15.2	13.9	19.4	19.7	5.9	7.1	21.1
W_{fP} - Pilot Fuel Flow, g/s	14.4	15.2	13.9	13.9	13.9	0	0	14.0
W_{fR} - Reactor Fuel Flow, g/s	0	0	0	5.5	5.8	5.9	7.1	7.1
f - Total Fuel/Air Ratio	0.0120	0.0143	0.0143	0.0198	0.0201	0.0060	0.0072	0.0214
f_p - Pilot Fuel/Air Ratio*	0.0236	0.0282	0.0282	0.0279	0.0278	0	0	0.0289
f_R - Reactor Fuel/Air Ratio*	0	0	0	0.0159	0.0163	0.0169	0.0204	0.0204
ΔP_{fP} - Pilot Fuel Injector Pressure Drop, kPa	558	669	552	558	510	0	0	545
ΔP_{fR} - Reactor Fuel Injector Pressure Drop, kPa	0	0	0	30	46	39	63	61
Combustion Exit Data								
$\Delta P/P$ - Total Pressure Loss, %	1.83	2.33	2.51	2.83	3.46	2.80	2.94	3.14
T_{R1} - Reactor Exit Temperature No. 1, K								
T_{R2} - Reactor Exit Temperature No. 2, K								
T_{R3} - Reactor Exit Temperature No. 3, K								
T_{R4} - Reactor Exit Temperature No. 4, K								
T_R - Average Reactor Exit Temperature, K								
T_4 - Average Combustor Exit Temperature, K	1221	1374	1401	1471	1428	894	914	1435
PTF - Pattern Factor	0.31	0.30	0.30	0.20	0.25	0.80	1.17	0.29
Gas Analysis Data								
EICO - CO Emission Index, g/kg	7	4	3	3	3	5	3	3
EIHC - HC Emission Index, g/kg	2	1	1	0	1	3	1	0
$EINO_x$ - NO_x Emission Index, g/kg	6.1	11.6	17.8	16.0	15.8	7.6	8.2	13.1
f_g - Fuel/Air Ratio (From Gas Sample)	0.0226	0.0277	0.0253	0.0280	0.0303	0.0053	0.0070	0.0327
η_g - Combustor Efficiency (From Gas Sample), %	99.6	99.9	99.9	---	99.9	99.6	99.8	99.9
SN - Smoke Number								
Metal Temperatures								
$T_{P,Max}$ - Maximum Pilot Liner Temperature, K	675	830	894	915	920	754	773	927
$T_{R,Max}$ - Maximum Reactor Shell Temperature, K	496	637	717	883	884	898	958	961

*Based on Pilot Airflow = 0.507 * WA
Reactor Airflow = 0.354 * WA

Table B-8. Clean Catalytic Combustor - Sector Test Data Summary. (Concluded)

Combustor Configuration: Parallel Flow With Reduced V_{REF}.

Run: 11 Date: December 21, 1981

Reading Number	2	3	4
Nominal Power Setting, %	60	60	60
Combustor Inlet Data			
Fuel Split, Pilot/Total	1.0	1.0	0.629
T_3 - Inlet Temperature, K	713	719	716
P_3 - Inlet Pressure, kPa	416	417	414
WA - Airflow, kg/s	0.998	1.23	1.24
W_f - Fuel Flow, g/s	19.7	17.5	26.8
W_{fP} - Pilot Fuel Flow, g/s	19.7	17.5	16.9
W_{fR} - Reactor Fuel Flow, g/s	0	0	9.9
f - Total Fuel/Air Ratio	0.0197	0.0143	0.0217
f_P - Pilot Fuel/Air Ratio*	0.0389	0.0281	0.0269
f_R - Reactor Fuel/Air Ratio*	0	0	0.0227
ΔP_{fP} - Pilot Fuel Injector Pressure Drop, kPa	1096	861	820
ΔP_{fR} - Reactor Fuel Injector Pressure Drop, kPa	0	0	102
Combustion Exit Data			
$\Delta P/P$ - Total Pressure Loss, %	1.99	4.30	3.83
T_{R1} - Reactor Exit Temperature No. 1, K			
T_{R2} - Reactor Exit Temperature No. 2, K			
T_{R3} - Reactor Exit Temperature No. 3, K			
T_{R4} - Reactor Exit Temperature No. 4, K			
T_R - Average Reactor Exit Temperature, K			
T_4 - Average Combustor Exit Temperature, K	1429	1241	1289
PTF - Pattern Factor	0.29	0.37	0.24
Gas Analysis Data			
EICO - CO Emission Index, g/kg	50	4	28
EIHC - HC Emission Index, g/kg	1	0	54
$EINO_x$ - NO_x Emission Index, g/kg	16.1	13.5	10.9
f_g - Fuel/Air Ratio (From Gas Sample)	0.0396	0.0283	0.0273
η_g - Combustor Efficiency (From Gas Sample), %	98.8	99.9	94.7
SN - Smoke Number			
Metal Temperatures			
$T_{P,Max}$ - Maximum Pilot Liner Temperature, K	929	1108	1090
$T_{R,Max}$ - Maximum Reactor Shell Temperature, K	715	795	856

*Based on Pilot Airflow = 0.507 * WA
Reactor Airflow = 0.354 * WA